WARWICK
THE UNIVERSITY OF WARWICK

A Thesis Submitted for the Degree of PhD at the University of Warwick

Permanent WRAP URL:
http://wrap.warwick.ac.uk/97618

Copyright and reuse:
This thesis is made available online and is protected by original copyright.
Please scroll down to view the document itself.
Please refer to the repository record for this item for information to help you to cite it.
Our policy information is available from the repository home page.

For more information, please contact the WRAP Team at: wrap@warwick.ac.uk

warwick.ac.uk/lib-publications

Innovation Report

Vision Based Environment Perception System for Next Generation Off-road ADAS

By
Anna Gaszczak

Engineering Doctorate Portfolio Submission
This work is submitted in partial fulfilment for the degree of
Engineering Doctorate (EngD)

Warwick Manufacturing Group
University of Warwick

Abstract

Advanced Driver Assistance Systems (ADAS) aids the driver by providing information or automating the driving related tasks to improve driver comfort, reduce workload and improve safety. The vehicle senses its external environment using sensors, building a representation of the world used by the control systems. In on-road applications, the perception focuses on establishing the location of other road participants such as vehicles and pedestrians and identifying the road trajectory. Perception in the off-road environment is more complex, as the structure found in urban environments is absent. Off-road perception deals with the estimation of surface topography and surface type, which are the factors that will affect vehicle behaviour in unstructured environments.

Off-road perception has seldom been explored in automotive context. For autonomous off-road driving, the perception solutions are primarily related to robotics and not directly applicable in the ADAS domain due to the different goals of unmanned autonomous systems, their complexity and the cost of employed sensors. Such applications consider only the impact of the terrain on the vehicle safety and progress but do not account for the driver comfort and assistance.

This work addresses the problem of processing vision sensor data to extract the required information about the terrain. The main focus of this work is on the perception task with the constraints of automotive sensors and the requirements of the ADAS systems. By providing a semantic representation of the off-road environment including terrain attributes such as terrain type, description of the terrain topography and surface roughness, the perception system can cater for the requirements of the next generation of off-road ADAS proposed by Land Rover.

Firstly, a novel and computationally efficient terrain recognition method was developed. The method facilitates recognition of low friction grass surfaces in real-time with high accuracy, by applying machine learning Support Vector Machine with illumination invariant normalised RGB colour descriptors. The proposed method was analysed and its performance was evaluated experimentally in off-road environments. Terrain recognition performance was evaluated on a variety of different surface types including grass, gravel and tarmac, showing high grass detection performance with accuracy of 97%.

Secondly, a terrain geometry identification method was proposed which facilitates semantic representation of the terrain in terms of macro terrain features such as slopes, crest and ditches. The terrain geometry identification method processes 3D information reconstructed from stereo imagery and constructs a compact grid representation of the surface topography. This representation is further processed to extract object representation of slopes, ditches and crests. Thirdly, a novel method for surface roughness identification was proposed. The surface roughness descriptor is then further used to recommend a vehicle velocity, which will maintain passenger comfort. Surface roughness is described by the Power Spectral Density of the surface profile which correlates with the acceleration experienced by the vehicle. The surface roughness descriptor is then mapped onto vehicle speed recommendation so that the speed of the vehicle can be adapted in anticipation of the surface roughness. Terrain geometry and surface roughness identification performance were evaluated on a range of off-road courses with varying topology showing the capability of the system to correctly identify terrain features up to 20 m ahead of the vehicle and analyse surface roughness up to 15 m ahead of the vehicle. The speed was recommended correctly within +/- 5 kph. Further, the impact of the perception system on the speed adaptation was evaluated, showing the improvements in speed adaptation allowing for greater passenger comfort.

The developed perception components facilitated the development of new off-road ADAS systems and were successfully applied in prototype vehicles. The proposed off-road ADAS are planned to be introduced in future generations of Land Rover products. The benefits of this research also included new Intellectual Property generated for Jaguar Land Rover. In the wider context, the enhanced off-road perception capability may facilitate further development of off-road automated driving and off-road autonomy within the constraints of the automotive platform.

Table of Contents

List of Figures

List of Tables

Acknowledgements

I would like to thank numerous people for the support and help that they have given me through the Engineering Doctorate programme.

First, I would like to express my gratitude to my supervisor Prof. Paul Jennings and my co-supervisor Dr Kurt Debatista for their continuous support and constructive discussions during the course of this project. Discussing my ideas with them has provided me with multiple perspectives of the theoretical and practical aspects of this work. Their confidence and patience throughout this process were invaluable.

The creative and productive atmosphere at the Research Department in Jaguar Land Rover, provided me with great working environment, helping the ideas presented in this work materialise. My gratitude goes to all my colleagues and friends in Jaguar Land Rover for supporting my work with fruitful discussions, work reviews, software integration and testing.

This work would not be possible without the support from my managers in Jaguar Land Rover Dr Carl Pickering and Nigel Clarke to whom I am in debt for the opportunity to pursue this research. I would like to thank to all of my colleagues for their support and input especially Dr Andrew Fairgrieve, Dereck Webster, Jithesh Kotteri, Jithin Jayaraj, Binesh Ravi, Neenu Isaac and Dr Thomas Popham.

My family and friends were such as tremendous support during that time; giving me encouragement and being a constant source of motivation when it was needed. I would like to thank my family and friends. I would like to thank Gosia, Agata, Alicja, Diana, Josefa, Lukasz, David and Linus for supporting me during the final efforts to complete this programme.

Declaration

The work presented in this document is entirely my own. All published work and sources have been acknowledged. This work has not been submitted or presented in any previous application for a degree or award.

Anna Gaszczak

List of Abbreviations

ABS	*Anti-Lock Braking System*
ACC	*Adaptive Cruise Control*
ADAS	*Advanced Driver Assistance System*
AEB	*Automatic Emergency Braking*
ANN	*Artificial Neural Network*
ATPC	*All-Terrain Progress Control*
CPU	*Central Processing Unit*
DARPA	*Defence Advanced Research Projects Agency*
DFM	*Direct Functional Mapping*
ECU	*Electronic Control Unit*
FOV	*Field of View*
FPGA	*Field Programmable Gate Array*
FPR	*False Positive Rate*
GPS	*Global Positioning System*
HDC	*Hill Descent Control*
HMI	*Human Machine Interface*
IMU	*Inertial Measurement Unit*
IP	*Intellectual Property*
ISO	*International Organisation for Standarisation*
JLR	*Jaguar Land Rover*
LDW	*Lane Departure Warning*
LKA	*Lane Keeping Assist*
MLS	*Multi Level Surface Map*
PC	*Personal Computer*
PSD	*Power Spectral Density*
RGB	*Red Green Blue*
ROC	*Receiver Operator Curves*
SAE	*Societey of Automotive Engineers*
SIFT	*Scale-Invariant Feature Transform*
SLAM	*Simultaneous Localisation and Mapping*
SURF	*Speeded Up Robust Features*
SUV	*Sport Utility Vehicle*
SVD	*Singular Value Decomposition*
SVM	*Support Vector Machine*
TBSA	*Terrain Based Speed Adaption*
TPR	*True Positive Rate*
TR	*Terrain Response*

Portfolio Plan

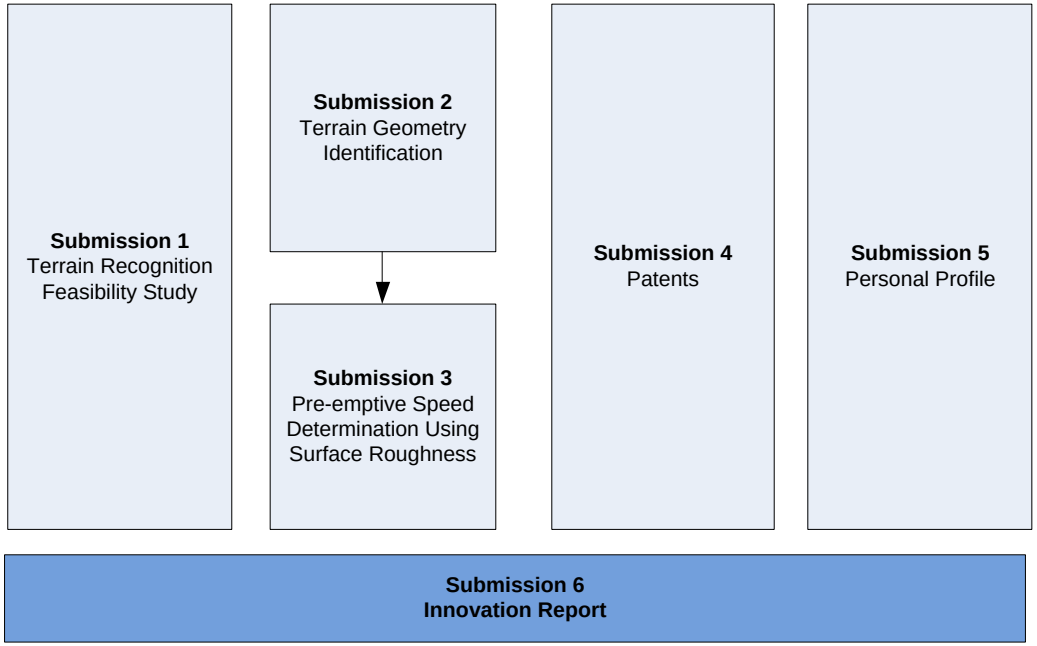

1 Introduction

Autonomous vehicles have gained much publicity over the recent years as non-automotive and automotive firms such as Google and Tesla announced that they have been driving safely for thousands of miles. Whilst this has set the goal for the next generations of automotive products, full automation still requires significant developments. Meanwhile, some highly automated driving features are available in the market in the form of Advance Driver Assistance Systems (ADAS) such as adaptive cruise control, lane centring, highway autopilot and automatic parking.

In the last two decades, numerous projects have shown advances in autonomous driving. In the early 1990s, the European project PROMETHEUS demonstrated successful autonomous highway driving from Germany to Denmark [1]–[3]. In the 2000s the Defence Advanced Research Projects Agency (DARPA) organised a number of challenges to showcase autonomous vehicles. The two Grand Challenges featured autonomous off-road ground vehicles in the Nevada desert [4], [5]; the first challenge took place in March 2004 and the second challenge in October 2005. The DARPA 2007 Urban Challenge featured autonomous vehicles driving in an urban traffic [6]–[9]. Recently the most publicly noticed activities are: Google autonomous vehicle driving thousands of miles in California [10], University of Parma BRAiVE successfully navigating in urban traffic in Parma [11] and Mercedes Bertha driving autonomously the historic route of the first Mercedes vehicle from Mannheim to Pforzheim [12]. However, production systems currently focus on expanding automated single driving scenarios such as driving on a motorway or parking. Most luxury vehicle manufacturers offer highway assist [13] and urban stop and go traffic jam assist [14], [15]. While vehicle manufacturers have already introduced highly automated driving features to reach higher levels of automation, these systems are not designed nor expected to operate in off-road environments.

At the core of any ADAS system lies the perception of its environment, allowing the vehicle to extract relevant information about its surrounding to be able to perform the desired action. The richness of the attributes and the quality of the information have direct ramifications on the capability of the system. On-road perception systems can semantically describe the environment in terms of the existence of other road participants (vehicle, pedestrian and obstacle detection) and the road trajectory (lane detection), which provide sufficient level of detail to follow a clearly marked urban road. However, when no lane marks exist, the system is not capable of operating [16]. While the perception in the on-road environment is simplified due to the assumption of driving on a tarmac road, perception in the off-road environment is much more complex as the terrain in its topography and composition is more varied.

Perception is also inherently dependent on the type of sensors used by the ADAS system. While active sensors such as lidars provide robust and rich information sets preferred by developers of autonomous cars such as Google and DARPA participants, they are expensive and problematic to package on a

production vehicle. Other active sensors such as radars and ultrasonics provide a limited perception capability, since it is only possible to detect objects such as cars, road furniture and pedestrians. Recent developments in the area of computer vision lead to a widespread use of camera systems in production vehicles. Cameras may offer further perception capability due to the more rich description of the scene in the visual spectrum, however the type of information produced by the perception system entirely depends on the employed computer vision methods.

1.1 Sponsoring company - Jaguar Land Rover

Jaguar Land Rover (JLR) produces high-end sedan and sport utility vehicles (SUV). Land Rover has been leader in the development of off-road ADAS technologies, introducing first to market features such as Hill Descent Control, Terrain Response and All-Terrain Response. With increased levels of on–road automation, there is an expectation that in the future a similar level of automation will become available for off-road driving. While automotive manufacturers compete with the offering of on-road automated features, the off-road capability offers a unique selling point for Land Rover.

JLR vehicles are fitted with an increased number of sensors (camera, radars, ultrasonic). The forward-looking camera has also become a standard equipment on JLR vehicles, driven by the requirements of EuroNCAP safety rating for pedestrian protection and collision mitigation [17]. Although the main purpose of these sensors is to support on-road ADAS functionality, they could be repurposed to enable off-road ADAS to become a new revenue stream.

1.2 Project Aim

The aim of the research project described in this document is to develop a vision based sensing techniques, including measurement of the surface roughness, terrain geometry and the presence of grass, to enable the next generation of Jaguar Land Rover off-road assistance features.

Following a review of existing sensing capability provided by current supplier solutions, it was established that the sensor data processing methods do not provide the required information in the off-road environment. It concluded that there is no commercially available perception system capable in off-road environments. The following research question was thus formulated:

Can a vision-based perception system provide an understanding of the off-road environment to enable the next generation of off-road ADAS features within the constraints of automotive systems?

In the first part of the project, JLR was interested in improving the performance of existing Terrain Response system by recognising the terrain type ahead of the vehicle, and more specifically prioritising grass surfaces. After an initial feasibility study which was conducted into the development of a vision-based method for grass detection, a change of strategy was decided. With the decreasing costs of camera

sensors and introduction of stereo-cameras in the automotive market a new range of opportunities opened. The stereo camera provides the measurements of 3D structure of the environment, hence could potentially more advanced functionality including lateral and/or longitudinal motion control. This hardware choice with enhanced capabilities brought new opportunities in the feature development leading to the second part of the project.

In the second part of the project, JLR wanted to develop a feature called Terrain Based Speed Adaption. This would allow the vehicle to control its speed automatically in off-road conditions and adjust it depending on terrain conditions. Terrain geometry and surface roughness were identified as key factors to be detected pre-emptively.

As a result, the following objectives were formulated:

- Develop and validate a terrain classification system capable of detecting grass surfaces
- Develop and validate a terrain geometry identification system.
- Develop and validate a pre-emptive speed recommendation system based on surface roughness.

As the off-road perception system is to be deployed in an automotive environment, the proposed solutions should also take into account the following constraints:

- Processing power available on the vehicle

  Processing power on vehicle is limited therefore real-time solutions which fit with the available computational power shall be developed. A typical automotive camera system pre-processes the image by FPGA extracting lower-level image features and computes disparity, before the CPU can perform the classification tasks. The same processor may be used to run many other tasks therefore its computational load is an important factor to consider.

- Available sensor limitations

  The project objectives shall be met with the current sensor availability and their limitations. Available sensors already support safety related functions and their specification cannot be changed without significant development cost. The sensor constraints are a major factor that affects the perception system performance.

- Robustness

  As discussed in [18] the perception system needs to be robust against varying illumination conditions and vehicle dynamics that induce camera motion (including roll, pitch and yaw). If the perception system cannot handle certain environmental conditions, it shall report the low quality of this output to the system that relies on this information.

1.3 Overview

This development of the off-road perception system has been a new activity within the company, as previously the perception capability have been delivered by suppliers even in the research stage; only when perception component already existed the feature development was undertaken. This led to longer feature development time and risk that the perception component does not fully fulfil the requirements as the requirements evolve during the development process. In addition, it can be commercially challenging if a supplier develops a system for a manufacturer if it cannot be applied by other customers to leverage economies of scale. The development of perception in-house offered faster development time and more flexibility with requirements specification. In addition, commercial benefits included generated Intellectual Property during the course of this project.

The development undertaken during this doctorate delivered off-road perception capability. Perception is a mechanism of interpretation and identification of sensory information to understand the environment. The vehicle interacting with the world has access only to the world representation delivered by sensors. Perception builds this world model based on the interpretation of the sensor data and extracting the relevant objects and attributes of the environment relevant to the driving task and scenario.

The proposed off-road perception system can be broken down into three conceptual components representing important attributes of the terrain as shown in Figure 1.1.

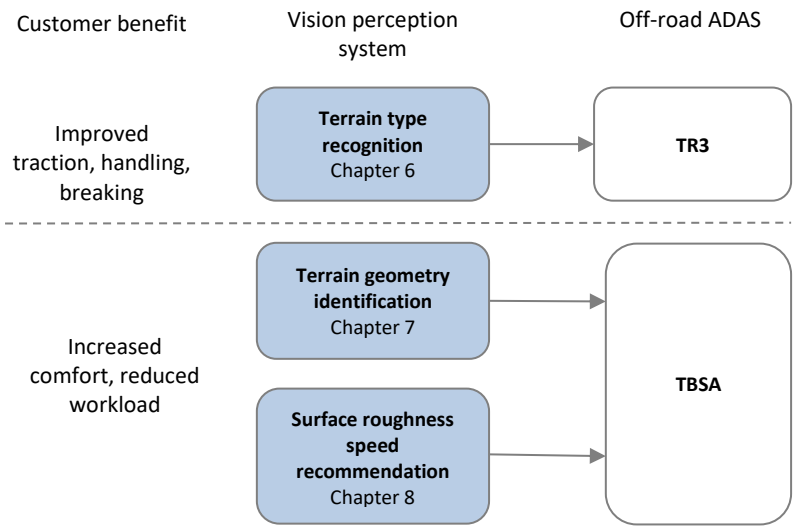

Figure 1.1. Proposed off-road perception system and its building blocks linked to individual off-road ADAS functions.

- Terrain type recognition - Terrain type may provide an indication about the surface composition and traction. This module was developed so that the appropriate Terrain Response mode can be chosen in anticipation of the terrain.

- Terrain geometry identification– Terrain geometry relates to macro terrain features such as slopes, ditches, crests and obstacles that will affect vehicle behaviour in an off-road environment. This module was developed so that the vehicle can adjust its speed in anticipation to the macro terrain features affecting vehicle progress.

- Surface roughness and speed recommendation – Surface roughness relates to micro terrain features, which can cause excessive vehicle acceleration levels leading to passenger discomfort. In addition, to relate the surface roughness to recommended vehicle speed, a mapping function was derived experimentally. This module was developed so that the vehicle can adjust its speed in anticipation to the micro terrain features affecting the comfort of the progress.

1.4 EngD Portfolio Structure

The portfolio consists of five submissions. Three of the submissions present an individual sensing problem with relation to different off-road ADAS features, proposed solution and validation. Each submission can be read independently, however, to understand the evolution of development, it is recommended to read them starting with this Innovation Report and the follow from the first submission progressing incrementally to the last submission.

Submission 1: Terrain detection feasibility study. This document describes the intended evolution of Terrain Response system and proposes a method for grass classification using colour camera. The document reviews state-of-the-art vision based terrain classification methods and machine learning methods with a focus on complexity, computational requirements and robustness. This is followed by design of a new computationally light way method for grass detection. This document finishes with experimental validation of the proposed method.

Submission 2: Terrain Geometry Identification. This document describes the sensing requirements posed by Terrain Based Speed Adaptation and the proposed solution to identify terrain geometry characteristics. This submission covers analysis of sensing requirements, followed by analysis of sensor characteristics to understand if the requirements can be fulfilled. It also covers a review of related work in off-road perception systems. Further, a method for terrain geometry identification is proposed and experimental validation results are presented.

Submission 3: Pre-emptive Speed Recommendation Using Surface Roughness. This document describes the proposed surface roughness measurement method and vehicle speed recommendation method based on the measured roughness. This submission covers a review of off-road perception in the context of surface roughness, surface roughness measurement methods and impact of surface roughness on passenger comfort. Further, experimental validation results are presented.

Submission 4: Patents. This document summarises patent applications submitted as a result of this work.

Submission 5: Personal Profile. This document summarises how the author fulfils the required EngD competences.

1.5 Structure of the Innovation Report

Chapter 2 is an introduction and review of Advanced Driver Assistance Systems. It describes the capability of the ADAS and associated perception systems currently available on the market.

Chapter 3 reviews related work in the area of off-road perception.

Chapter 4 describes the approach taken to address the research question.

Chapter 5 discusses the target off-road ADAS systems and discusses the perception requirements in order to achieve the expected functionality of ADAS.

Chapter 6 describes the design and implementation of the terrain recognition method. The results of the experimental performance evaluation are presented.

Chapter 7 describes design and implementation of the terrain geometry identification method. The performance of the perception system as well as its influence on TBSA performance are discussed.

Chapter 8 describes the design and implementation of the speed recommendation method based on surface roughness. The performance of the surface roughness assessment method and speed recommendation method is evaluated. Further the impact of pre-emptive speed recommendation on TBSA performance is discussed.

Chapter **Error! Reference source not found.** discussed the impact of the research, its limitations and recommends streams of further work.

Chapter 10 concludes this document.

2 Advanced Driver Assistance Systems

The main drive behind the introduction of ADAS is the improvement of safety. It is estimated that the forward collision avoidance systems can prevent 75% of rear-end crashes and save around 5000 fatalities and 50,000 serious injuries per year across the EU [19]. Another type of accident caused primarily by driver inattention or fatigue are off-path crashes where driver leaves the course of the road. The lane keeping assistance systems can reduce the number of off-path crashes by alerting the driver when the vehicle is in danger of leaving the lane unintentionally or by actively steering the vehicle to stay in the path. The use of lane keeping assistance is estimated to reduce the number deaths by a 15% and the number of injuries by 8.9% according to the European Commission funded project eIMPACT [20].

Growing importance and increased public acceptance of highly automated vehicles drives the development and market introduction of ADAS features even further. The main aim of ADAS system is to improve safety and comfort of driving. ADAS systems monitor vehicle surroundings to perform difficult of repetitive tasks, hence improving comfort and lowering driver's workload. Studies into ADAS systems that automate part of the driving task (longitudinal or lateral control) indicate that use of ADAS reduces driver workload [21]–[23] hence can improve safety. In critical situations, such as emergency braking, the ADAS warns the driver helping to prevent accidents or intervenes to support the driver mitigating the consequences. This is leading to increased road safety as shown in studies [24], [25]. ADAS system can substitute certain human actions with repeatable and reliable machine control, eliminating human errors that lead to accidents.

This chapter will review existing ADAS systems and the research efforts in the domain of highly automated driving. Since the capability of the existing ADAS systems highly depend on the perception systems, this chapter will also cover review and analysis of the available sensing systems. The concept of perception system will also be introduced and discussed in the context of ADAS, specifically discussing what and how is sensed to provide the required information about the vehicle environment.

2.1 ADAS market

The market for ADAS system according to ABI Research is estimated to be worth $11 billion by the end of 2016, with the compound annual growth rate of 29% [26]. By 2026 the market is expected to be worth $132 billion [26]. By 2020, almost 25 million cameras are expected to be fitted into cars in Western Europe each year, with annual revenues surpassing €2 Billion as predicted by SBD [27].

The experienced growth in the market for ADAS is driven by multiple factors:

- Legislation pressure to introduce more safety features. European Commission mandated fitment of Lane Departure Warning (LDW) and Autonomous Emergency Braking (AEB)

systems for heavy commercial vehicles from 2014, with 100% fitment required by the final quarter of 2015 [28].

- The inclusion of active safety systems: AEB and LDW into EuroNCAP safety rating [17]. From 2014 only models that have 50% fitment rates for AEB will be able to claim an extra 3 points in the Safety Assist category, with points also being awarded for 50% fitment rates of LDW and Lane Keeping Assist (LKA). From 2017 this fitment rate will increase to 100%.

- Higher market penetration of low cost camera-based ADAS applications. Low-cost camera-based systems supporting Land Departure Warning, Lane Keeping Assistance and low-speed Emergency Breaking has been introduced on high volume vehicle models such as Ford Focus, Mercedes C-Class, Volkswagen Passat, Fiat 500.

- Technical advances in sensor design and manufacturing driving the sensor cost down. Larger market penetration allows the supplier to leverage economies of scale driving the cost of new components even lower.

Typically, automotive manufacturers introduced ADAS features in the top vehicle segment first as the cost of new technology introduction in high as it requires new hardware, sensors and has an impact on vehicle communication architecture. While the cost of ADAS is going down with the economies of scale achieved by suppliers, the ADAS systems are introduced in lower cost vehicles.

2.2 Automotive feature development

The purpose of this section is to set the frame of reference for the work presented in this report. Automotive development process consists of two stages *concept phase* and *series development* as shown by the generic model proposed by Knapp [29] presented in Figure 2.1. Due to confidentiality restrictions, specific development process as adopted by JLR cannot be presented. The generic model though reflects the key stages relevant to system development and the split between research concept development and series development by Centre of Competence (CoCs). In the *concept phase*, the initial idea of a feature is evaluated, taking into account multiple aspects of the project including business case, technical feasibility of the system and expected customer functionality. Proof of concept is built to evaluate technical feasibility and expected customer functionality of the proposed feature. Proof of concept prototype plays an important role in the early development stages as noted by Elverum [30] due to its role in providing detailed characteristics of the system performance. Initial performance assessment is essential to understand detailed product or system requirements. The *concept phase* aims at finalising the system level requirements, which are handed over to the CoC for series development. System specification describes the functionality of the system, defines system inputs and outputs, system performance and users' interactions.

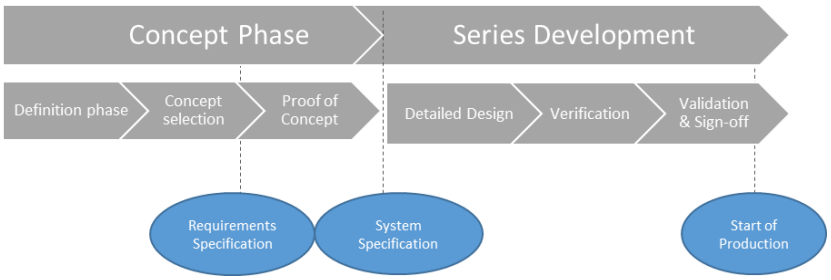

Figure 2.1. Generic automotive development process flow.

In the s*eries development* phase, the vehicle manufacturer's main role is to integrate all the systems provided by external suppliers into the vehicle. The integration of the systems is based on agreed lists of specifications and interfaces. Usually, the software contained within the system provided by the supplier is treated as 'black box' and the specific methods implemented in the system are part of supplier's Intellectual Property (IP) [31].

Quality and precision of the requirements passed onto suppliers is a crucial factor when integrating the systems. Hence the proof of concept in the *concept phase* is so important, as it allows to understand the interactions between different components of the systems and derivation of functional requirements.

2.3 Automated driving taxonomy

Driverless, autonomous vehicles, highly automated driving and Driver Assistance widely used terms describing different levels of automation. The terminology used in industry, research publications and media varies describing systems of different capabilities hence the industry put forward efforts to standardise the taxonomy of automated driving. German Federal Highway Research Institute (BASt) [32] and Society of Automotive Engineers (SAE) [33] independently proposed a congruent taxonomy for on-road automated vehicles as presented in Table 2.1. Highly Automated (SAE level 3) and Fully Automated (SAE level 4) systems do not require constant driver supervision as opposed to Partial Automation (SAE level 2) and Driver Assistance (SAE level 1) system. Highly automated driving systems that do not require driver attention are currently under development with prototypes being tested by vehicle manufacturers, Google and various research consortia. Although currently available ADAS systems can automate certain driving scenarios, such as driving on a motorway, they are only SAE level 1 and 2 systems as they require the driver to monitor the system at all times and take over the vehicle control if required.

BASt level	Definition	SAE level
Driver Only	Human driver executes manual driving task.	**0**
Driver Assistance	The driver permanently controls either longitudinal or lateral control. The other task can be automated to a certain extent by the assistance system. The driver shall **permanently monitor** the system and shall be prepared to **take over control** at any time.	**1**
Partial automation	The system takes over longitudinal and lateral control. The driver shall **permanently monitor** the system and shall be prepared to **take over control** at any time.	**2**
High automation	The system takes over longitudinal and lateral control. The driver is **no longer required to permanently monitor** the system. In case of a take-over request, the driver must take over control with a certain time buffer.	**3**
Full automation	The system takes over longitudinal and lateral control completely and permanently. In case of a takeover request that is not followed, the **system will return to the minimal risk condition by itself**.	**4**

Table 2.1. BASt automated driving taxonomy [32] *with corresponding SAE classification* [33].

2.4 On-road ADAS

Currently available ADAS systems aim to free the driver from monotonous or tedious tasks such as driving on the motorway, driving in a traffic jam or parking. A comprehensive list of ADAS system available in modern vehicles is presented in Table 2.2. At the moment these functions offer only partial automation, designed to work only in specific scenarios and being supervised by the driver at all times.

These ADAS systems are characterised by relying on the permanent perception of the vehicle environment through one or more sensors as shown in Table 2.2. These sensors acquire the information about the vehicle surroundings with a certain level of abstraction describing objects in the scene (pedestrians, vehicles, lines). Depending on the specific ADAS function, the processed sensor data is used for warning or actively controlling the lateral or longitudinal vehicle motion e.g. by steering the vehicle to keep in the lane or executing emergency braking. Some of the limitations of these systems stem from the limited capability of the environment perception – what the car can *'see'* and react to. For example, Lane Keeping functionality only works when clear road marks are present, Emergency Breaking system is only designed to brake for pedestrians and other vehicles, but not for any other obstacle.

Vehicle environment perception is delivered by a range of sensing technologies including radars, cameras and ultrasonic due to the fact that no single modality can provide a comprehensive and robust understanding of the environment. Although radar can detect moving vehicles with a high degree of range measurement accuracy, it is not suited to detect lane markings. Hence, Emergency Braking System uses mainly radars, whereas Lane Keeping Assist is supported by cameras. Parking Assist, on the other hand, is delivered by ultrasonic sensors, which can provide short-range distance measurements to any

type of object. SAE level 2 systems use a combination of both radar and camera. The primary sensing modality used by each ADAS function is marked in Table 2.2.

Feature	Description	Camera	Radar	Ultrasonic	SAE Auto Level
Adaptive Cruise Control (ACC)	System maintains vehicle speed at a level pre-set by the driver. If it is not possible due to a slower preceding vehicle, the system will adapt the vehicle speed to maintain a safe headway distance to the lead vehicle.		✓		**1**
Forward Collision Warning (FCW)	System issues a warning if there is an impending collision with the vehicle in front.	✓	✓		**0**
Advanced Emergency Braking System(AEBS)	System issues an audible warning if a potential collision is detected. If the driver does not respond, the system applies the breaks to reduce the severity of the possible impact. New generation of systems also perform emergency braking if the vehicle is going to collide with pedestrian.	✓	✓		**1**
Lane Departure Warning (LDW)	System detects unintentional lane drift and issues audio/haptic warning.	✓			**0**
Lane Keeping Assist (LKA)	System detects unintentional lane drift and steers the car back into its lane.	✓			**1**
Blind Spot Detection (BSD)	System monitors vehicles entering the blind spot to issue a warning when the driver wants to change lanes. System also detects fast approaching vehicles from behind.	✓			**0**
Highway Assist (HA)	In highway scenario, the system controls the lane-keeping and speed adaptation task. The driver can initiate lane change manoeuvre by indication, the system will check for other vehicles in the next lane and perform manoeuvre if safe. The system is intended to be used on roads with no intersections and no oncoming traffic.	✓	✓		**2**
Traffic Jam Assist (TJA)	The system follows a preceding vehicle in a stop and go traffic. The system will keep vehicle in its lane and if no road marks are present it will follow the vehicle in front, keeping distance from the vehicles in the neighbouring lanes.	✓	✓		**2**
Intelligent Speed Limiter (ISL)	System detects speed limits signs and if the driver exceeds speed limit issues a warning. Optionally, depending on driver's selection, the system may limit the vehicle speed according to the speed limits.	✓			**0 or 1**
Parking Assist	The system measures possible parallel and perpendicular parking spots. Once activated the system controls vehicle acceleration and steering to park in free parking spot. The parking spot is defined as free space between vehicles.			✓	**2**
Remote Control Parking	The system can remotely drive into or reverse into a parking spot or garage. The vehicle needs to be centred and straight into the parking spot. The driver can intervene if necessary using remote.			✓	**1**

Table 2.2. ADAS features currently available on the market.

2.5 Off-road ADAS

Although on-road/off-road classification suggest that the off-road driving considers only off the public roads scenarios which are rarely encountered by a driver in developed countries, actually in most of the developing countries unpaved and gravel roads or poorly paved roads constitute a large portion of the public roads. According to the World Bank database [34], the percentage of paved roads in the country road network for Australia is only 43%, Argentina 32%, China 62%, whereas European Union countries on average have more than 90% of paved roads. While in Europe off-road features may not be used by the majority of drivers, they offer needed assistance for the drivers in other parts of the world.

Off-road assistance features help the driver to control the vehicle and keep vehicle progress in rough and difficult encountered while driving off-road or unpaved roads. The off-road feature range encompasses Hill Descent Control (HDC), All-Terrain Progress Control (ATPC) and Terrain Response (TR), which are described in Table 2.3. The level of automation offered by theses system is significantly lower than on-road ADAS, as mainly these systems improve traction or control longitudinal progress by monitoring the vehicle response to the terrain it is traversing.

The two new proposed systems, that are a basis of this work, are included in this summary marked in grey in Table 2.3. Both of the systems have been classified as pre-emptive, meaning that they need to anticipate terrain ahead of the vehicle. In contrast to reactive systems, which only need to react to terrain the vehicle is currently traversing. Terrain Response 3 (TR3) needs to be able to anticipate the terrain ahead to choose appropriate Terrain Response mode automatically before the vehicle starts to react to the terrain. This is particularly important on low friction surfaces; the vehicle can lose traction and ground itself before the appropriate terrain mode is selected. Terrain Based Speed Adaptation (TBSA) should be able to anticipate upcoming terrain to choose appropriate vehicle speed for safe and comfortable traversal without the need of driver intervention.

Feature	Description	Reactive	Pre-emptive	SAE Auto Level
Hill Descent Control (HDC)	System controls vehicle traction and speed to allow controlled descent in off-road conditions.	✓		**1**
Terrain Response (TR)	System adjusts vehicle chassis, transmission, throttle and breaks according to the terrain type selected. For example driving in grass and snow needs smoother torque mapping which will induce less wheel spin on a slippery surface. While driving in mud and ruts the suspension is raised to provide more height to traverse ruts and more responsive throttle to overcome wheel slip in mud. The driver can choose appropriate program using the rotary control.	✓		**0**
Terrain Response 2 (TR2)	System monitors speed, wheel slip, wheel articulation and brakes to select appropriate Terrain Response mode automatically.	✓		**0**
All Terrain Progress Control (ATPC) ***Land Rover*** **Crawl Control** ***Toyota***	System takes over vehicle longitudinal control similar to Cruise Control on road feature. The driver can select desired vehicle speed and the system will control the accelerator and breaks to maintain the speed in all conditions. The system uses information from wheel speed sensors and accelerometers fused together to determine how much power to deliver to each of the wheels and when to brake each of the wheel individually.	✓		**1**
Terrain Response 3 (TR3)	System detects the surface type ahead of the vehicle to pre-set the TR mode accordingly. In particular, this would avoid vehicle being grounded on low friction surfaces.	✓	✓	**0**
Terrain Based Speed Adaption (TBSA)	System takes over vehicle lateral control similar to Adaptive Cruise Control on road feature. The driver can select desired vehicle speed and the system will control the accelerator and breaks to maintain the speed in all conditions. The system detects upcoming terrain and adjust the vehicle speed according to the topography of the terrain ahead.	✓	✓	**1**

Table 2.3. Off-road ADAS features.

2.6 Sensors

This section will cover review of sensing systems employed in ADAS solutions, showing the key differences between sensors and their capabilities and the impact on the feature functionality. The summary of all reviewed sensors is presented in Table 2.4.

Following terms used within the Table 2.4 shall be clarified

Sensor Technology	Range	FOV	Objects classified	Measurements	Sensing robustness	ADAS applications
Radar 76GHz Long Range Automotive	120-200m	Horizontal 5° - 30° Vertical 5°	**Vehicles**	Distance, bearing, speed	Not influenced by weather	Adaptive Cruise Control Forward Collision Warning Autonomous Emergency Braking
Radar 24GHz Medium range	40-60m	Horizontal 30° - 90° Vertical 5°-10°	**Vehicles**	Distance, bearing, speed	Not influenced by weather	Adaptive Cruise Control Forward Collision Warning Autonomous Emergency Braking Blind Spot Monitoring
Lidar Multi-Beam (4 beam)	120-200m	Horizontal up to 180° Vertical 10°-40°	**Vehicles** **Pedestrians** **Generic obstacles**	Distance, object width, lateral position	Decreased range in rain and fog	Adaptive Cruise Control Forward Collision Warning Autonomous Emergency Braking
Lidar Scanning (180-360° 64 beam)	50-120m	Horizontal up to 360° Vertical 30°	**Vehicles** **Pedestrians** **Generic obstacles**	Distance, object width, lateral position, object shape	Decreased range in rain and fog	NA
Ultrasonic	2-6m	60°	**Obstacles**	Distance	Decreased range in rain	Park Assist Autonomous Parking
Mono camera	50-70m	40°-60°	**Vehicles** **Pedestrians** **Traffic Signs** **Lane Marking**	Object position in the image, from that can infer distance	Decreased detection range in low light conditions,(below 10 Lux) rain, fog	Forward Collision Warning Autonomous Emergency Braking Pedestrian Detection Traffic Sign Recognition Lane Keep Assist Lane Departure Warning
Stereoscopic Camera with Computer Vision	50-70m	40°-60°	**Vehicles** **Pedestrians** **Traffic Signs** **Lane Marking**	Object position and its distance	Decreased detection range n low light conditions,(below 10 Lux) rain, fog	Forward Collision Warning Autonomous Emergency Braking Pedestrian Detection Traffic Sign Recognition Lane Keep Assist Lane Departure Warning
Infrared	50-70m	40°-60°	**Vehicles** **Pedestrians**	Object position in the image, from that can infer distance	Decreased detection range n low light conditions,(below 10 Lux)	Pedestrian Detection

Table 2.4. Automotive sensors

2.6.1 Radar

Radar is an active sensor that emits high-frequency radio signal and registers objects based on the signal reflected back to the sensor. The relative speed of objects is measured using Doppler effect (shift in frequency between the reflected and transmitted signals) and distance to the object can be determined by the time lag [35]. Radar can reliably detect vehicles in all weather and visibility conditions as is not affected by ambient lighting and adverse weather conditions (fog, rain) [36], but it is not capable of registering other road features such as lane markings, recognising the road signs content and traffic signals state. Hence, currently, its applicability to more advanced ADAS functionality and autonomous driving is limited to detecting and tracking other vehicles.

Two types of radar are currently available in the market [37]: long range 76 GHz radar with a detection range of up to 200m and field of view up to 30° and medium range 24 GHz radar with a range of up to 60m and wider field of view up to 150°. Long-range radar is utilised in ACC and FCW, whereas medium range radar is used in Blind Spot Monitoring.

Research efforts into interpretation of the sensor data beyond vehicle detection shows promising results [38] including traffic sign detection [39], dense point cloud generation [40], [41], vehicle ego-motion estimation for localization [41], localization using SLAM [42], pedestrian detection [43]. While the research results look promising, this functionality still requires further development, it also requires potential hardware changes and needs to be proven in the industry.

2.6.2 Lidar

Lidar (Light Detection and Ranging) is an active sensor that emits laser light pulses and detects objects based on the light reflected back to the sensor. Currently, lidars have been shown to be able to classify vehicles and pedestrians [44], as well as generic obstacles [45]. Automotive specification lidars used in series ADAS applications are however more simple, usually comprising of one or two laser lines [46], which limits the application scope to detecting generic obstacles. In terms of the environment conditions impact on sensor capability, lidars are not affected by ambient lighting conditions. However precipitation, snow, dust and heated exhaust fumes have been shown to degrade lidar performance [47].

More expensive 64 beam lidars such as those utilised in the Google Self-Driving Car or Urban Grand Challenge [48], may enable real-time detection and classification of many other objects and environment features such as pedestrians, kerbs, road furniture and intersections that are required for more complex ADAS features. Lidars have been a primary sensor on the majority of vehicles in DARPA Grand Challenge allowing the vehicle to detect obstacles and drivable areas.

Although multiple beam lidar provides unmatched sensing performance, the cost and complexity of the hardware is very high, including problems with packaging, and therefore multibeam scanning lidars are

currently utilised only within the applied robotics research community and advanced vehicle prototype development.

2.6.3 Ultrasonic

Ultrasonic sensors generate high-frequency sound waves and calculate the distance to a detected object or surface based on the time between sending and receiving the signal, similar in principle to radar. Ultrasonic sensor has typically a range of up to 6 m and can provide accurate distance measurements when an array of sensors is mounted in a bumper [37]. The sensor array allows localisation of an object by triangulating the response signal received from each individual sensor. Ultrasonic sensors are common and relatively low-cost solution applied in parking assistance systems [37]. Currently, the systems based on ultrasonic sensors do not have the capability to classify the detected objects.

2.6.4 Camera

Camera is a sensor that detects the visible/infrared light reflected from the scene providing a visual sensing modality similar to a human vision system. The visual spectrum contains the information human drivers use to operate vehicles and the perception capability of the vision-based system depends on the employed image processing algorithms. Existing automotive systems are capable of classifying pedestrians [49], [50], vehicles [51]–[53], traffic signs [54] and lane marking [55] due to a range of image processing algorithms.

Although vision-based ADAS systems are versatile and offer support to a wide variety of functions, they are prone to major limitations including performance degradation under poor weather/lighting conditions and range measurements limitations. In poor lighting conditions (too low or high light levels exceeding dynamic range, an abrupt change in light levels) camera-based systems can exhibit some performance degradation, as the quality of the image decreases. Similar effects may be induced by bad weather conditions (heavy rain, fog, and snowfall) where the maximum detection range of camera-based systems will be degraded.

Currently in the automotive market, there are two camera technologies supporting forward facing ADAS applications: mono and stereo cameras. The main difference between mono and stereo cameras is that the stereo camera can provide distance measurements of all the objects within the environment, whereas mono camera infers the distance of the detected objects based on their nominal size and the object size appearing in the image.

2.6.5 Sensors summary

Perception is inherently dependent on the type of sensors used by the ADAS system. Recent developments in the area of computer vision lead to widespread use of camera systems in production vehicles. While active sensors such as lidars provide more robust and rich information set, preferred by

developers of autonomous cars such as Google and DARPA participants, they are expensive and problematic to package on a production vehicle. Other active sensors such as radars and ultrasonics provide a limited perception capability since it is only possible to detect objects such as cars, road furniture and pedestrians using these sensors. While cameras offer further perception capability due to more rich description of the scene in the visual spectrum, the type of information produced by the perception system depends on the employed computer vision methods.

2.7 Perception

Any intelligent vehicle system can be viewed as composed of three conceptual modules: sensing, planning and acting. The vehicle interacts with the physical world, but it only has access to the information about this world through the measurements obtained from the sensors. Interpretation of the sensors' measurements to provide necessary information to plan vehicle actions is the task of perception. Without perception, any automated vehicle system would not be able to take actions. In this work, the perception will be referred to as a process of acquiring sensor data and processing it to acquire relevant information about the environment. More precisely the definition is:

"Perception is the process of transforming sensor measurements into a world model" [56]

From this definition, the perception can be further broken down into three areas:

- World model – How is the world represented? What attributes of the environment should the vehicle know about?
- Sensor measurements – What is the sensor actually measuring?
- Transforming sensor measurements into a world model – How to process sensor data to extract the required attributes of the environment?

The posed questions do not have single answer because what the vehicle needs to know about the environment depends on the specific task. The requirements are posed on the perception system by the expected functionality of ADAS and the scenarios in which the system should operate. For example, ACC modulates the vehicle speed based on the presence of other vehicles; hence the perception system needs only to detect vehicles. However, since the system operates at highway speeds, the perception needs to provide sufficient range, hence long-range radars are used.

A conceptual processing model of ADAS system adopted from [57] is presented in Figure 2.2. The *world model* is an explicit representation of the world and consists only of a subset of semantic objects based on which the vehicle is controlled; it is an interface between the sensor and control component.

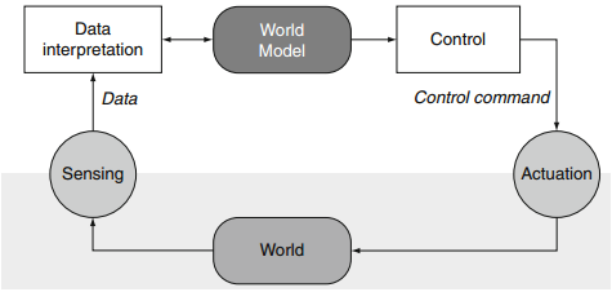

Figure 2.2. Abstract representation of ADAS system [57]

Existing ADAS systems have limited understanding of the environment. The *world model* is built based on the existence of objects such as vehicles, pedestrians and obstacles, complimented by lane marking and traffic signs. Such a limited representation of the world with the assumption that the vehicle is travelling on a road is sufficient to provide existing on-road ADAS functionality described in section 2.4. However, highly automated driving will require a richer description of urban scenes [16], as the car cannot be expected to travel only on roads with road marks; semantic description could include road surface and road boundaries including kerbs, grass verges and railings.

Current semantic representation of the world is of very limited use off-road, where the topography and the condition of the terrain have primary impact on the vehicle behaviour. None of the classified objects describes any attribute of the terrain. To illustrate this point Figure 2.3 shows environmental representation obtained from the automotive stereo system in urban (left) and off-road (right) environment. In urban scenario, system detects vehicles (blue), pedestrians (red), generic obstacles (green) and lane marking (green). In off-road environment, the only classified objects are obstacles (green). Note that not all of the obstacles are detected, as some of the bushes and trees do not conform to the obstacle model that the system employs. This highlights the limitation of the on-road perception system, which makes assumptions about the structure of the environment, which does not hold off-road.

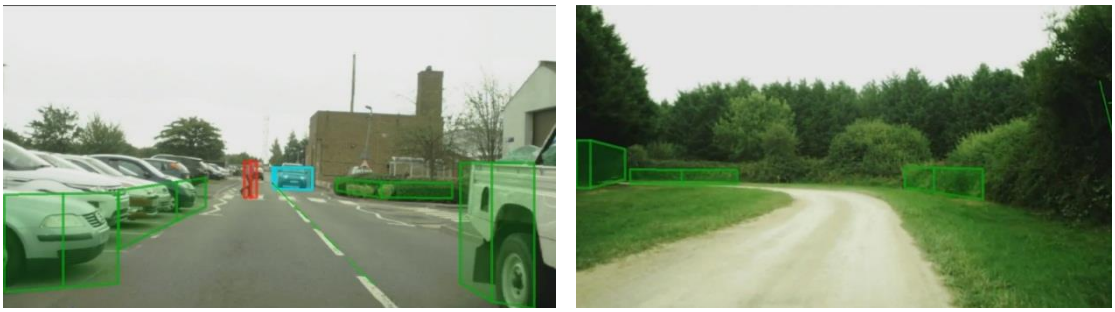

Figure 2.3. Automotive supplier stereo camera object detection – urban scenario (left), off-road scenario (right).

3 Off-road perception

This chapter presents related work in the domain of off-road perception. Off-road perception is of most interest in robotics community, as the majority of the proposed systems and methods were developed for autonomous navigation of unmanned ground vehicles.

3.1 Off-road robotic systems

Perception in off-road context is a complex problem and has been researched for various applications ranging from planetary rovers, search and rescue robots and autonomous off-road vehicles. There is an increasing interest in the development of autonomous systems that can operate in difficult unstructured terrains to limit human involvement especially in search and rescue scenarios or military operations. Mobile robots development has been a major contributor to the development of perception systems in unstructured terrain. The most notable autonomous platforms that showed the capability of sensing platforms include DARPA Grand Challenge vehicles and Mars rovers [6], [58]–[63]. These systems operating in wide variety of environments need tackle three main problems: assessment of terrain traversability, path planning and actually performing the required manoeuvres. This review will focus on the perception and the way the sensor information is processed to provide meaningful abstracts that describe the terrain in terms of surface type, surface roughness, obstacles, slopes and other terrain features that will affect not only traversability but also the vehicle speed. We review the literature with the aim of classifying and analysing the proposed approaches with respect to identifying terrain features of interest that affect the vehicle progress and the vehicle the speed.

One of the most prominent showcases of the application of off-road sensing for autonomous navigation has been the DARPA Grand challenge competition organised by U.S government in 2005. The aim of the competition was for an autonomous vehicle to traverse a predefined route in the desert and only five vehicles completed the route. The vehicles have been equipped with a range of sensors including Velodyne lidars, laser scanners, stereo and mono cameras, accelerometers and GPS to provide a sensing horizon which would allow high speed driving [5], [64]–[66]. In addition, digital maps of the road network with complimentary aerial images were provided to all the teams. It is worth noting that all of the vehicles that completed the course used laser range finders to detect obstacles, surface roughness and road, aided by the vision systems to detect drivable path, or to extend the range of perception as demonstrated by the self-supervised monocular road detection in desert terrain [67], [68]. The systems focused on detecting the road surface and identifying roadside obstacles, as the vehicles were following a known route, with the assumption that the road is always traversable. Hence the problem was simplified to find and navigate on an unstructured road. The approaches to the road detection considered using colour descriptors and a self-learning classifier [67], ant colony optimisation for road boundary detection [69], region based growing with the use of texture descriptors to extract path boundary. The emphasis

of the obstacle detection algorithms was to apply geometrical constraints on the returned lidar signal. Due to the fact that multiple lidar scans had to be aligned the majority of the approaches focused on estimating the vehicle state and aligning laser scans and not on analysis of the terrain geometry or surface roughness. Similar systems using laser scanners are used in on-road autonomous vehicles.

Although the systems presented during the competition showed off-road terrain sensing capability, the application of these systems is limited in the automotive domain, since they use bulky and expensive laser scanners such as Velodyne lidar. Stanley, the vehicle that won the competition is shown in Figure 3.1, with a range of lidar mounted on top of the vehicle. Due to the fact that autonomy in off-road scenarios has been successfully shown, the impression may be that the off-road perception task has been solved. However, this is not the case in terms of onboard sensing for automotive applications, where the exact map of the environment is unknown and the sensor set is constrained to vision and radar sensors. The lack of cost constraints on the autonomous vehicles such as presented in DARPA Grand Challenge [4], [5], [62], Google [70], Oxford Labs [71], the availability of highly accurate GPS and/or point cloud maps and extensive sensor suite led to solutions that are not currently directly applicable in the automotive domain.

Figure 3.1. Stanley – the vehicle that won DARPA Grand Challenge in 2007

Another program sponsored by DARPA which focused on the development of planning and perception modules for autonomous ground vehicles was Learning Applied to Ground Robots (LAGR) [72]–[75]. Within this program, a hardware platform has been standardised and consisted of a small ground robot equipped with two sets of stereo cameras, accelerometer and GPS sensor. These program has led to a progress of a stereo and monocular based sensing, especially extending the range of sensing by learning the short range information from stereo images and propagating the information onto monovision images. A majority of the proposed solutions rely on the obstacle detection in the short range and build a visual model of a path to detect drivable surfaces in the far range [76], [77], [78]–[80] as the scenarios on which the platforms were tested always consisted of a drivable, flat path. These solutions are not also directly applicable in the automotive domain since the problem of off-road driving cannot be simplified to avoiding obstacles, but rather quantifying the features of the challenging terrain so that the vehicle systems can be adjusted appropriately.

3.2 Terrain traversability

The problem of terrain traversability considers the ability of the vehicle to negotiate a particular terrain. Terrain constitutes the material that comprises the surface as well as the geometry of the surface [81]–[83] and both of these factors affect the performance of the vehicle on the terrain. According to Shoop trafficability is "*the ability of the terrain to support and provide traction for vehicle operation*" [83] and the field of terramechanics studies interaction between the soil and the vehicle. Trafficability is influenced by many factors, most important being soil strength, soil composition and the ambient conditions (temperature, moisture) [84]. The mechanical properties of different surfaces vary considerably under a range of environmental condition e.g. dry soil has different traction that the same surface after the rain. In addition the surface characteristic may vary depending on the depth, the top layer may be loose such as gravel track, but underlying surface may provide traction, whereas for grass surface the opposite is true; the top layer of grass may provide traction but once the grass is damaged the soil/mud underneath may induce wheel slip. In the view of the research on the trafficability, currently only limited number of methods that enable robust remote sensing of the soil composure has been shown in the operation of Mars Rover [59]. This includes thermal inertia measurements through multispectral imaging and the use of ground penetrating radars. These methods, however, require specialised sensors and typically are not real time. More traditional methods for measuring soil parameters involve the use of measurement tools directly inserting in the soil such as bavemeters, cone penetrometer or engineer crowbar [83]. Research conducted in the field of off-road vehicles and autonomous robots provides a multitude of methods for an approximate terrain characterisation through the measurement of the vehicle response to the conditions e.g. measuring wheel slip, vibration or wheel sinkage. In particular, most popular methods classify terrain type into a number of predefined classes e.g. tarmac, packed gravel, soil using unsupervised or supervised learning methods [85]–[87]. In work by DuPont [88] the acceleration of the vehicle body with neural networks is used to create terrain signatures that are used for vehicle navigation. Also Iagnemma proposed to use the vibration of the rover suspension measurement to classify the terrain traversability [89] and in his later work proposes use of camera system mounted near the wheel to measure wheel sinkage [90][91]. The limitation of proprioceptive sensing methods is that that the vehicle is already traversing the terrain which is being classified. This means that the changes in the terrain are not anticipated and when travelling at higher speed the vehicle may sustain damage before any action is taken.

Looking at the perception problem from the point of view of identifying relevant terrain features which may be traversable but will affect passenger comfort e.g. a rough patch, a step or a rock, differentiates this problem from the largely researched problem of classifying environment into traversable/non-traversable class. Historically, traversability has been a binary problem, when the area around the vehicle has been classified into traversable/non-traversable regions and the vehicle path has been planned accordingly [92]. Non-traversable regions are classified as obstacles, typically defined as steep slopes, tall

objects and ditches [93], [94], [95]. The complexity of the off-road scenes led also to classification approaches focusing on detecting specific terrain hazards such as water [96] and slip hazards (e.g. grass surfaces , sandy slopes) to aid the navigation of the robot.

More recent approaches has identified the limitation of binary traversability classification and introduced continues traversability scores which take into account either surface appearance, roughness estimates, location of water bodies and obstacles [93], [97], [98]. Howard and Seraji [93] introduced traversability index with fuzzy logic which quantifies the difficulty of the terrain based on its physical properties such as slope and roughness. In this approach the vehicle speed is (low/high) is associated with the difficulty of the terrain (low/high index). The traversability index concept has been further employed in many studies considering autonomous vehicle navigation [94], [99]–[101].

The world model created by most of the robotics system considers the navigation problem as finding least cost path, where the cost is defined by terrain characteristics such as surface type, surface roughness, obstacles and slopes. The resulting world model is a cost map with associated traversability index. The weighting factors of different terrain characterisations are either manually tuned to achieve target vehicle behaviour [98], [102], [103]or learnt from expert behaviour [104]. Traversability estimation from perception perspective requires knowledge of the robot physical limits and experimental or simulation based adjustment of the cost function used to derive the traversability map.

The most dominant research streams in the analysis of local traversability consider the geometry of the terrain and/or appearance of the surface. Various geometry based approaches create a 3D representation of the scene that corresponds which is analysed to identify drivable terrain, obstacles and other relevant terrain features [98], [105], [106]. Appearance-based methods, on the other hand, rely on the visual appearance of object and surfaces. Traversability can be assessed using visual cues such as colour and texture either to classify terrain type, identify obstacles, identify water bodies or find free space.

At this point it is worth mentioning that in this work, the traversability of the surface to provide a decision of go/no-go is not considered. The interest of this work driven by the application is two-fold: classification of terrain type based on visual features for improvement of terrain response and terrain geometry identification for the purpose of speed adaptation. Further review of the methods and world models employed for traversability analysis will provide an understanding if some of the proposed techniques could be adapted for proposed applications.

3.2.1 Local vs global maps

General direction of the autonomous research is to build a map of the environment to align multiple sensor readings and then use it for path planning purposes. This is the idea behind Simultaneous Localisation and Mapping (SLAM) which is extensively used by state-of-the-art systems such as Oxford

Autonomous Car, Google Car, next generation of Mars Rovers. In particular, perception is achieved through a previously build environment map and the vehicle tries to localise itself within the mapped environment. State-of-the-art systems propose also the semantic classification of the build maps into traversable/non-traversable regions [107], urban semantic classes and surface maps. Although SLAM achieves long range sensing capability through maps created prior to the vehicle deployment, it is not realistic to expect 3D environmental maps for all the off-road environments to be used for in-vehicle sensing. Existing automotive solutions focus on local sensing as the environment may change quickly, and no map information is needed for the majority of ADAS systems where the driver directs the vehicle. Hundelshausen [108] argues that instead of using SLAM approaches a local understanding of the environment and path planning using 'tentacles' is sufficient to drive in unknown terrain. This approach has been successfully employed in urban and non-urban environments in DARPA urban challenge and Elrob competitions [108].

While lidar measurements may need a SLAM approach in order to align the measurements from multiple scans even to create only a local map, the stereo-vision provides a static map of the environment with each frame. Hence as argued by Hundelshausen [108] a single frame local map may be sufficient to provide enough information about the environment.

3.2.2 Geometry-based methods

The majority of methods obtain a geometry of the scene through a 3-dimensional point cloud, which is then processed to obtain information about surface roughness, slopes and obstacles. The creation of the geometrical representation of the terrain can be achieved through a variety of sensors including lidar, stereo cameras and time of flight cameras. The scene is represented by a dense 3D point cloud where depth measurements are converted into 3D world coordinates. These methods have been successfully employed in Mars Rover systems, LAGR and DARPA challenge [6], [60], [62], [108].

Processing methods of the range data can be split into two groups: methods directly processing point cloud to extract regions of interest and methods that build a more compact representation of the world which is then processed further. Methods that process directly point clouds extract regions and objects of interest such as flat ground planes, obstacles, non-traversable regions. Methods, which build a more compact representation of the world in a form of Cartesian grid maps, use this intermediate representation to assess terrain geometry, slopes, surface roughness, detect both positive and negative obstacles in order to assess traversability.

Processing the point cloud directly aims at extracting semantic representation of the environment. The semantic representation differs depending on the application and robot capabilities. For example, robots may not be able to traverse height differences of more than 10 cm or cover a slope steeper than 15 degrees, hence these areas can be classified as obstacles. In robotic applications, semantic representation

will include obstacles, non-traversable areas, flat surfaces, rough surfaces. Lalonde [109] classifies the environment into *scatter* (foliage, grass), *linear* (tree trunks, wires) and *surface* (ground) based on the point cloud statistics building a Gaussian Mixture Model and using Expectation Maximisation for classification. Similar classification methods on the point cloud data are used to segment drivable or ground areas in work by Navaro [107]. Larson [110] detects negative obstacles directly from lidar point clouds using Support Vector Machines. Ballone [111] proposes a novel Unevenness Point Descriptors to identify roughness of the terrain, which can be used for assessment of traversability. These methods are computationally expensive and do not provide a medium level description of the terrain geometry including slope measurements.

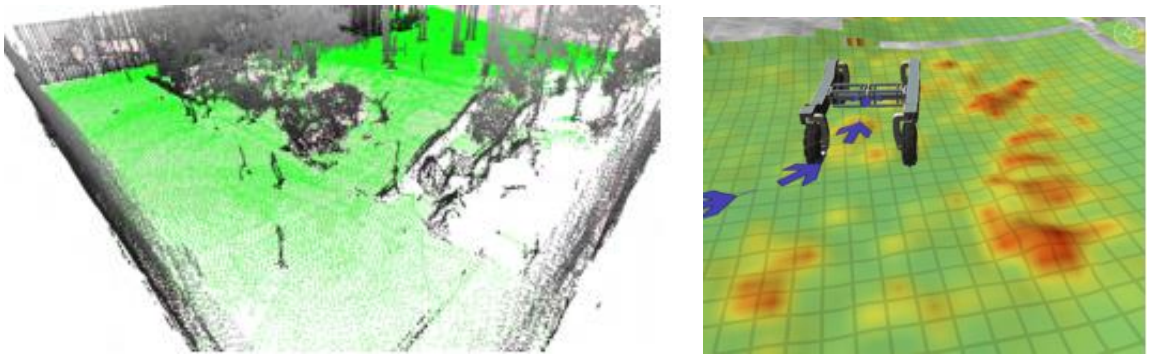

Figure 3.2. Left - Point cloud classification showing green points classified as ground [109]*. Right – traversability map, red indicates higher traversability cost based on slope and roughness* [112]*.*

In order to reduce the amount of data that needs to be processed more compact representation of the data has been proposed such as Occupancy Grids [113]–[115], Digital Elevation Maps [116]–[118], Multilevel Surface Maps [119]–[121] and Octo Maps [122]. In contrast to the raw set of 3D points, these methods provide a compact representation (Cartesian grid) with explicit connectivity between adjacent grid cells. Reducing the data representation from multiple points to a grid, reduces the required processing and the explicit connectivity between the cells enables grouping of adjacent cells into objects.

A 2D grid map introduced known as an occupancy grid, uses the discrete values for each cell assigning a class of obstacle, free space or unknown [113] [123] or a probability of occupancy [114]. Such a world model assumes that the free unoccupied space is drivable and is used for path planning. 2D representation known as Digital Elevation Maps holds only elevation values for each grid cell. This representation is not sufficient in the off-road environment where slope and the height variation of points within the cell may provide an indication of the terrain. 2.5D representation such as Multi Level Surface Map can hold attributes of the terrain such as height, roughness and slope information. This representation has been widely used to navigate in unstructured terrains to navigate around perceived hazards such as rough surfaces and steep slopes [98], [124], [101], [94], [125], [126], [127], [128], [129], [130]. Full 3D voxel occupancy maps describe occupancy of the environment as a 3D cell. 3D voxel map required considerably more memory and is more computationally complex to process. The 3D voxel maps are used for robots that need to navigate avoiding obstacles in all dimensions such as

submarine or flying robots [131], [132]. Most of the ground robots use 2.5D approach, which holds much more information than 2D map or occupancy grid, but is less complex than voxel maps.

Macro terrain features usually pose a risk to the robotic vehicles. Hence the traversability analysis assigns a cost based on the inclination of the surface and the vehicle constraints are used to adapt the cost map weighing depending on the physical capabilities of the platform to traverse slopes, step edges and obstacles. In these approaches macro terrain features are not directly identified but rather described in terms of cost. These approaches are validated based on the robot system performance of safe traversal slopes [98], [124], [101], [94], [125], [126], [127], [128], [129], [130].
Other methods propose to identify and classify objects such as positive and negative obstacles [133]–[135], tree trunks [124], tree lines [109], excessive slope [98], low overhangs [98], and water bodies [96], [136], which are treated as non-drivable surfaces. Most methods apply thresholds to the terrain slope, plane fit residual representing roughness, and elevation standard deviation representing spread of points in the grid map to classify the terrain as ground, obstacles and unknown.

3.2.3 Disparity-based methods

Disparity-based methods aim at processing disparity maps obtained from the stereo system without the need to compute point clouds. The advantage of this approach is that the processing is significantly reduced. The disparity based methods are used mainly for obstacle and path detection. With the assumption of relatively flat road area, any obstacles can be detected using V-disparity representation as proposed by Labayarde [137] and further extended by Broggi [65], Caraffi [106]. Since the actual geometry of the scene is not recovered using disparity, these methods are limited in their application to obstacle detection. Furthermore, the assumption of relatively flat road area, limit the application of these methods in more severe off-road environments.

3.3 Vision-based Terrain Type Classification

Terrain classification approaches proposed in the literature are mainly used for autonomous robot navigation to asses if the robot can traverse a particular surface or to adjust wheel speed and torque to improve traction in unstructured environments [60], [74], [138], [139]. The main advances in this field in recent years can be attributable to the development efforts for the Mars rover robots [60], [138] as well as unmanned ground vehicles (UGVs) for military purposes [74]. These approaches consider visual based terrain classification as a complementary recognition scheme to vibration analysis and range data classification. This is important to note as the range data provides valuable information about the structure of the scene such as obstacles ahead and the surface roughness. These features can improve classification performance in comparison to the purely visual based classification as some surface types may be difficult to distinguish based on their visual features e.g. sand and soil [140].

Colour-based methods are incorporated into almost every terrain classification method presented in literature, as they are computationally inexpensive. Colour classification is however challenging in outdoor environments as perceived surface colour depends on sensor type, lighting conditions, weather conditions and viewing angle [141]–[143]. There is no agreed colour model or colour space which is best suited for terrain recognition task and the methods proposed in literature use different colour descriptors depending on particular application [143]. Even when considering multiple terrain classification problem approaches differ significantly - Manduchi [134] and Jansen [144] proposed colour classification in normalised RGB colour space with Gaussian Mixture Models, Dima [145] classifies image patches in LUV colour space using first order statistics of colour content, Angelova [140] uses RGB histograms with hierarchical classifier. The choice of colour descriptor depends on the complexity of problem, number of classes and additional features used for classification such as texture or 3D structure information.

Texture-based methods analyse local variation in pixel intensity which correspond to texture of the surface. In general texture based methods are computationally expensive but prove to be effective for terrain classification for close range images [91], [140]. Work by Castano [146] exclusively deals with texture classification in outdoor scenarios. He proposed to use Gabor filter banks with Gaussian Mixture Model to four model terrain classes: soil, trees, grass, sky. The method was tested on a data set containing only 18 images and the reported classification performance was in region of 65%. Castano [146] notes that classifier of such a performance may be used in conjunction with other colour or range based classifiers. Also run time was not stated in the paper, however it is well known that filtering image with bank of Gabor filters is computationally expensive with high memory requirements [147].

More recent work by Mioulet [148] shows real-time implementation of road type classification using Gabor filters, however this real-time performance is achieved by specialised hardware designed solely for the purpose of fast image filtering using Gabor filters. Most of the terrain classification methods presented in literature are in the domain of autonomous robot navigation. In most cases it is a small robot with the camera viewing the surface within a small distance providing detail information [79], [134], [145]. The difference is that texture features are stronger in images at close range than when viewed from further away [140], [143]. Angelova [140] shows that classification performance using texture drops from 76% for image regions closer than 3 m to 65% for image regions which are further than 3 meters from the camera. Similar findings are reported also by Batlle [143]. Similarly methods proposed for SUV based autonomous vehicles as in Dahlkamp [67] or Jansen [144] focus on the colour features as usually the camera is placed further away from the surface providing less detailed view.

3.4 Roughness

In robotics roughness assessment is primarily used for navigation an path planning purposes. In work by Seraji [93], [102], [149] the traversability score is assessed based on the slope and roughness. However

roughness is assessed based on number of rocks and classified in one of the fuzzy levels (low, medium, height). More granular surface roughness assessment is based on the deviation of the points from the fitted plane in the cell in a Surface Map. This type of roughness metric has been extensively used for traversability assessment [98], [124], [101], [94], [125], [126], [127], [128], [129], [130]. All of these approaches, however, use the roughness estimate to identify potentially hazardous regions so that the robot can plan its path avoiding these areas. Most of these works do not validate and link the roughness descriptor with vehicle response but rather identify the hazard regions to be avoided. In addition, the limitation of calculating local roughness score in a single patch is that the traversal of multiple map cells affects the vehicle response as traversing two consecutive smooth patches which have a vertical offset (e.g. a kerb) will generate impact on the vehicle but will not be detected by such a metric. Work by Loh [112] addresses this problem by analysing the local neighbourhood of the cells. The roughness metric considers the surface residuals and the height differences between the neighbouring cells. Again this approach is limited in terms of analysis of the impact on the vehicle, as the map is used to avoid hazardous terrains. Bellone [111] proposes an Unevenness Point Descriptor (UPD) derived directly from the raw point cloud data by calculating the surface normal for each point and looking at the differences of surface normals. This approach addresses the deficiencies of previous approaches for the purpose of path planning. However it does not discuss or validate how the roughness metric is correlated to the vehicle response. Dragazany [103], [150] uses a combination of UPD with visual superpixel segmentation to classify the traversability of the surfaces. These roughness descriptors provide indication on potential hazards, so that the vehicle can choose the most optimal path. None of these descriptors, however, considers the actual response of the vehicle in terms of acceleration and vibration levels which would affect passenger comfort.

3.5 Roughness in road maintenance and vehicle dynamics

In on-road applications road roughness can be described as an elevation profile along the vehicle wheel tracks which the vehicle traverses. Since road profiles can be described as random signals, the descriptor can be the profile itself or its statistical properties [151]. Road profiles can be measured through a range of instruments including profilometers, lasers, portable inclinometers and ultrasonics [152]. A road profile represents elevations along a longitudinal direction of travel, usually measured along two lines per lane of the road. The profiles need to be further processed to extract the information that describes the surface roughness.

Road maintenance applications and vehicle durability simulations often use International Roughness Index (IRI) [153] and Power Spectral Density (PSD) [152]. In road maintenance application this indices are used to characterise the state and quality of road networks [154]. These indices are also used as mathematical models to simulate the road profiles employed in the vehicle durability and dynamics simulation studies [155]–[157].

A popular indicator of surface roughness the International Roughness Index (IRI) originally developed in 1986 is measuring a response of a quarter-car model to road profile at a nominal driving speed of 80 km/h. The quarter-car simulation was a theoretical representation of the nominal vehicle when the IRI was developed [154] [158]. The IRI value is determined by processing the measured profiles and accumulating the suspension displacement of the quarter car model characterized by suspension damping rate, suspension spring rate, tire spring rate, sprung mass and unsprang mass. The IRI is influenced by a frequency range of 10-12 Hz and measures vehicle body response but is not the optimal indicator to measure the ride comfort in terms of human body vibration as concluded by [159]–[161] and [154]. IRI is a convention due to the dynamic properties of the car that are defined by the standard hence is not correlated to the parameters of the real vehicle used in experiments. Moreover, IRI is a numerical index that was designed to summarize the roughness of the road surfaces over entire road networks and long road distances. IRI summarizes that impact of the model vehicle response, but it may not be the optimal roughness descriptor for other applications.

ISO standard 8608 "Mechanical vibration - Road surface profiles - Reporting of measured data" [162] describes a method of reporting measured vertical surface profile with use of Power Spectral Density (PSD). The PSD represents spectral components that are proportional to the square of the sines amplitudes represented in the road profile. Since the ISO Standard 8608 refers to characterisation of road network it requires kilometres of elevation data with high resolution (usually 1 cm), hence the method of reporting the surface roughness cannot be directly applied to data measured with stereo camera. Several studies interested in impact of road roughness on passenger comfort indicated that with increased PSD of the surface and increased vehicle velocity passenger comfort decreases [159]. Passenger comfort was measured using the weighted mean-square acceleration amplitude as prescribed by the ISO standard 2631-1 [163], which describes how to quantify impact of vehicle vibration on comfort. Therefore, PSD was investigated in this work as a roughness descriptor.

3.6 Ride quality comfort

Ride quality is an important factor in the driver's experience especially in off-road conditions where the terrain is uneven causing more vehicle vibration than in normal on-road conditions. Ride perception is influenced by a number of factors such as surface unevenness causing vibration, noise and vibrating elements in the vehicle, friction, lighting conditions [151]. It is the unevenness of the road in the longitudinal direction that has been identified as a major parameter associated with poor ride quality [164][165]. As discussed by Gillespie [151], when the vehicle traverses the surface, the road unevenness acts as a vertical displacement input to the wheels, therefore exciting the vehicle vibrations. The resulting level of vibration within the vehicle depends on the magnitude and frequency of the surface height displacements, the vehicle suspension response characteristics and the vehicle speed. Most of the

literature states that the road roughness is the most significant factor with respect to the driver perceived ride quality [164][165].

Ride quality has been associated with a range of frequencies described in ISO standard 2361-1 "Mechanical vibration and shock - Evaluation of human exposure to whole-body vibration" [163]. The passenger comfort is affected by the frequencies of 0.5 Hz and 80 Hz and the ISO standard prescribes the use of weighted acceleration based metric as the basic evaluation of vibration for a seated person, which occurs in all six axes on the seat. The ISO 2361-1 defines the weighting filters to apply to the data, providing more emphasis to the vibration frequencies, to which humans are most sensitive. The frequency weightings Wk(f) for vertical axis was used in this work to asses passenger comfort. ISO states that the proposed evaluation procedure provide means to estimate from vibration (magnitude, frequency and direction) its likely effects on comfort. Hence, the proposed metric can be used to assess relative passenger comfort and adjust the vehicle speed to minimize the vibrations which will affect the comfort. The details including frequency weighting are described in detail in the ISO standard.

3.7 Application - vehicle speed selection

Autonomous off-road vehicle speed adaptation mostly considers minimising hazards of vehicle damage or immobilization. Desired vehicle speed can be determined based on the obstacles ahead of the vehicles [124], water bodies [98] and ditches [166]. Although the identification of these terrain features might be sufficient for low-speed manoeuvring, when considering high-speed off-road driving surface roughness should also be considered. Vehicle traversing rough off-road terrain is subject to vibration and shock and various studies have shown that the effect of shock can be detrimental to the vehicle [85] and affect passenger comfort [162]. With the increasing number of applications of unmanned robotic vehicles [64], [167], [168], surface roughness is considered as a hazard where avoidance behaviours are employed [60], [169]. Other methods propose to manage the vehicle speed to minimise excessive shock to the vehicle on rough surfaces [170]. Within the literature, the speed selection methods can be classified into two groups – reactive and pre-emptive. In the reactive mode, the vehicle only reacts to the terrain conditions and adjusts the speed, whereas in the pre-emptive mode the vehicle senses the terrain ahead and adjust the speed before the vehicle reaches the terrain.

3.7.1 Reactive speed selection

Reactive speed control uses proprioceptive vehicle sensors and adjusts the vehicle speed based on the vehicle state (vibration, speed, etc.). Speed selection can be dependent on a shock, vibration experienced by the vehicle [168], [171], [172] or be terrain class dependant. Thrun [64] proposed a method for speed selection based on the vehicle state (pitch estimate and vertical vibration of vehicle frame). Based on the derived linear relationship between surface roughness and the vehicle allowable speed, the system recommends the vehicle speed. Extension of this work is a reactive algorithm [170] which slows the

vehicle down when a high shock event is detected based on a supervised learning technique, where the shock threshold and acceleration rates are derived using machine learning.

The speed selection systems proposed for autonomous vehicles consider the shock and possible damage to the vehicle, whereas systems used in passenger vehicles consider passenger comfort as a input to the control system. Kelly [173] proposed a system for adaptive speed control of 4x4 passenger vehicle which accelerates and slows down the vehicle dependant on the passenger comfort metrics derived from vehicle excitation including vibration, lateral acceleration, roll and pitch angles. This work is the basis of the reactive Terrain Based Speed Adaptation method.

These methods require the vehicle to traverse the terrain before a speed selection can be made. When considering high-speed vehicles this is undesirable since interacting with a rough terrain could cause severe and immediate damage or discomfort if the speed of the vehicle is too high in situations where the terrain type changes suddenly, the inclination of the terrain changes (steep slope) or vehicle encounters discrete terrain features such as ditch or rock.

3.7.2 Pre-emptive speed control

In literature, there are few works that analyse both the traversability and assess the navigation speed. Most of the pre-emptive methods focus mainly on the derivation of the best possible path but do not consider the vehicle speed, as the vehicle speed is either very low or pre-set based on the previous knowledge of the route. The early work that considered the vehicle speed assessment was the fuzzy logic traversability assessment by Seraji [149] used for planetary rovers. Vehicle speed selection considered three levels (low, medium, high) dependent on the combination of roughness and slope. A similar approach to speed selection using fuzzy logic was also proposed by Sezer et al. in [174] where the speed selection was based on the proximity of the obstacles and the direction of vehicle travel. In Tunstel's [99] work the speed selection was proportional to the traversability score. The main limitation of this work is that the surface roughness was assessed based on the visual features and mainly focused on detecting rocks, as the intended use was planter exploration where the variability of the terrain types is low. Another limitation of these approaches is that conservative navigation regime, which will consider most of the terrain features as hazardous and try to find the safest path. When considering off-road driving in a passenger vehicle, the route of the vehicle can contain steep slopes and very rough surfaces which are not catered for by these approaches.

The most similar work to the one presented in Chapter 8 is work by Stavens and Thrun [64][175][170] where the vehicle speed is selected based on the surface roughness measurement obtained with the laser scanner. The pre-emptive speed determination was however not implemented on the original DARPA Challenge vehicle, but rather this work retrospectively analyses the data showing that the pre-emptive

roughness measurement would allow the vehicle to complete the route faster and limit the number of high shock events experienced by the vehicle.

El-Kabbany [167] proposed a technique that correlates the terrain geometric properties and the vehicle response (vertical acceleration) to determine the maximum speed based on a roughness score. This work extended by Wilson [176] uses a geometric terrain identification technique where a range sensor captures a 3D terrain point cloud and uses the standard deviation of the terrain point elevations to determine a roughness score. The point clouds in this work were constructed by concatenating multiple measurements, where measurement errors can be introduced if the vehicle state estimate is not accurate. Another limitation of this work includes the assumption that the vehicle is not subject to linear or angular accelerations due to throttle or turning control, which limits the application of this technique in real-world conditions where the vehicle will very rarely travel at a constant speed. Although this work shows that it is possible to predict the vehicle vertical acceleration from the input terrain profile, the authors note the limitations of this technique due to the 3D point cloud measurement system and the prediction of only vertical acceleration. The predicted z-acceleration is on the suspension and not on the vehicle frame which will affect the occupants of the vehicle. The work also does not cover any experimental validation on a real vehicle.

In a similar manner, Dubey [177] proposed an approach that incorporates the relation between the shock experienced by the vehicle, the vehicle's speed and terrain roughness as a cost in a local planner for autonomous navigation. Surface roughness is measured from a point cloud using Difference of Normals approach. The results show that the commanded speed for rough surfaces is slower compared to a baseline path planner, however, this work does not provide any comparison of the commanded speed and the vehicle response, hence the results do not show if high shock events could have been avoided.

3.8 Differences between robotics and automotive

As discussed in Section 2.7 perception of the environment is task dependant and within robotics community the task of the robot is to autonomously navigate in unstructured environments. Navigation in unstructured environments from perception perspective is simplified to find a path that minimises the cost of traversal in term of safety, stability, traversability or energy consumption. The vehicle chooses a least cost path where hazards such as slopes, rough surfaces and terrain classes obtain high cost. In the ADAS domain, where the driver is always in control of the vehicle, the driver may choose to drive over a steep slope or rough terrain; hence the task of. ADAS systems encompass considerations regarding the involved human factors such as passenger comfort and safety measures. Accounting for the factors that affect human driver and the effect of human driver on the control of the vehicle is what differentiates ADAS and robotic systems. These consideration drive a different control strategy, which in turn requires a different perception system.

While no commercial solutions offering off-road perception capability exist, there is a vast amount of research conducted in the area of robotics that deals with the perception of unstructured environments. The literature review pointed to number of potential solutions, however, limitations of the applicability of existing methods for off-road ADAS applications were found:

- Off-road perception systems in robotics are mainly deployed for the purpose of autonomous navigation. The perception methods are used to assess traversability of the terrain, to establish a safe path for the vehicle. The goal is to navigate around hazards, whereas in proposed ADAS applications the driver is in control of the vehicle. The driver may decide to drive through any surface and object, hence the purpose of this work is to model the world with set of attributes that are applicable for particular ADAS and not assess the traversability of the terrain.

- The off-road perception solutions proposed in the literature vary with the sensor set employed hence it is not possible to establish if similar results can be achieved with a stereo camera. A particular sensor of choice in robotics is high precision lidar, which as discussed in Section 2.6.2 provides very accurate and dense description of the environment. Stereo cameras are more limited in terms of detection range and field of view as discussed in Submission 2 [178].

- Standardised performance evaluation is uncommon in the field of robotics since each system is developed for a different application with a different sensor set. Therefore, it is difficult to compare published results and to establish the validity of proposed solutions to the particular requirements of the system proposed in this work.

4 Approach

This research was a part of off-road feature development undertaken within Jaguar Land Rover. The lack of available off-road perception capability was a limiting factor in intended feature development. Although vision sensors could offer a potential to deliver off-road perception capability, there was a need to establish how attributes of the off-road terrain could be sensed. It was necessary to develop a proof of concept system in order to understand if the requirements posed by the ADAS on the perception system can be fulfilled to deliver intended feature functionality. In order to deliver the expected perception capability and asses its performance, the following approach was taken, as illustrated in Figure 4.1. The project can be viewed as two independent stages, since the perception system was tailored to the needs of two different off-road ADAS applications. As introduced in Section 2.5, these were Terrain Response 3 (TR3) and Terrain Based Speed Adaptation (TBSA).

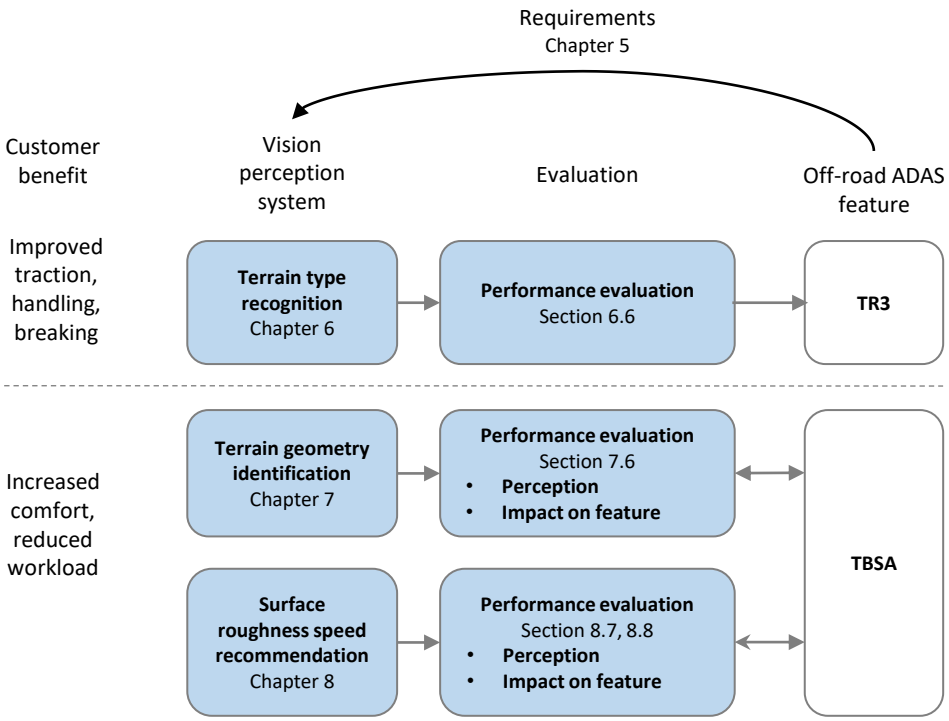

Figure 4.1. Overview of proposed approach

TR3 is intended to improve traction handling and braking by applying terrain dependant vehicle settings which affect throttle response, gearbox settings and ABS. In order to improve performance of the automatic mode selection, the perception system should detect pre-emptively low friction surfaces such as grass and snow. More detailed discussion on the perception requirements posed by the ADAS system follows in Section 5. Based on the requirements a terrain recognition method was proposed and is described in detail in Chapter 5. The study aimed at developing a real-time method for grass detection. The terrain type was narrowed down to grass, due to methodological constraints of capturing a representative data set of snow conditions. The availability of snow conditions in test facilities in UK was limited and the cost of testing abroad was prohibitive at the initial stage of the study. The

performance of the method was evaluated on a diverse set of off-road and on-road scenarios in order to understand if the proposed method can cope with variety of different terrains and illumination conditions.

Commercial conditions had an impact on the change of study direction. Within the automotive industry, the choice of sensors is mainly driven by the trade-off between cost and the capability to support multiple ADAS functions. During the course of the project, the sensor strategy changed and a new stereo camera sensor replaced the initially planned colour camera. This had profound implications on both the proposed off-road ADAS functionality and the perception capability. As the stereo camera provides depth perception capability, which can provide more information about the terrain, it opened an opportunity for sensing the topography of the terrain to support TBSA. Therefore, the focus of the research changed to facilitate the development of perception system supporting TBSA.

The goal of TBSA is to reduce drivers' workload and improve comfort by automatically managing vehicle speed. In order to achieve this goal, the perception system needs to pre-emptively identify terrain geometry and surface roughness to complement reactive based system TBSA system as discussed further in Section 5.2. The TBSA perception system was further split into two separate components: one analysing macro terrain features such as slopes, ditches and crest and a second which analyses micro terrain features constituting surface roughness. The split was driven by the fact that different methods were needed for recognizing macro and micro terrain features.

The proposed terrain geometry identification method is described in detail in Chapter 7. In order to establish the performance of the perception system in terms of its capability to detect macro terrain features (range and accuracy), experimental evaluation was performed. Further, the impact of the terrain geometry identification on the TBSA performance was qualitatively evaluated in off-road conditions to establish if the inclusion of vision perception system provides benefits in terms of speed adaptation.

Speed recommendation based on surface roughness method is described in Chapter 8. The performance of the system is evaluated based on its ability to recommend appropriate, expert chosen vehicle velocity for surfaces of different roughness. Further, the impact on the TBSA performance in qualitatively and quantitatively assessed to understand the benefits of vision based surface roughness measurement.

Design and implementation of prototype solution

The proposed perception modules were implemented on a PC based platform providing a prototype solution. The perception prototype system provides a means to:

- understand the performance of the perception system in realistic scenarios
- validate that the perception system fulfils the requirements posed by the feature
- validate the expected behaviour of the feature

- specify system interfaces and requirements for further series development

Performance evaluation

The purpose of performance evaluation is two-fold: to establish if the proposed method fulfils functional requirements cascaded from the feature level and to establish the limitations of the system performance. Each of the perception modules is designed to tackle a separate set of problems linked to a specific vehicle behaviour. Hence each of the perception modules is separately validated on the data set representing different use cases.

Validation of the system is performed on real-world data. Real-world data gathered with the representative sensor set provides an indication of the feasibility of the solution within the constraints of production representative sensors. This, in turn, builds confidence that the system can be passed to series development.

5 Requirements

As discussed in section 2.7, each ADAS system imposes its own requirements on the information that the perception system should provide. These requirements are discussed individually for each of the systems. This chapter provides a more detailed discussion on the target off-road ADAS systems and analyses the functional requirements of the perception system taking into account the interactions with the intended application. Understanding the required perception functionality drives the design of the proposed computer vision methods, which analyse the sensor data to extract the relevant information about the environment.

5.1 Terrain Response 3

As introduced in Section 2.5, TR3 is an incremental improvement on the previous version of Terrain Response 2 and Terrain Response. Terrain Response is a feature that aims at maximising vehicle capability in difficult off-road terrains. It aims at helping the driver by adjusting the throttle response, gearbox mode, ABS to achieve maximum traction and control. There are five terrain modes available: general (for normal conditions), grass/gravel/snow, mud and ruts, sand, rock crawl [4]. Next generation of the system Terrain Response 2 (TR2) introduces an automatic selection of one of the TR terrain modes by classifying the terrain type based on the measurement of articulation, wheel slip and vibration.

5.1.1 Surface type transition

While transitioning between different surfaces, some surface types are difficult to detect for TR2 system - traction event needs to occur before selection can be made. In case of grass/gravel/snow mode detection of the low friction surface relies on detecting wheel slip. This can have detrimental effect especially on grass and snow surfaces, as wheel slip on deformable surfaces can result in excavation of soil around the wheel, leading to wheel sinkage, and this in extreme cases may lead to vehicle being grounded as illustrated in Figure 5.1. By providing the information of the surface ahead, the system could apply the appropriate pre-set mode to reducing wheel slip ratio and avoiding surface damage.

Figure 5.1. Illustration on TR2 system behaviour vs expected improvement in performance with TR3 system.

Although it would be beneficial to be able to classify all terrain types to improve the robustness of the terrain classification used in TR2, classifying multiple terrain classes using vision based methods is challenging [6]. Also as discussed previously, due to the limitations of obtaining snow data in the UK test locations and prohibitive cost of obtaining data abroad the scope of terrain classification system, the decision was made to limit the scope of terrain type recognition. Based on the performance gap identified in the TR2 performance it would be more beneficial to tackle the problem of grass detection as the first step of vision-based terrain classification system. If a solution to the problem of grass classification can be shown to be robust against various real-world use cases then the solution space can be expanded to multiple terrain types.

5.1.2 Perception requirements

The requirements of the perception system is to detect grass surfaces under different lighting and weather conditions with minimum false positive detection rates especially on tarmac so that the system does not engage unnecessarily. In addition, the system should be able to detect the surface ahead to provide the required 200 ms for the TR system to engage, hence the sensing range should be at least 5 m. TR2 requires 200 ms to switch mode, hence assuming top velocity of 80 kph the sensing horizon need to be at least 5 m. The bound on the operating speed of 80 kph is an assumption based on the expectation that driver would not choose higher speeds on low friction surfaces [179].

5.2 Terrain Based Speed Adaptation

Terrain Based Speed Adaption (TBSA) is an ADAS feature that is intended to manage vehicle speed depending on the environment conditions. A similar ADAS system, which reduces driver's workload by managing longitudinal vehicle motion on road, is the Adaptive Cruise Control (ACC) feature. ACC is designed to keep vehicle speed at a level selected by the driver. If there is a preceding vehicle, which would warrant the car to slow down, ACC would slow down to keep a safe headway to the vehicle in front. TBSA can be described as an off-road version of ACC, in a sense that the driver will select a maximum target vehicle speed and if the surface topography and roughness will warrant reduction of speed the vehicle will slow down automatically.

The system builds on an existing feature called All-Terrain Progress Control (ATPC). ATPC is an off-road feature that controls the vehicle speed to a target speed selected by the driver. This feature only maintains the selected vehicle speed regardless of the conditions of the surface. Similarly, an earlier version of ACC called Cruise Control only maintained selected vehicle speed, thus the driver was responsible for slowing down the vehicle if there was a slower vehicle in its path.

ATPC maintains automatically a set speed during off-road driving by maximising required traction. ATPC manages the engine output and brakes to avoid loss of traction allowing the vehicle to maintain the desired speed. This allows the driver to focus on steering and assessing the terrain ahead. TBSA is a

progression of ATPC, which manages vehicle speed in more holistic manner taking into account the terrain on which the vehicle is driving and choosing appropriate vehicle speed. It is important to note that the driver is in control of the vehicle at all times hence the system will not make any decision regarding the traversability of the selected path.

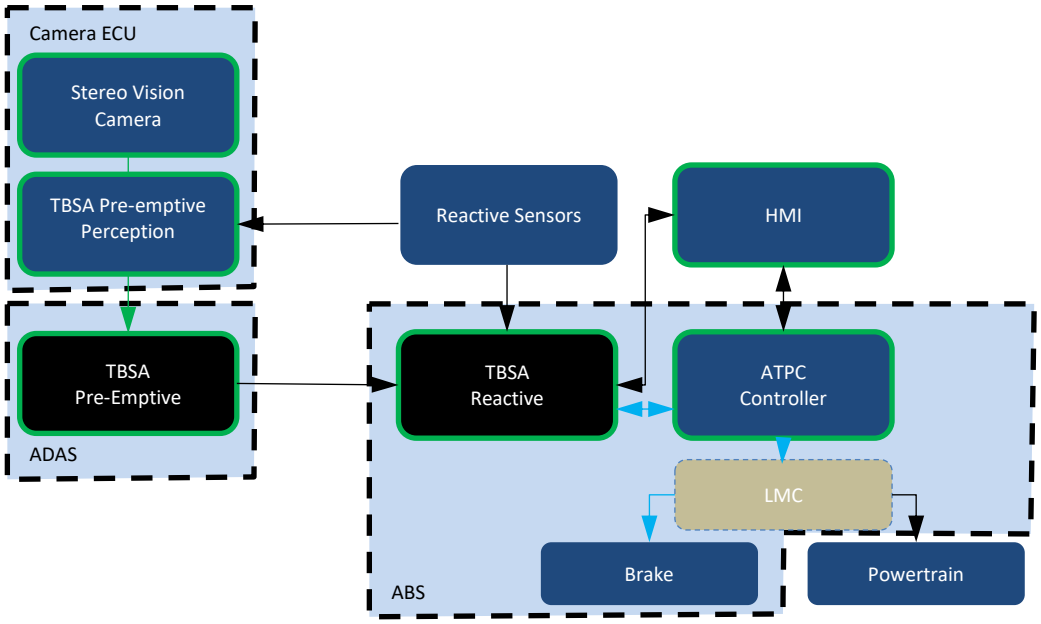

Figure 5.2. Terrain Based Speed Adaptation Architecture

Component	Description
Stereo Vision Camera	Image, Disparity
TBSA Pre-emptive Perception	Convert stereo vision camera images into terrain features (Slope Gradient, Ditch, Crest, Roughness) and distance information.
TBSA Pre-emptive	Converts terrain features (Slope Gradient, Ditch, Crest, Roughness) and distance information into a speed target.
Reactive sensors	Restraint Control Module Inertial Measurement Unit (RCM IMU), Suspension Height, Wheel Speeds, Steering Angle/Rate, Terrain Response Programs
TBSA Reactive	Converts the sensor information into unmeasured states (Gradient, Comfort) & then adapts the ATPC target speed based on these states
HMI	Human Machine Interface (HMI) ADAS (Cruise Control Buttons) and instrument cluster.
ATPC Controller	Manages driver's speed request and converts to a speed and acceleration target for the Longitudinal Motion Control
LMC	Longitudinal Motion Control (LMC) converts the speed and acceleration targets into positive and negative torque requests

Table 5.1. Terrain Based Speed Adaptation Components

The TBSA architecture is shown in Figure 5.2 and Table 5.1. TBSA consists of two components: reactive and pre-emptive system. A reactive system can adjust the vehicle speed based on the response of the vehicle to the terrain, the system measures vehicle state and the acceleration levels experienced by the vehicle, as follows:

- System monitors vehicle gradient and adapts the vehicle speed depending on the gradient severity different target speeds are applied.

- When vehicle transitions from positive gradient to no gradient, the cresting event is detected and the vehicle slows down to allow the driver to assess the situation.
- System monitors lateral vehicle acceleration and adapts vehicle speed while cornering to maintain constant lateral acceleration.
- System monitors vehicle vertical acceleration and calculates *comfort metric* based on ISO standard for passenger vibration [163]. If the target comfort level exceeds predefined limits the system accelerates vehicle, if the target comfort levels are below target level the system decelerates vehicle.

Since the system adjusts the vehicle speed reactively, there are several situations, when the vehicle reacts too late to the terrain events. This may cause excessive excitation of the vehicle or driver intervention; in turn this may lead to customer dissatisfaction with the product. These use cases are described below. Detailed descriptions of the use cases is contained within Submission 2.

5.2.1 Slope – transitions

Transition between the gradients can be illustrated with an example of traversing a steep hill as illustrated in Figure 5.3. As the vehicle approaches crest of the hill the driver may not be able to see what lies ahead hence the vehicle should slow down to enable the driver to assess the situation (this is marked with pause symbol in the illustration). The vehicle needs more torque while climbing the hill hence there is a risk of the vehicle overshooting the crest if the speed is too high while cresting. Similarly, when the vehicle starts to descend the velocity should be minimum if the slope transition is severe again limiting the drivers view of what is ahead.

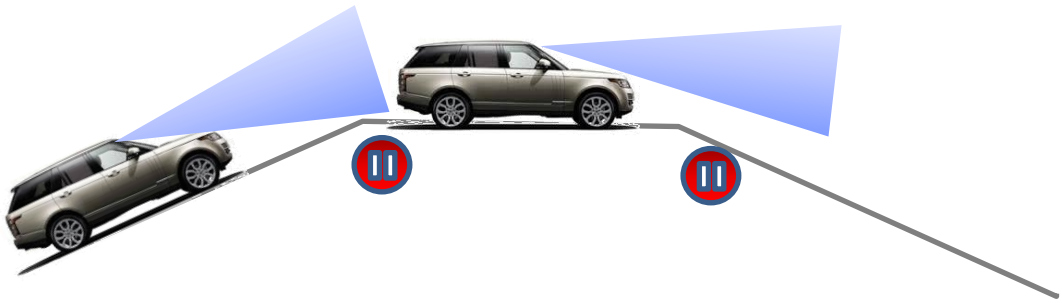

Figure 5.3. Transitions between slopes

While approaching the slope the physical limits of the vehicle also needs to be considered. Steep slopes close to the approach and departure angles will warrant the minimum speed to ensure that the vehicle will not be damaged. The approach angle, as illustrated in Figure 5.4, is the maximum gradient difference that the vehicle can clear without damage to the front bumper while approaching a gradient transition. Departure angle is the maximum gradient difference when the back of the vehicle clears the gradient change without damage.

Figure 5.4. Approach and departure angle.

5.2.2 Ditches and fords

Ditches and fords are common features found in off-road environments and if traversed too fast, they can cause damage to the vehicle. Since it is difficult to establish the depth of a ditch from shallow viewing angle as shown in Figure 5.5, it should be approached with low speed. Similarly, fords should be approached with care, as the depth of the water is unknown. Moreover, high velocity impact with water creates a bow wave, which may be higher than the maximum wading depth of the vehicle, posing additional hazard.

Figure 5.5. Ditch scenario

5.2.3 Surface roughness

Apart from macro topography features such as hills and ditches, surface roughness is another important factor that warrants the adjustment of the vehicle speed. For example, transitioning from a smooth surface to a rough surface requires the driver to slow down the vehicle; even the presence of potholes and sporadic undulations requires the driver to slow down. When a rough terrain is approached with high velocity, the terrain exerts forces on the vehicle suspension that result in higher acceleration levels of the vehicle body [151]. High levels of vibration are known to cause discomfort to the vehicle occupants [163].

There are two particular scenarios associated with surface roughness, which reactive TBSA cannot accommodate:

- Discrete terrain feature such as kerb, rock or log – Single terrain event which causes excessive shock to the vehicle, once passed over there is no need to slow down. Hence the reactive system cannot cope with this scenario.

- Transition from smooth to rough surface – While transitioning between surfaces the vehicle experiences excessive levels of vibration, before the reactive system sufficiently lowers vehicle speed. Figure 5.6 shows the effects of transition between surfaces on the vehicle vibration (*AccelZ*) and passenger comfort (*IsoPsngrExit*). As the vehicle travels on a smooth surface with high velocity (30 kph) the vertical acceleration experienced by the vehicle is low, resulting in low levels of passenger excitation indicating comfortable travel. When the vehicle transitions to rough surface, the passenger excitation increases causing the vehicle to slow down. Once the vehicle velocity reaches 10 kph, the passenger excitation metric stabilises and the vehicle maintains this speed.

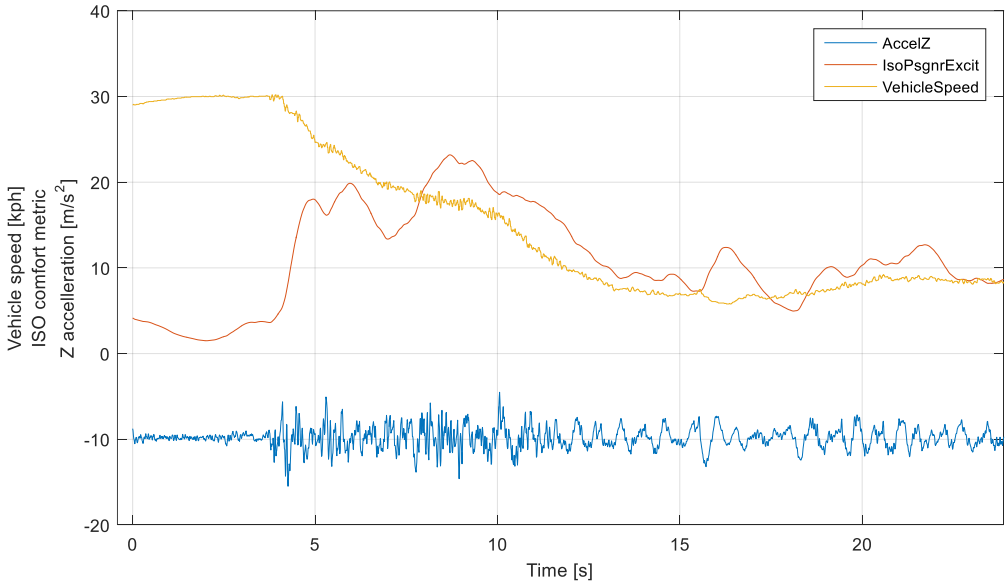

Figure 5.6. Vehicle transitioning between smooth and rough surfaces.

5.2.4 TBSA operating limits

TBSA is intended to operate in the same speed limits as its predecessor system ATPC allowing the driver to select the target speed in the range between 1.8 kph and 30 kph. Due to the nature of driving in the off-road environment, the lower bound has been set to 1.8 kph since on low friction surface it may not be possible to stop the vehicle. Especially on low friction such as mud or snow applying brakes and stopping the vehicle may cause vehicle to slide. On the other hand managing the torque and slowing

down the vehicle to a crawl poses less hazard. Additionally, since all the vehicle wheels may slip there is no guarantee that the vehicle has stopped. The upper operating limit stems from the availability of other off-road vehicle subsystems that has been designed to operate at a maximum speed of 30 kph.

In order for the vehicle to slow down in the situations presented in the previous sections, it is important to consider the maximum operating speed. In the worst-case scenario, the vehicle driving with top speed may encounter a slope or a ditch that will require the vehicle to slow down to the minimum operating speed. The analysis of the worst-case scenario forms a basis for the analysis of sensing requirements presented in the next section.

There are also constraints posed on the maximum acceleration and deceleration rates applied by the vehicle. According to ISO standard "Adaptive Cruise Control systems — Performance requirements and test procedures" [180] the average maximum deceleration rate for ACC is 3.5 m/s^2 on tarmac roads. In terms of comfort, longitudinal deceleration rate of 2 m/s^2 is considered comfortable [181]. Maximum deceleration rate of 2.25 m/s^2 was chosen as it is within the comfort limits and is safe taking into account possible low friction surfaces.

5.2.5 Sensing horizon

The vehicle can react in time for the change if the terrain only is the information about upcoming terrain features is provided with enough preview distance. The required preview distance or sensing horizon will be defined by the bounding operating speeds of the vehicle. Since the vehicle needs to slow down if a terrain that requires lower vehicle speed is detected, the sensing horizon is bounded by the vehicle slowing down distance. Vehicle slowing down distance can be calculated as follows:

$$d = \frac{(v_0 - v_1)^2}{2a} + v_0 T_r + B\,, \qquad (5.1)$$

where d is the slowing down distance, a is the vehicle deceleration, v_0 is the initial vehicle velocity, v_1 is the desired final velocity, T_r is the system reaction time, B is the safety distance buffer.

For the purpose of this analysis, a worst-case scenario is considered. The vehicle drives over a smooth straight surface with the maximum speed of 30 kph followed by a large ditch/ford in the path which the vehicle should traverse with minimum speed of 1.8 kph.

Given the following values the slowing down distance can be calculated as a function of initial velocity,: initial vehicle velocity v_0, target velocity v_1=0.5 m/s, system reaction time T_r=200 ms, safety distance buffer B=0.5 m. System reaction time of 200 ms is an estimate considering processing the information, controller requesting the vehicle slow down and the vehicle systems applying requested deceleration. For safety, additional 0.5 m of distance buffer is added.

The slowing down distance as a function of initial speed is plotted in Figure 5.7. The vehicle needs to be able to slow down for potentially hazardous terrain features from the maximum operating speed of 30 kph to 1.8 kph, which results in the slowing down distance of 15 m. Therefore, the sensing range of the proposed pre-emptive sensing solutions needs to be at least 15 m.

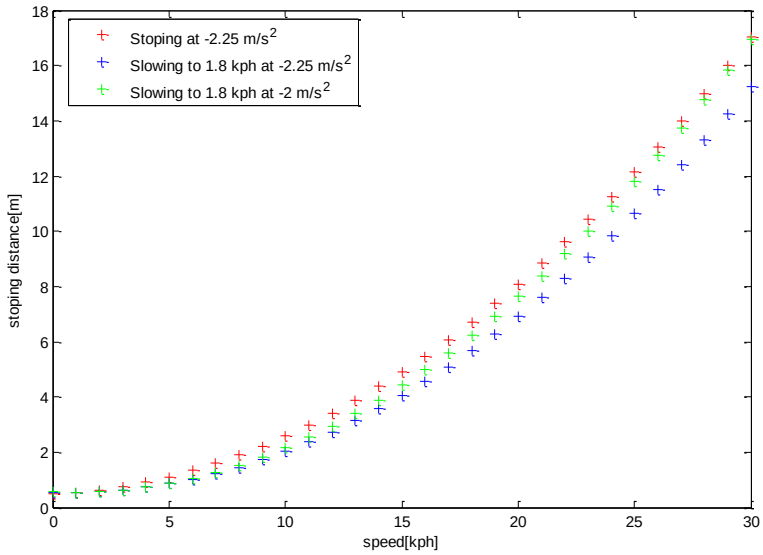

Figure 5.7. Vehicle slowing down distance as a function of initial velocity.

5.2.6 Sensing requirements

Based on the use cases identified in Section 5.2, the perception system needs to:

- measure upcoming slopes up to 15 m ahead of the vehicle
- detect crests up to 15 m ahead of the vehicle
- detect ditches up to 15 m ahead of the vehicle
- measure surface roughness up to 15 m ahead of the vehicle

5.3 Summary

This chapter provided a detailed review of the intended functionality of the proposed off-road ADAS systems. In order to achieve the expected functionality the requirements of the perception system were derived. The design of the computer vision algorithm proposed in subsequent chapters is driven by these requirements.

6 Terrain type recognition

This chapter addresses the question of how to identify terrain types which have been identified in Section 5.1 as an enabling sensing technology for Terrain Response 3. As discussed in Chapter 1, in this stage of the project a mono colour camera was planned to be introduced on the vehicle. Therefore, this chapter addresses the terrain recognition problem using mono vision based methods.

Vision-based terrain type detection is a problem of recognising surface types from video images acquired by the camera mounted on the vehicle. Although this perception task is very easy for humans, it is a non-trivial task for a machine. There are several factors such as dynamically changing lighting and weather conditions, various environments and sensor characteristic that have an impact on how objects are perceived hence affecting the performance of any video processing algorithms. Robust real-world applications utilising video processing need to consider these factors. Moreover, during development, it is virtually impossible to expose the system to all kind of variations. Therefore, the challenge lies in designing an algorithm that can robustly operate in new and unknown environments and adapt to changing conditions.

This chapter describes a novel approach to robust terrain type recognition in the context of classifying grass surfaces in real-time via a monocular camera. Within the scope of this work grass is considered as a surface vegetation consisting of long, narrow leaves characterised by its green appearance due to the content of chlorophyll. By comparison with presented state-of-the-art methods, the novelty of the proposed approach is two-fold. Firstly, the proposed method uses straightforward and computationally inexpensive descriptors, which are shown to be invariant to illumination and shadows. This results in a clear separation between the grass and non-grass classes, providing high detection rates with minimal false positive detections in a broad range of conditions. Performance issues, especially false detections and inability to deal with illumination conditions have been identified as a major issue when applying image processing algorithms in the automotive domain [18]. Secondly, using a combination of Support Vector Machine (SVM) and aforementioned straightforward descriptors with a practical sampling strategy provides real-time performance with low memory footprint as opposed to more complex methods proposed in the literature.

The algorithm achieves real-time performance with classification time of 15 ms per image. The robustness of the solution under a wide range of illumination conditions has been shown on a dataset containing more than 50 000 image samples taken under different conditions (cloudy, high sun, dusk, dawn). Currently, the algorithm can detect the grass surface in front of the vehicle in daytime conditions with an average accuracy of 97% for the test case scenarios. Use of the existing algorithm for night time conditions does not provide sufficient performance with an average accuracy of 75%.

This chapter presents a terrain classification method based on the requirements posed by Terrain Response system (Section 5.1) as the system is designed to operate in the automotive environment. The design of the method is presented in Section 6.1 . The proposed method is then validated on a realistic dataset containing more than 50 000 image samples taken under different conditions lighting (cloudy, sunny, night) with results presented in Section 6.6.

6.1 Terrain classification method

The proposed terrain classification method follows a machine learning-based object detection paradigm. Supervised learning algorithms build classifiers by taking a set of labelled samples represented by a feature vector and a class label in a form $D = \{(x_1, y_1), \dots, (x_n, y_n)\}$ and finding a function $: X \to Y$. In general classification is the process of taking a sample x_i and assign a class label y_i to it. Here only a simple description is provided, more detailed description of the classification pipeline is discussed in Submission 1. The processing pipeline is depicted in Figure 6.1.

The classifier is trained on a sample training set consisting of positive $\{grass\}$ and negative $\{non-grass\}$ samples in the training phase. The sample set consists of a compact representation of the image called descriptor. Once a classifier is trained, it is used to classify new data in the testing phase. Classifier represents a function that maps the feature vector extracted from the image into a class label$\{grass\ /\ non-grass\}$.

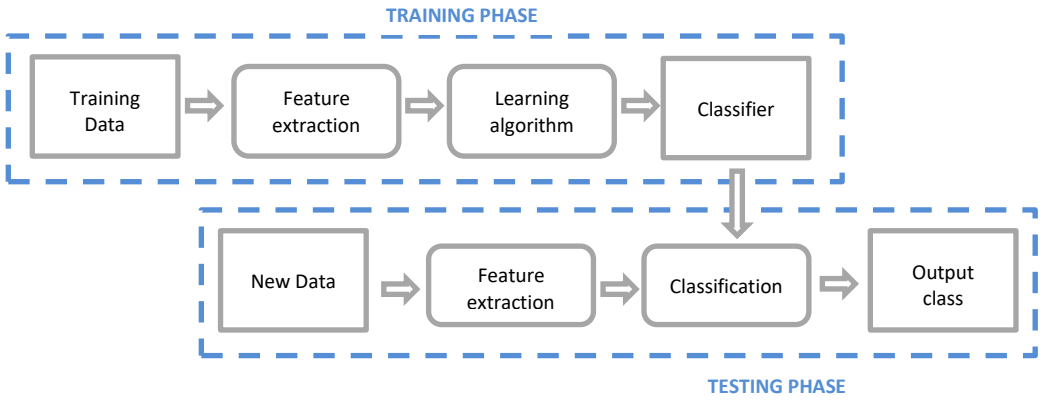

Figure 6.1. Classification processing pipeline

A result from classification pipeline on test data is shown in Figure 6.2. The image on the left is the correctly classified grass sample, whereas image on the right represents correctly classified non-grass sample. Since only a portion of the image corresponds to the surface that the vehicle will drive on, a rectangular region corresponding to the vehicle path was chosen for classification. The sampling strategy allows limiting the required computation as only region of 300 x 150 pixels is classified.

The sample region was chosen to correspond to an area of ground between the two vehicle wheels. This area is located in the range of 5-6 m in front of the vehicle. In this implementation, the sampling area was fixed, since the experimental setup did not allow logging of the data from the vehicle. However, as shown in Chapter 7 it is possible to use the driver steering inputs to sample the region corresponding to the vehicle predicted path.

Figure 6.2. Example images of the classified samples. Only the area highlighted by the colour rectangle is used as an input of the classification algorithm. The colour of the bounding box signifies the result of the classification process: green - grass (left), red non-grass surface (right).

As discussed by practitioners Duda [182] and Ponce [183], the choice of descriptors and the classifier are paramount to achieving robust performance. The understanding of the underlying data is important to choose a meaningful descriptor that can provide maximum separation between two classes even in the presence of noise. There is no single classifier that works best on all given problems (a phenomenon that may be explained by the no-free-lunch theorem). Various empirical tests have been performed to compare classifier performance and to find the characteristics of data that determine classifier performance. Within the literature many classification method exists and a choice of classifier depends on the underlying data [182].

The following sections will justify the descriptor and classifier choice, providing guidance on robustness of the proposed methods and their computational performance. The datasets used for training and evaluation of the classifiers will also be introduced.

6.2 Dataset

The dataset comprises more than 50 000 images of various surfaces in different weather and lighting conditions. The data collection was performed on the off-road track in Gaydon and various roads in Warwickshire with varying illumination conditions. When choosing the locations the goal was to obtain a representative set of different terrain types and lighting conditions. This was possible in the Land Rover off-road track in Gaydon. This facility is used to test the off road-performance of the JLR vehicles as selection of different terrain types is similar to the wide range of surfaces in different parts of the world. There are gravel tracks, dirt roads, different tarmac types, wade fords, red sand, mud tracks, forest tracks and different types of grass paddocks. In addition, data was also collected on public roads in Warwickshire in order to include representative road driving scenarios (urban environment and motorways) and surfaces containing road markings. Video sequences were captured in different times

of day and under varying illumination conditions (sunny, cloudy, dusk, dawn, night). A detailed break down and description of the data sets is covered in Submission 1 [184]. Example images are shown in Figure 6.3 and Figure 6.4. The choice of the terrains contains cross-section of the terrains most commonly driven on both off-road and on-road including tarmacked public roads, gravel tracks, mud and grass taken under different lighting conditions including sunny, cloudy conditions and night time. A breakdown of the sample set with respect to the terrain type and lighting conditions in shown in Figure 6.5.

Figure 6.3. Off-road scenarios – typical driving surfaces including gravel and grass.

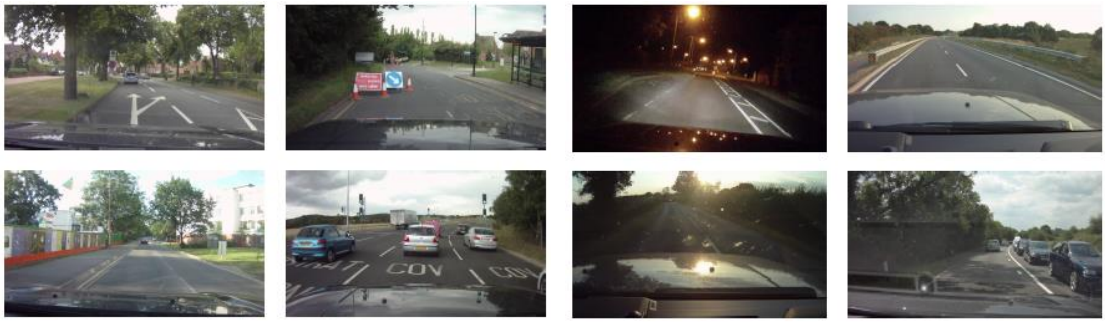

Figure 6.4. Urban scenarios – selection of tarmac road with and without road marks under different lighting conditions.

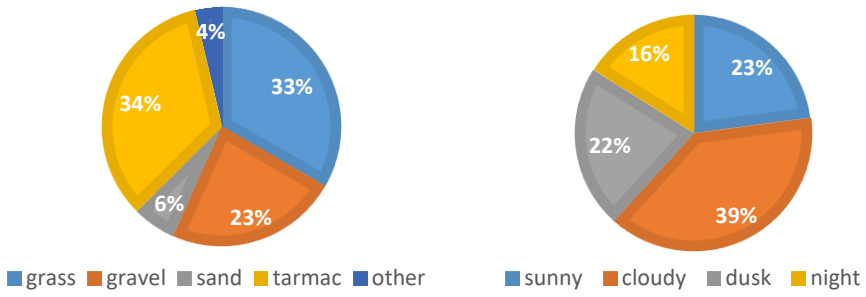

Figure 6.5. Dataset composition with respect to the terrain type and lighting conditions.

Each of the images was manually annotated, highlighting the region of interest and assigning a class label$\{grass\ /\ non-grass\}$. Only a subset of the 3 000 grass and 3 000 non-grass samples were chosen

for training; the rest of the samples were used as a test set to evaluate the performance of the proposed method. Samples include variety of different grass types, tarmac and gravel under different illumination conditions as shown in Figure 6.6. Mixed samples that contain both grass and non-grass areas are not included in the training set as they do not clearly belong to any of the class hence it is not possible to label them clearly as $\{grass\ /\ non-grass\}$.

Figure 6.6. Examples from the training data set.

6.3 Image features

Image descriptors are a compact representation of the image extracting key characteristic such as colour, texture or keypoints [185] (e.g. SURF [186], SIFT [187]). In order to establish the most suitable classifier first, available image descriptors were reviewed focusing on complexity and robustness to lighting conditions, and secondly the image data set was analysed to establish if the proposed descriptors can discriminate grass/non-grass classes.

Colour descriptors were most promising, as colour has been shown to distinguish natural terrains. Texture descriptors were disregarded, as due to the camera location behind the windscreen, the visual texture of the surface was not visible. Most of the work presented in literature uses texture descriptors when the camera is located closer to the ground and texture granular terrain features are clearly visible. Keypoint descriptors were also disregarded due to their computational cost.

From the literature review contained within Submission 1 [184] the following conclusions were derived guiding the design of the descriptor:

- Colour-based methods are computationally inexpensive as they require calculation of only first and second order statistics. The number of operations required is directly proportional to the number of pixels. First order statistics (mean and standard deviation) are faster to compute than histograms, though both operations are only linearly dependent on the number of pixels.

- Texture-based methods are computationally expensive and provide moderate to high classification performance depending on the application. Because of the fact that texture methods use k-th order statistics (k>2) and perform an operation on pixel neighbourhood for

each pixel, the processing time required exceeds the real-time requirements for our application as discussed in Submission 1.

- Keypoint feature based methods are computationally expensive and unsuitable for real-time applications, as even on a capable processing platform it takes more than a second [188].

- Processing demand increases with the number of pixels used in classification. Classification of each pixel within the image may not be necessary for the terrain classification of the proposed application. Processing only region of interest within the image reduces computational load.

Colour-based methods are incorporated into almost every terrain classification method presented in the literature as they are computationally inexpensive. Colour classification is, however, challenging in outdoor environments as perceived surface colour depends on lighting conditions, weather conditions and viewing angles [142], [143]. There is no agreed colour model or colour space which is best suited for terrain recognition task and the methods proposed in the literature use different colour descriptors depending on the particular application [143].

The normalised RGB colour space was chosen, since it was shown in the literature to provide invariance to camera viewpoint, illumination direction and intensity [189]. The data set showed also the separation between the classes with mean and standard deviation used as a descriptor. The plots with the normalised RGB descriptors for the training set images are shown in Figure 6.7. Other colour spaces (HSV and RGB) did not show clear separation between the classes; however they were still used in the classifier training to evaluate their performance. Although, the classes may not show clear separation the machine learning method may still be able to create non-linear separation function, hence further investigation was required.

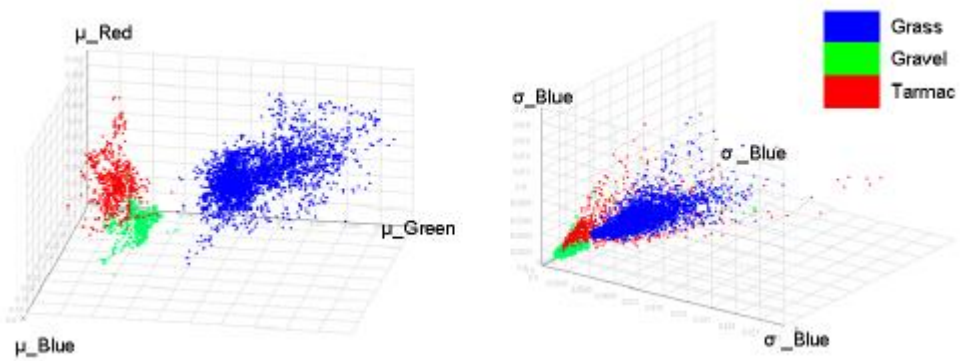

Figure 6.7. Feature spread of the training sample set in the normalised RGB colour space. Each point on the plot corresponds to one image sample. The plot on the left shows spread of the samples in the space denoted by the mean values for each colour channel, whereas plot on the right shows space denoted by standard deviations for each colour channel.

Apart from mean and standard deviation, the colour descriptor can be built based on histograms. Histograms for each colour space were also evaluated for the purpose of grass classification, however

the performance of histogram based descriptors was inferior to the first order statistic descriptors as discussed in Section 6.4. Further discussion on colour spaces and descriptors is included in Submission 1.

6.4 Classification

Two machine learning methods were used to train the classifier: Artificial Neural Network (ANN) and Support Vector Machine (SVM). These two supervised learning methods are popular choices in object recognition using monocular images ([182], [183]) for objects ranging from faces , vehicles , pedestrians. The performance of both methods was analysed in terms of the detection accuracy and computational requirements.

Both classifier parameters were optimised using 5-fold cross validation as discussed in detail in Submission 1. The combination of RGB, normalised RGB (denoted in figures as *rgb*) and HSV colour spaces were used with two descriptors: first order statistics (mean and standard deviation for each colour channel) and histogram (64 bin histogram for each colour channel). The results of training are plotted on Receiver Operating Curves in Figure 6.8 and Figure 6.9. As SVM and ANN produce a continuous output (distance or probability), different thresholds may be applied on the outputs to predict class membership. The ROC curve is produced by plotting the true positive rate (TPR) vs. the false positive rate (FPR) at various thresholds. This depicts the trade-off between hit rates (TPR) and false alarm rates (FPR). The better performing classifiers produce ROC curve closer to the top left corner with lowest FPR for the same TPR.

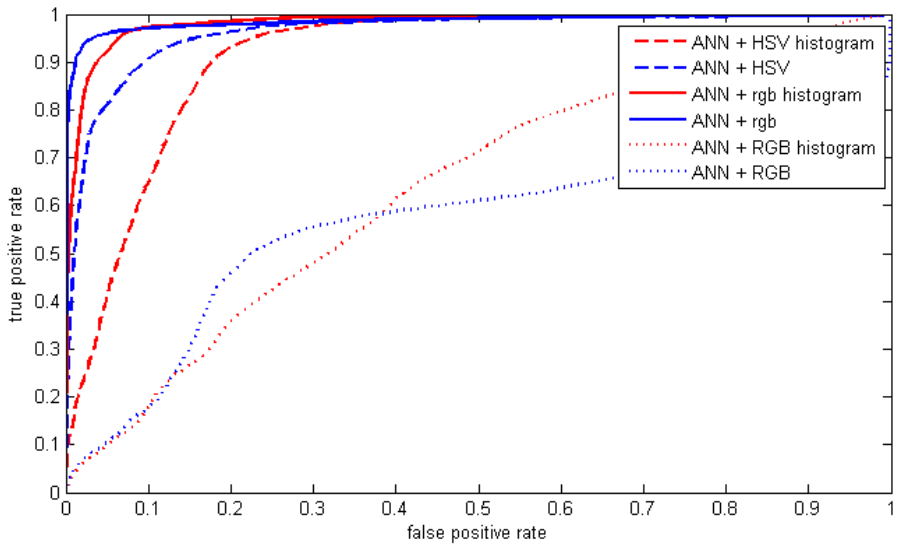

Figure 6.8. Artificial Neural Network training performance.

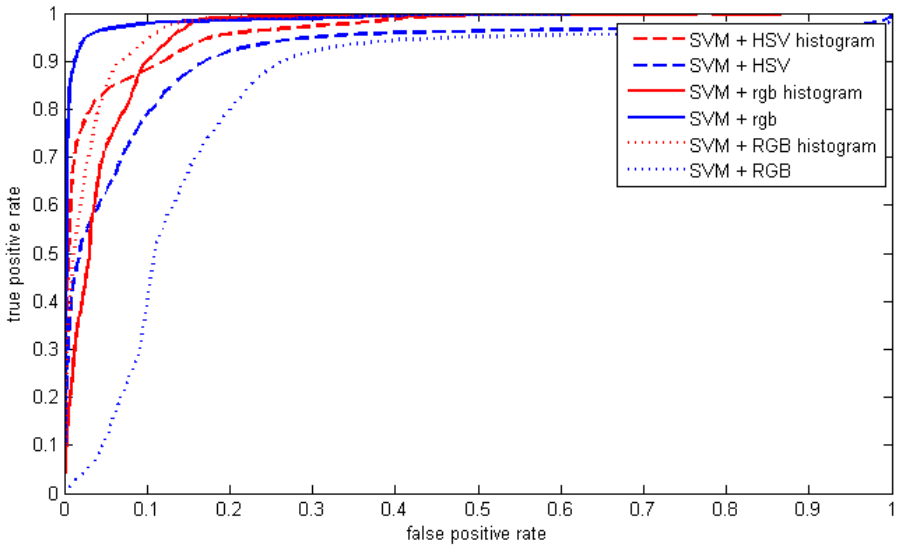

Figure 6.9. Support Vector Machine training performance.

From the results it is clear that the RGB colour space with first order statistics descriptor offers better performance than the other colour spaces and histogram descriptors. In terms of comparison of SVM and ANN using the best performing descriptor, the performance is comparable as seen in Figure 6.10. Both ANN and SVM with RGB descriptor achieve TPR exceeding 95% for FPR of 2%.

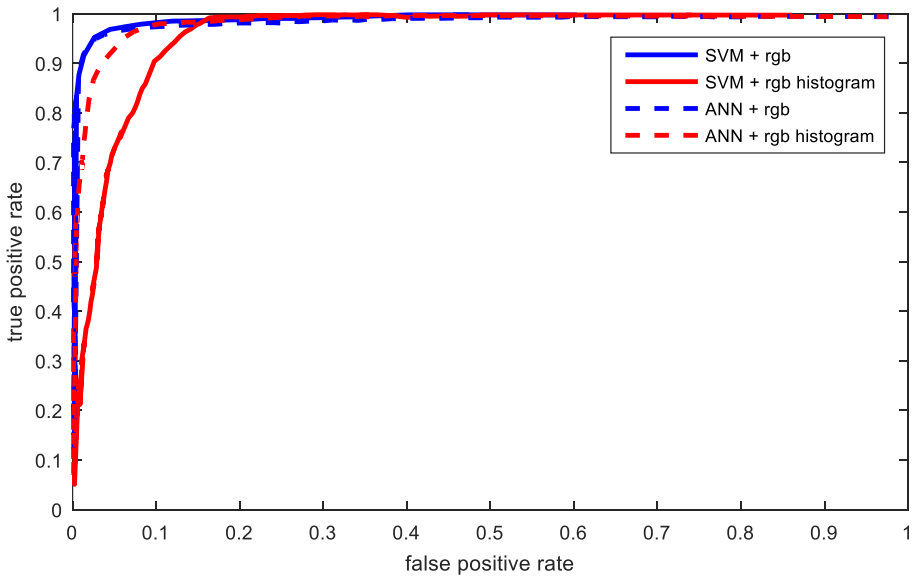

Figure 6.10. SVM and ANN ROC curves.

Although both classifiers achieve similar performance and the difference in performance is negligible, the SVM based classifier was chosen for further validation. SVMs generalize well even in with small training sample conditions as SVM training always finds global minimum by finding the hyperplane separating the classes with highest margin. Whereas ANN finds local minima [190], hence it could find a separating function that is tailored to the training set.

6.5 Computational performance

Computational performance of the classifiers plays an important role, as the processing resources on a vehicle are limited. The main load on processing is demanded for the computation of the descriptor with 10^6 operations required to compute normalised RGB descriptor and only 10^3 operations to apply classifier. The processing takes 15 ms on 3.2 GHz Intel i5-650 processor to calculate descriptors and classify the image. Both classifiers can be stored in less than 1MB of memory, which is suitable for automotive ECU. The proposed method is hence suitable from the computational performance perspective on an automotive ECU.

6.6 Experimental evaluation

The proposed approach was validated on the sequences that were not used for training. Assessing the performance on previously unseen data set aims at understanding if the classifier can actually perform well in real-world scenarios in wider range of operating conditions. There were total of 33 video sequences taken, resulting in more than 1,5 hour of annotated video footage. In comparison, other works proposed in literature evaluate the performance of terrain detection methods on the tests sets consist only of hundreds of images. Jansen [191] reports the result on a test set of 89 images, whereas Castano [146] only on 18 images. In addition, vast majority of the methods presented in literature does not consider robustness against various lighting conditions. This is understandable, since the majority of these approaches were designed specifically for robots only used off-road. Although work by Manduchi [192] and Jansen [191] emphasise the influence of illumination and weather conditions, the limited number of test images does not provide sufficient evidence that the proposed approach can operate robustly in the range of unseen conditions. The data used for validation of the proposed approach consist of sequences taken under various lighting conditions including night conditions. In addition, validation data set incorporates challenging and diverse scenarios (vehicles in the camera field of view, different types of tarmac, road markings). Most of the methods proposed in the literature consider mainly off-road conditions and do not focus on the false detection caused by traffic and various road marks. The detailed description and break down of the dataset and the experimental setup is contained in Submission 1.

The performance of the proposed method was measured using balanced accuracy calculated as:

$$acc = \frac{1}{2}\left(\frac{TP}{TP + FN} + \frac{TN}{FP + TN}\right), \qquad (6.1)$$

where TP is number of true positive, FN false negative, FP false Positive, TN true negative.
Balanced accuracy measures the number of samples correctly classified taking into account inter-class distribution.

SVM provides class label as an output of classification. In addition, SVM can output a distance between the currently classified sample and the separating hyperplane, since SVM separates the two classes by calculating the maximum margin hyperplane as shown in Figure 6.11. The distance metric can be used as a measure of confidence in the classification. Certain methods such as Platt scaling [193] have been proposed in literature to map the SVM distance to probability output, however this was not implemented in the current method. Instead, here the SVM distance is used to illustrate the difference in classification results between correctly classified samples with high confidence and misclassified samples usually with low confidence. The distance between hyperplane and classified point will be denoted as *d*. Evaluation of the classifier performance on mixed type surfaces and during transition between the surfaces shows that the hyperplane distance could indicate the uncertainty of the classification result.

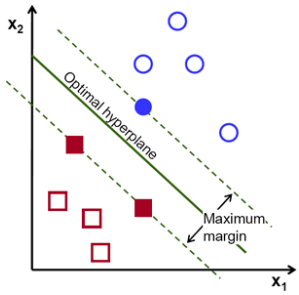

Figure 6.11. Support Vector Machine with maximum margin hyperplane.

6.6.1 Results

Experimental validation results are presented in Figure 6.12. Obtained accuracy for the video sequences obtained in daytime conditions exceed 97% and is significantly lower in night time with average of 75%. The reduced accuracy is caused by misclassified samples which are discussed in Section 6.6.2 and 6.6.3.

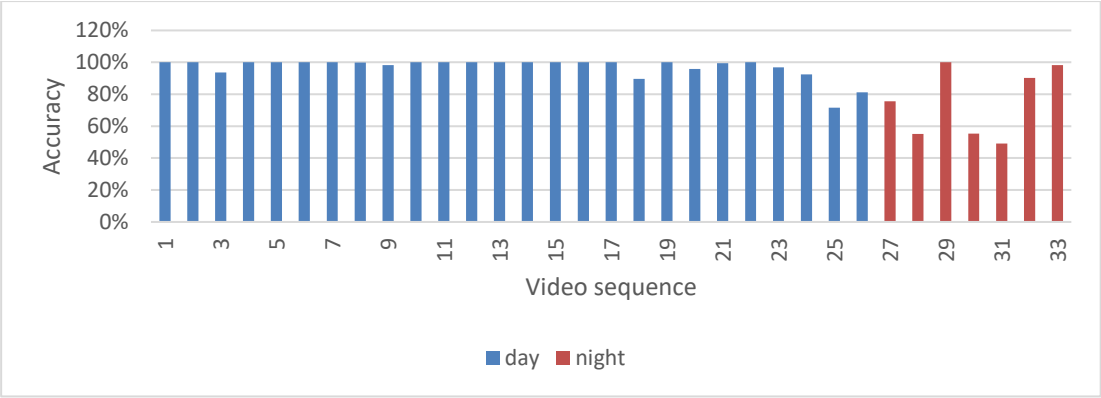

Figure 6.12. Validation results on 33 test video sequences.

6.6.2 Daytime scenarios

The non-grass samples were correctly identified in a range of different on-road and off-road scenarios with example classification results shown in Figure 6.13. Tarmac, cobblestones, gravel, sand, road marks,

different tarmac colours and even vehicle appearing in the camera field of view were correctly classified as non-grass class with 99% of non-grass samples classified correctly.

The correctly classified grass samples are shown in Figure 6.14. Grass with different colours and height were correctly classified. 93% of the grass samples were classified correctly.

Figure 6.13. Correctly classified non-grass samples.

Figure 6.14. Correctly classified grass samples.

There were however cases of misclassification in both classes. The misclassification of the grass class occurs in the situations where grass is dry with brown and yellow in colour as shown in Figure 6.15.

This results in reduced accuracy for video sample 18 and 20 as shown in Figure 6.12. The misclassified non-grass samples correspond to ford with greenish water, dry yellow vegetation, resulting in reduced accuracy in video sequence 25 as seen in Figure 6.12. The misclassified urban features (yellow road marks and orange bus) correspond to video sequence 26 in in Figure 6.12. This misclassification stems from two different problems. Firstly, if a sample is visually similar in terms of colour as green water than the model will classify it as a grass sample. Second misclassification mechanism is a result of the computation of the descriptors. Since average colour values are used as a descriptor, a mix of black and yellow colours will result in the average green value being similar to grass class descriptor.

Figure 6.15. Misclassified samples

The bus misclassification scenario could be mitigated by a system check to see whether there is a vehicle present in the classification region. The road mark misclassification could potentially be acceptable as the terrain mode would switch only for short period and may not be noticeable by the driver, or existing lane detection system could be used to identify when yellow road marking is present in the classification region.

6.6.3 Night time scenarios

The performance during night time is worse than daytime as shown in Figure 6.12. The degraded performance stems from the fact that lights change the perceived colour of the surfaces. As seen in Figure 6.16 the perceived colour of grass illuminated by vehicle headlamps is washed out. Moreover, the tarmac surfaces appear differently under the illumination from headlamps and illumination from street lamps. The perceived colour of sample changes when the colour of the illumination changes. As the street lamps emit more yellow light than the headlamps and the natural sunlight, the colour distribution and model change. This shift in model boundaries result in misclassified samples of tarmac at night.

Even visually inspecting misclassified tarmac sample indicates a perceived green colour of tarmac. These changes to the colour captured by the camera make this method unsuitable for robust night time performance.

The illumination sources present at night such as headlamps and different types of street lamps emit light that varies in colour affecting the perceived colour of the surface. The bottom row of Figure 6.16 shows tarmac surface illuminated with only headlamps and street lighting and headlamps illustrating how colour changes with illumination. None of the colour descriptors are invariant to the change of illumination colour, hence in order to classify surface colour at night a colour model of the illumination source would be needed. Since it is possible to establish the colour of the light source, it is also not possible to train a single classifier which would perform well at night.

Figure 6.16. Example night samples.

6.6.4 Transition between surfaces

Not all of the video frames have been annotated as some of the samples contain both grass and non-grass image samples leading to ambiguity. To address this issue, the classifier performance is evaluated qualitatively on two scenarios with mixed samples. First scenario is the vehicle transitioning between grass and non-grass surfaces; second scenario is the vehicle traveling on a track with grass in patches in the area between the wheels (see Figure 6.17). The purpose of this evaluation is to understand how the classifier performs on mixed sample.

Figure 6.17. Examples of mixed surface samples: left – transition between gravel and grass, right – track with grass patch in the middle.

As introduced in Section 6.4, SVM outputs the distance to the separating hyperplane, which can indicate the confidence of the classification result. SVM distance is plotted in Figure 6.18 and Figure 6.19 for all the image frames in the sequence. The distance is a L2 metric and it is the absolute value of presented SVM distance values. In this notation, the sign corresponds to the target class: negative – grass class, positive – non-grass-class.

Figure 6.18 shows the transition between grass and gravel. The distance values change gradually from negative to positive with transition period of 35 frames, where the values are in the range <-0.5, 0.5>. These frames correspond to the situation where mixed sample is present in the classification region.

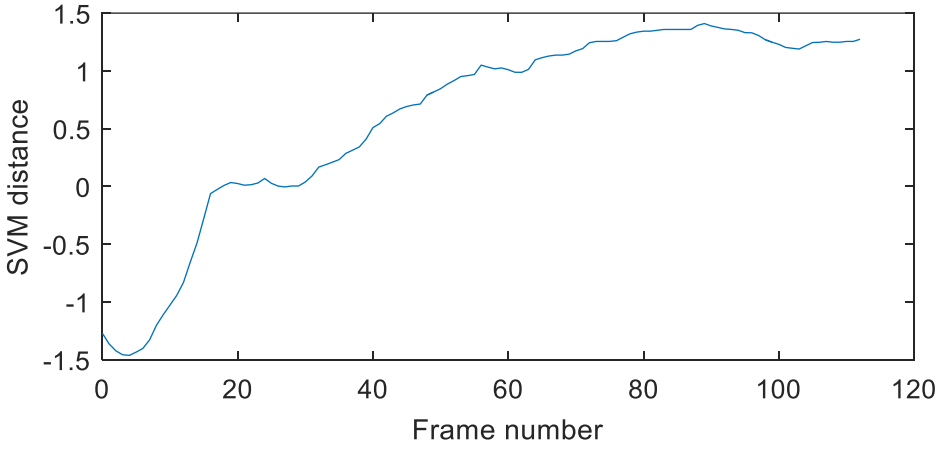

Figure 6.18. SVM distance when transitioning between grass and gravel surface. Sign represent classification output.

In case when the vehicle is driving on a track with a grass patch in the middle, SVM distance value oscillate depending on the proportion of the grass visible in the sampling window (see Figure 6.19). Although the confidence value drops below 0.2, all the samples in the sequence are correctly classified as non-grass surface.

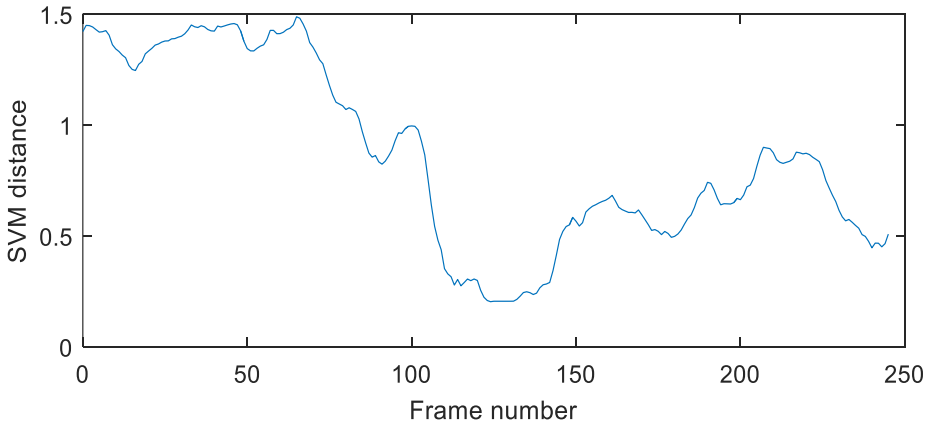

Figure 6.19. SVM distance on the track with grass. Sign represent classification output.

The obtained results show the applicability of SVM distance as a confidence measure to provide additional source of information to the subsequent control unit. The SVM distance could be used to judge how good the classification output is and in turn be utilised by the control module to decide if the terrain mode should be changed.

6.7 Conclusion

The research presented in this chapter focused on grass detection using single colour camera sensor and the aim was to develop a robust algorithm that can perform in real-world conditions. This work has developed an image processing framework for grass detection, showing the steps needed to achieve this, including the choice of discriminative image features, classifier choice and the performance of selected method. It was shown that mean and standard deviation in a normalised RGB colour space with SVM classifier provide classification accuracy of 97% in the daytime conditions. In the night time conditions the classification accuracy drops to 75% due to varying colour of light sources such as street lamps hence not conforming to the employed colour models. The reduced accuracy also stem from the fact that the brown, yellow grass was not classified as grass class. Taking the definition of grass as foliage type typically distinguishable due to its green colour, the classifier relying on the colour features was not able to correctly classify these samples.

The performance of the terrain classification system could be further improve in future with the use of texture descriptors, as with the higher image resolution, texture details such as individual grass straws would be visible. In addition, use of sensor fusion techniques such as multispectral imaging could leverage the distinctive spectral signature of vegetation for classification purposes. Further, fusion with proprioceptive sensors, where the system could learn both the appearance and the vehicle response, could lead to a self-learning system. In such a system, the taxonomy of the terrain classes would not be provided a priori, but rather be constantly updated depending on the situation that the vehicle is in.

Proposed solution was analysed in terms of the computational performance, showing that it applicable to employed on a real-time embedded platform due to low memory footprint and computational requirements. Experimental evaluation of the proposed solution shows that the execution time of less than 15 ms per frame, satisfying a real-time performance requirement.

This work assessed the performance of the proposed solution in a range of various environments and environmental conditions. The proposed solution has been evaluated on more than 1.5 hours of video sequences covering various surfaces (grass, gravel, tarmac, water), different on-road scenarios (traffic, road markings) and lighting conditions (daytime, night time). Many results reported in the literature operate on limited data sets, and do not consider the impact of these noise factors. Evaluation of our solution also focused on the classification performance on the previously unseen data. Achieved high classification accuracy shows that our approach can generalise well, and did not only perform well on the training data.

This work proposed a method for developing a vision-based terrain recognition system, considering the variety of operating conditions and the computational constraints. This system could be employed in the automotive environment, although robustness would need to be proven on a target production hardware. In conclusion, proposed solution could address a well know Terrain Response 2 problem by pre-emptively detecting grass surfaces in front of the vehicle and avoiding surface damage.

7 Terrain geometry identification

This chapter addresses the question of how to identify macro terrain features which were identified in Section 5.2 as a crucial element for pre-emptive perception system for TBSA. As discussed in Section 5.2 the semantic representation of macro terrain features contain slopes, crests and ditches. The system uses an existing production representative stereo-camera sensor that provides a 3D representation of the world; this is operated upon by a set of methods to analyse terrain geometry and provide the required inputs to the vehicle speed control system (TBSA).

Terrain geometry identification is the problem of analysing the structure of the terrain from range data acquired onboard the vehicle. Although many terrain geometry identification methods have been proposed in the literature it is not clear how well they would perform with sensors of limited capability such as automotive stereo camera. Methods proposed in literature use different world models, some incorporate slope and roughness as an indicator of terrain traversability. However, there is no indication how effective these representations are for the purpose of speed adaptation. Therefore, the challenge is to design a method, which is fit for purpose, can identify required macro terrain features and can fulfil the requirements posed by the TBSA system.

This chapter describes a method for terrain geometry identification in the context of identification of slopes, crests and ditches. The disparity information produced by the stereo-camera is processed into established compact representation Multi-Level Surface Map (MLS) as discussed in section 7.1. The MLS is processed to extract slope measurements (Section 7.2) and individual terrain features ditches (Section 7.3) and crests (Section 7.4). The novel component in the proposed method is crest detection, as none of the methods proposed in the literature employed crest as an element of semantic scene description. In the view of the state-of-the-art and lack of common evaluation methods and datasets, considerable amount of work focuses on experimental evaluation of the proposed system performance against the requirements of TBSA presented in Section 7.6.

The proposed method achieves real-time performance of 10 fps, which provides sufficient update rates for the TBSA system (Section 7.5). The proposed system has been evaluated on a range of off-road data sets and specific sets of quantifiable terrain features (Sections 7.6.1 and 7.6.2) to ensure that it fulfils the functional requirements posed by the TBSA system in terms of pre-emptive sensing capability. Furthermore, the performance of the system was qualitatively evaluated while operating as an input to TBSA system in Section 7.6.3.

7.1 Terrain Geometry Identification method

The proposed processing pipeline is presented in Figure 7.1. The system uses disparity images obtained from the stereo camera to reconstruct a 3D representation of the world (point cloud) which is further

processed to a world model of Multi-Level Surface Map (MLS). Since the driver will be in control of steering the vehicle, the predicted vehicle path from driver steering input is used to extract relevant terrain features from MLS in the area that will be relevant to where the vehicle will travel. The detected terrain features: ditches, crests and slopes are then passed to the vehicle control system to adapt the vehicle speed pre-emptively.

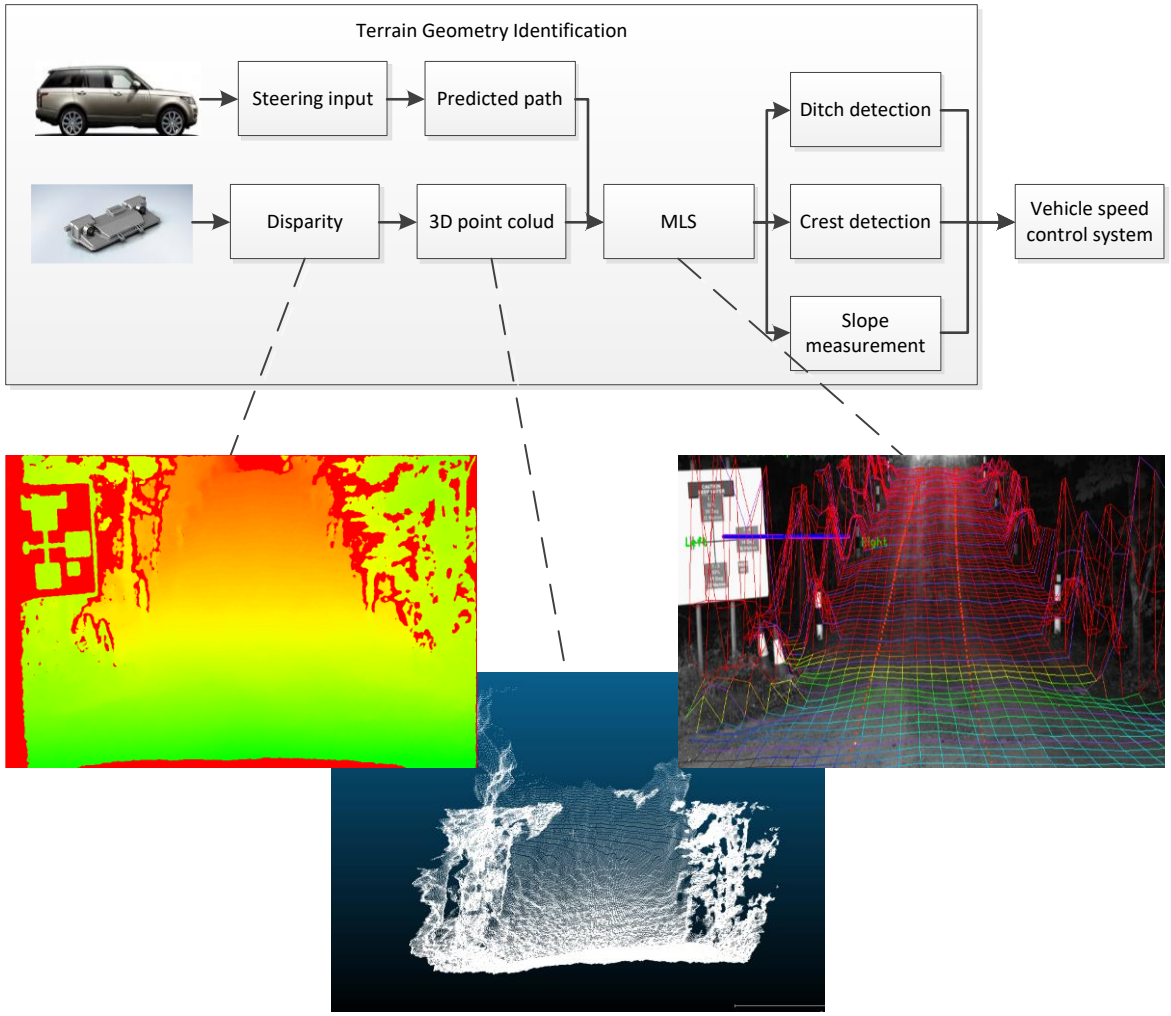

Figure 7.1. Overview of Terrain Geometry Identification system.

Section 7.1.1 describes point cloud generation form disparity. Section 7.1.2 introduces the point cloud transform from camera coordinate space to vehicle coordinates space. Section 7.1.3 describes MLS generation. Section 7.1.4 derives the predicted vehicle path from the steering input.

7.1.1 3D point cloud

A 3D point cloud is built from disparity map as follows. If camera parameters are known, given point in the disparity image $p = (x, y, d)$, where x, y are image coordinates and d is the stereo disparity, a

corresponding 3D point in camera coordinate space $P = (X, Y, Z)$ can be calculated based on the projective geometry equations as:

$$X = \frac{b(x - c_x)}{d},$$
$$Y = \frac{b(y - c_y)}{d}, \qquad (7.1)$$
$$Z = \frac{fb}{d}.$$

Camera parameters which need to be known are: b – camera baseline which is separation between two stereo cameras; f – camera focal length; c_x, c_y – camera principal point, point where optical axis intersects with image plane. In this work the camera calibration was performed by the supplier and the calibration parameters were provided. More details on stereo reconstruction are discussed in Submission 3. An example of a generated point cloud is shown in Figure 7.2.

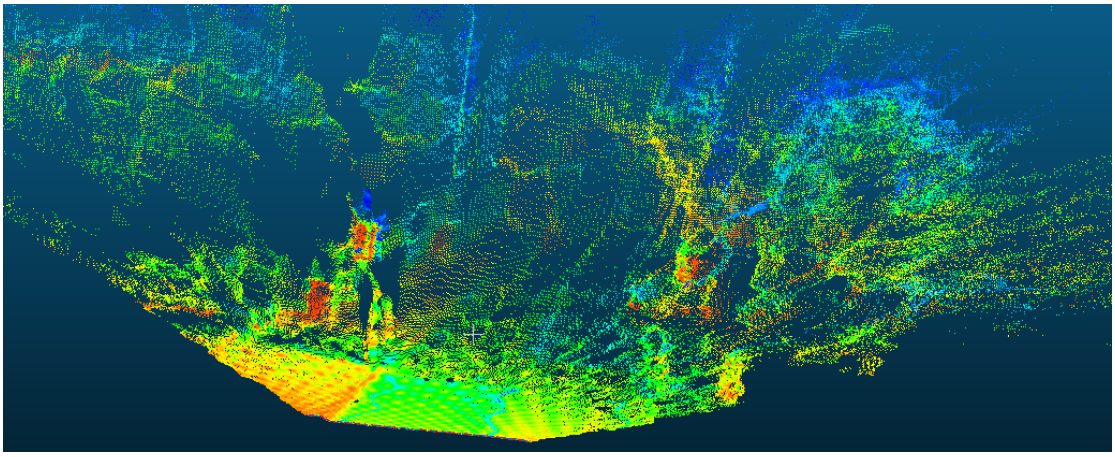

Figure 7.2 Point cloud generated from disparity image.

7.1.2 Vehicle coordinate space

3D point cloud represents unstructured data where each point is represented by $(x_{cam}, y_{cam}, z_{cam})$ coordinates in the camera coordinate space. The points are the translated into vehicle coordinate frame $(x_{veh}, y_{veh}, z_{veh})$ as show in Figure 7.3. The vehicle coordinate space is defined by a flat nominal ground plane underneath the vehicle, with origin of coordinate space being a middle point on the ground plane between the front vehicle wheels. This coordinate space has been chosen so that the distance to the objects would be reported with respect to the front wheels, which will come into contact with the surface first.

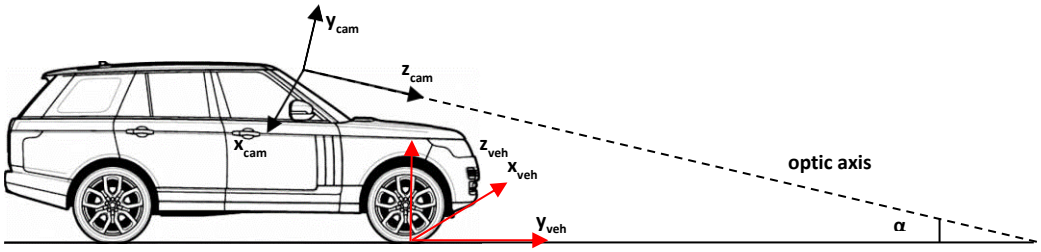

Figure 7.3. Camera and vehicle coordinate space.

7.1.3 Multi-Level Surface Map

The Multi-Level Surface Map (MLS) is a compact representation of a point cloud as discussed by Triebel [120], [194]. MLS map is a 2.5D representation, where the elevation points are grouped into Cartesian grid. The main advantage of using MLS is that it can represent multiple surfaces in the same grid cell, allowing disambiguation between ground surfaces and overhanging objects. In addition, each cell points are represented by a compact description, which includes mean, variance of points between in the cell, cell density and depth. This description reduces the memory and computational power required to further analyse the surface in comparison to point cloud as multiple points in a cell are described only by 4 descriptors. More details regarding this representation are included in Submission 3. Illustration of the MLS map is shown in Figure 7.4.

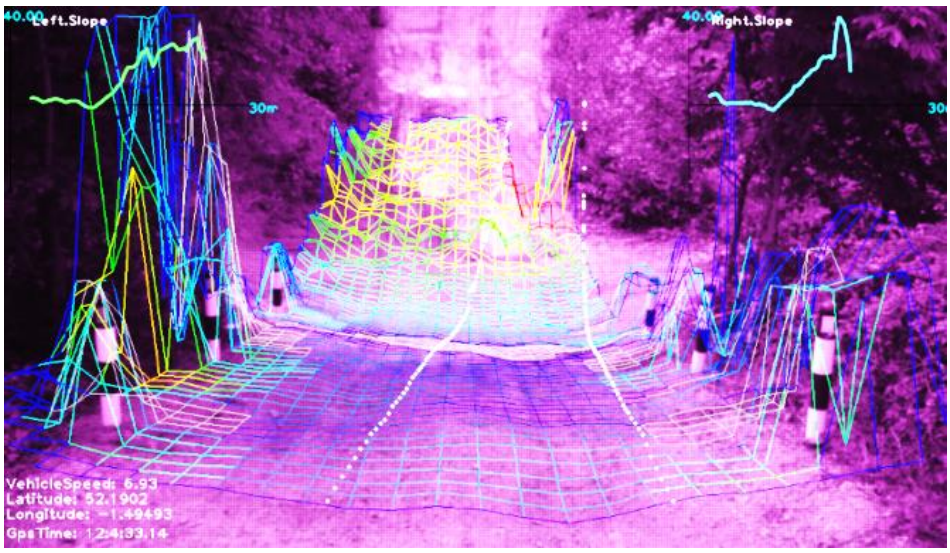

Figure 7.4. Multi-Level Surface Map. White dotted lines represent predicted vehicle path

In this implementation the cell size was chosen as *25 cm x 25 cm. 25 cm* as it is less than wheel diameter, hence objects which affect wheel – terrain interaction will be captured and *1 m x 1 m* coverage area will be represented only by 16 grid cells.

7.1.4 Predicted vehicle path

Terrain features will be identified within using the MLS map. However, only a subset of the features will be relevant to the predicted path of the vehicle. Since the driver is in control of the vehicle steering, the method to identify driver intended direction is based on driver's steering input. With the assumption of constant curvature and vehicle speed the path of the vehicle turning radiuses for both inner and outer front wheel can be calculated from trigonometry using Ackerman steering model [151]. The Ackerman steering is a term used to describe the vehicle geometry as presented in Figure 7.6. The ideal turning angles of the front wheels are given by $\theta_1$and θ_2 and define steering angles for the turn. Applied steering angle can be translated into the predicted path for left and right front wheels as shown in Figure 7.6.

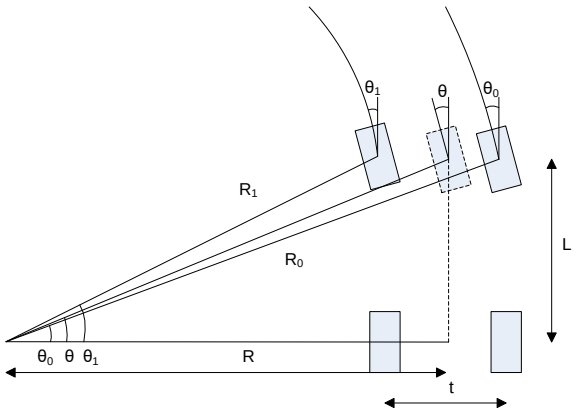

Figure 7.5. Turning radiuses for 2 front wheels based on Ackermann steering model

For each incremental distance of $cell\ size$ travelled along the circular path the x and y locations of the wheels as follows:

$$x_j(i) = R_n cos(\theta_j + i\theta_{inc}) - R$$
$$y_j(i) = R_n sin(\theta_j + i\theta_{inc}) - L \qquad (7.2)$$

where $\theta_{inc} = \frac{cell\ size}{R}$, $i \epsilon \mathrm{N}$, $j \epsilon \{0,1\}$, and R_1 is the corner radius length for inner front wheel, R_2 is the corner radius length for outer front wheel, L is the vehicle wheel base, t is the track width, R is the vehicle turn radius. The vehicle turn radius R is calculated from steering wheel angle θ:

$$R = \frac{L}{\tan\theta} . \qquad (7.3)$$

The wheel angles θ_0 and θ_1 can be calculated as:

$$\theta_j = arcsin\frac{L}{R_j}, \qquad (7.4)$$

$$R_1 = \sqrt{L^2 + (R - \frac{t}{2})^2}\ , \qquad (7.5)$$

$$R_0 = \sqrt{L^2 + (R + \frac{t}{2})^2}\ . \qquad (7.6)$$

7.2 Slope measurement

The measurement of the slope angle considers macro terrain features the size of which affects the vehicle orientation. Methods proposed in literature usually consider slope measurement as an input for traversability map, Seraji [102] incorporated only local slope of individual cells, Larson [105] consider the centre cell and its neighbouring cells within a window to generate measurement that has continues relationship within the local surrounding. The proposed method utilises the neighbourhood approach, as slope measurement of *25 cm* cell does not provide necessary scale to identify if a cell belongs to a larger slope. Hence this method proposes to utilise local neighbourhood of *7x7* cells as shown in Figure 7.6 representing a span of *1.75 m*. The local neighbourhood size been chosen to correspond to half of the vehicle length since the slopes of at least this length will influence the vehicle pitch angle significantly.

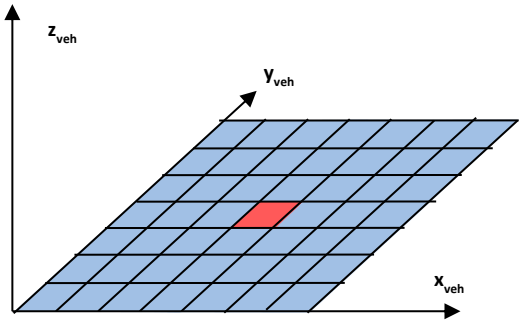

Figure 7.6. Local neighbourhood used for slope calculation. Central cell represented in red, local neighbourhood in blue.

The local neighbourhood and can be represented as a plane. The plane is fitted using the least square method based on Singular Value Decomposition (SVD). Data matrix *M* is shown in Equation (7.7), representing the set of *N* 3D points $(x_i, y_i, z_i), i \in N$ offset by the mean of the neighbourhood points $(\bar{x}, \bar{y}, \bar{z})$. After performing SVD the surface normal is represented by the vector corresponding to the smallest eigenvalue.

$$M = \begin{bmatrix} x_1 - \bar{x} & y1 - \bar{y} & z_1 - \bar{z} \\ \vdots & \vdots & \vdots \\ x_N - \bar{x} & y_N - \bar{y} & z_N - \bar{z} \end{bmatrix} \qquad (7.7)$$

The SVD of a matrix $A \in \mathbb{R}^{m \times n}$ is

$$A = USV^T \quad (7.8)$$

where $U \in \mathbb{R}^{m \times m}$, $V \in \mathbb{R}^{n \times n}$ and $S \in \mathbb{R}^{m \times n}$.

The columns of U are orthonormal eigenvectors ofAA^T, the columns of V are orthonormal eigenvectors of $A^T A$ and S is a diagonal matrix containing the square roots of eigenvalues from U or V in descending order.

Since the control system requires separate information about the forward slope (in the direction of the vehicle motion) the slope information is decomposed into forward slope as along z_{veh} axis illustrated in Figure 7.6. The calculated slope represents the continues relationship of the slope on a scale that will influence vehicle body position. This representation of the slope is used in this implementation and will be further referred to as *MLS slope map*. Illustration of *MLS slope map* is shown in Figure 7.7

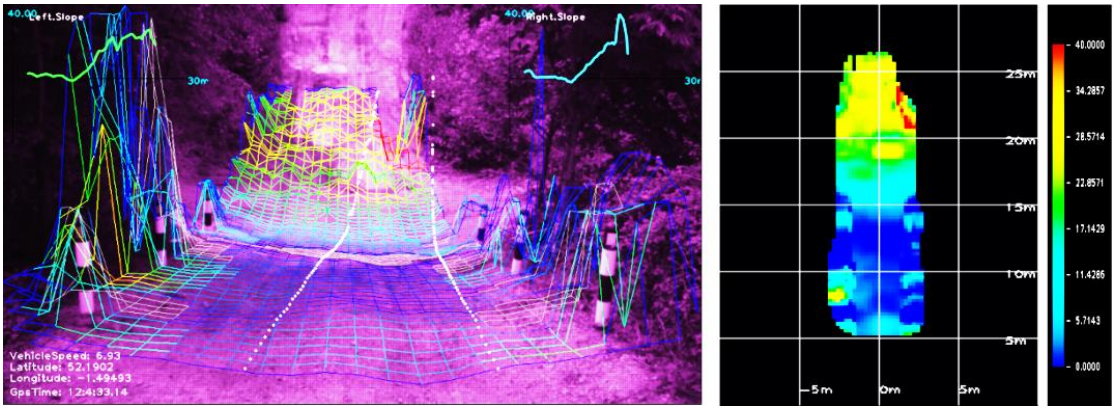

Figure 7.7. MLS slope map

The slope measured from a camera system is the relative slope between the vehicle and the surface. In order to obtain an absolute slope measurement, current vehicle pitch angle is added to the measured slope signal. Relevant *MLS slope map* cells corresponding to the predicted vehicle path are extracted, providing continuous slope measurement signal as a function of distance for left and right wheel paths as shown in Figure 7.8.

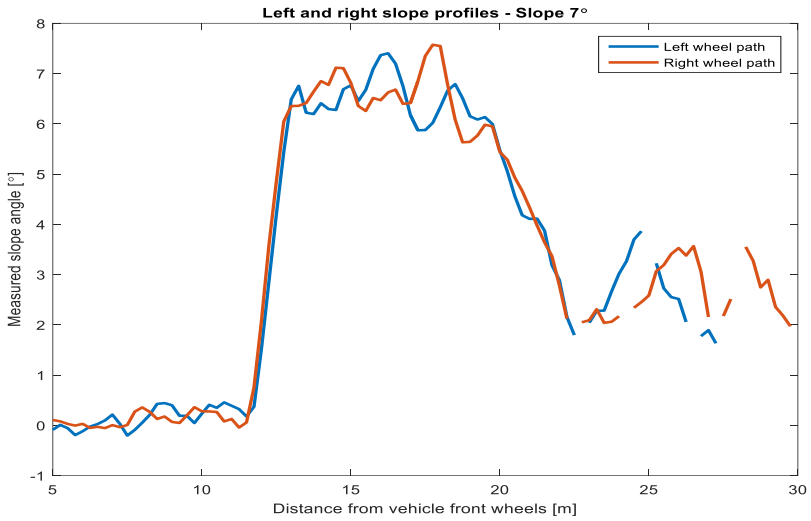

Figure 7.8 Measured slope profiles as a function of distance for left and right wheel predicted vehicle path.

7.3 Ditch detection

Negative obstacles such as ditches, potholes, terrain drops or steep negative slopes pose a challenge for the perception algorithms. In essence if the viewing angle does not allow a measurement of a surface a gap with missing measurements is observed in 3D world model. This is hazardous situation as it is impossible to know what is covered by the missing measurement patch. The proposed ditch detection method is similar to one proposed by Larson [94] where missing measurements from lidar scans were classified as ditches using SVM classification. The proposed method however does not use machine learning methods for classification, but rather relies on pure geometry based identification.

The proposed method leverages the fact that certain situations will result in *MLS map* cells not containing any measurements. Due to the camera shallow viewing angle, the bottom of the ditch is not visible hence cannot be measured, resulting in point cloud measurement gaps, as shown in Figure 7.9.

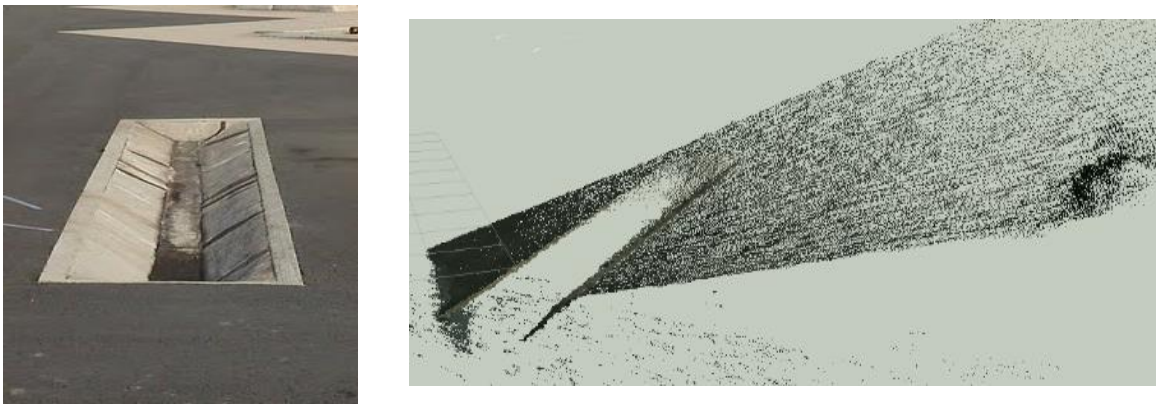

Figure 7.9 Example ditch (left) resulting in missing measurements in point cloud (right).

Empty cells in the MLS map are identified and grouped together. The empty cells are those that do not provide any measurements but are not the obstacle shadow cells. Obstacles are detected purely of the purpose of distinguishing between gap measurements resulting from a presence of large object or pothole. Obstacle detection is discussed in Submission 2. Empty cells are grouped together as an object and if the object lies in a predicted vehicle path as discussed in Section 7.1.4, the distance to the object is reported. Moreover the size of the reported object can be used further to implement different strategies depending on the object size.

7.4 Crest detection

Crest detection is achieved in a similar manner to ditch detection as crests are characterised as an area where a slope ends followed by a large gap where no data is available. Empty cells are merged as in case of ditch detection and if there is a preceding slope present it is classified as a crest. From the point of view of the vehicle behaviour there is a need to distinguish between ditches and crests as different vehicle behaviour is expected in each of these scenarios.

When approaching a crest, initially a relative slope is present in the data followed by a measurement gap, but once the vehicle is on the crest the slope becomes a flat plane followed by a ditch. Hence, the accelerometer data providing vehicle pitch angle is fused, providing measurements of the absolute slope.

In certain scenarios steep slope may cover the entire image area due to the camera FOV limits as shown in Figure 7.10. Figure 7.10 (right) shows top-down view of map identifying missing measurements - area with valid measurements in blue, followed by missing measurements in green, which would potentially be a valid crest. In order to differentiate this scenario from an actual crest, the detected crest position in the world model is projected back into image space to check if it is contained within the image bounds.

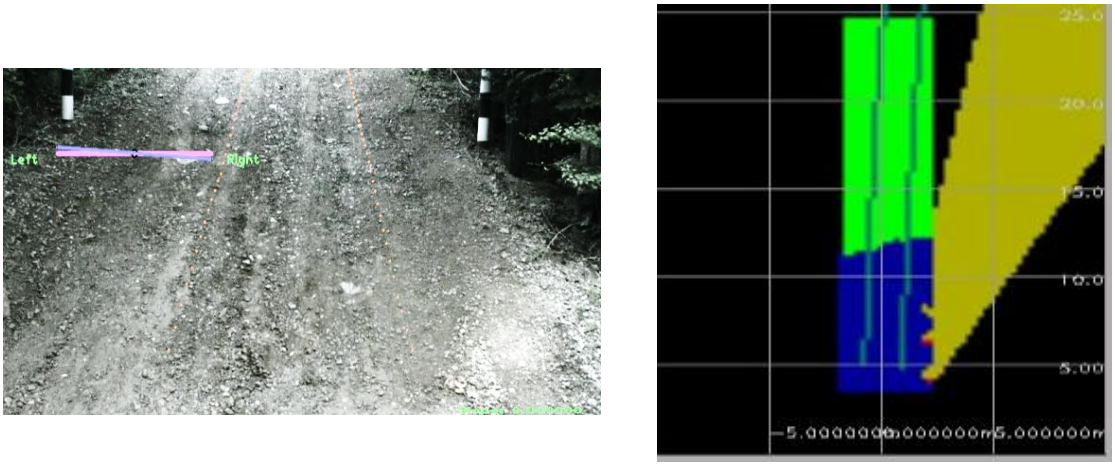

Figure 7.10. Illustration of steep slope in front of the vehicle covering entire field of view.

Further, the geometric constraints are applied to the detected missing measurement are. In order to be classified as crest, the width of the area needs to be at least 1.5 m to identify objects comparable with vehicle width with 0.5 m margin if not all the slope area is detected.

7.5 Computational performance

The system was tested on a PC machine with Intel i5-4670 processor. Since the computational performance of the proposed method is not constant as number of operations depends on the complexity of the scene, the average processing time over all the data sets is used as a metric of computational performance. Computation performance of the proposed method delivers processing of 10 fps. From the breakdown of the average computation time presented in Figure 7.11, it can be seen that the point cloud generation, MLS creation and slope calculation require the majority of the processing time. The processing time could also be reduced by not displaying the output, however during the testing it was essential to understand what the system detects hence the display time was included in the performance measurements.

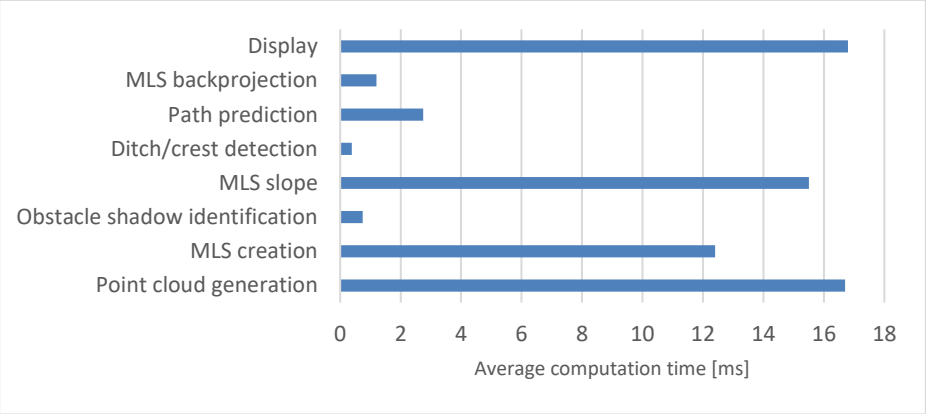

Figure 7.11. Average computation time for terrain geometry identification.

7.6 Experimental evaluation

The experimental evaluation was performed on real-world data sets. The real-world testing of the sensing system was preferred as it was not possible to model complex off-road environments within the commercially available toolset. Real-world testing highlights the limitations of the sensing system, hence the obtained results can be used to assess the expected performance of an overall TBSA system, providing confidence that it could be further progressed into series development.

The primary goal of this evaluation was to establish if production representative sensors are capable of delivering perception functionality required by the TBSA system. In order to validate the performance of each macro terrain feature identification method, a different set of experiments was performed for each component. In an off-road environment, it is difficult to obtain ground truth data, providing exact measurements of the terrain geometry. High resolution lidar scanners are used to establish a very accurate

measurement baseline for example when building high definition urban maps. However, these solutions are expensive, and not practical in off-road environments. Hence, instead of creating digital models, the ground truth data is provided by a set of available fabricated concrete objects for which geometry is known. These objects represent difficult to traverse geometries such as steep gradients, large concrete kerbs and ditches. Each of the detection components is evaluated based on the most important factors from the perspective of the control system: the accuracy the measurements, the accuracy of the reported distance and the detection range since these will affect the response time of the vehicle.

Furthermore, the terrain geometry identification method was qualitatively evaluated operating with TBSA system in an off-road environment. The validation within TBSA system was performed to identify if pre-emptive component operates in real off-road environments providing sufficient level of information for the vehicle to adapt the speed. As ground truth was not available, the pre-emptive component was evaluated qualitatively, showing that all the relevant terrain features were correctly identified allowing the vehicle to slow down pre-emptively in the presence of crests, ditches and slopes. Evaluation in the off-road environment also demonstrate performance issues which arise from the fact that the vehicle is steered by the driver and the pre-emptive measurements may not correspond to the actual vehicle path.

The following sections provide summary of the obtained results with more details presented in Submission 2.

7.6.1 Slope measurement accuracy

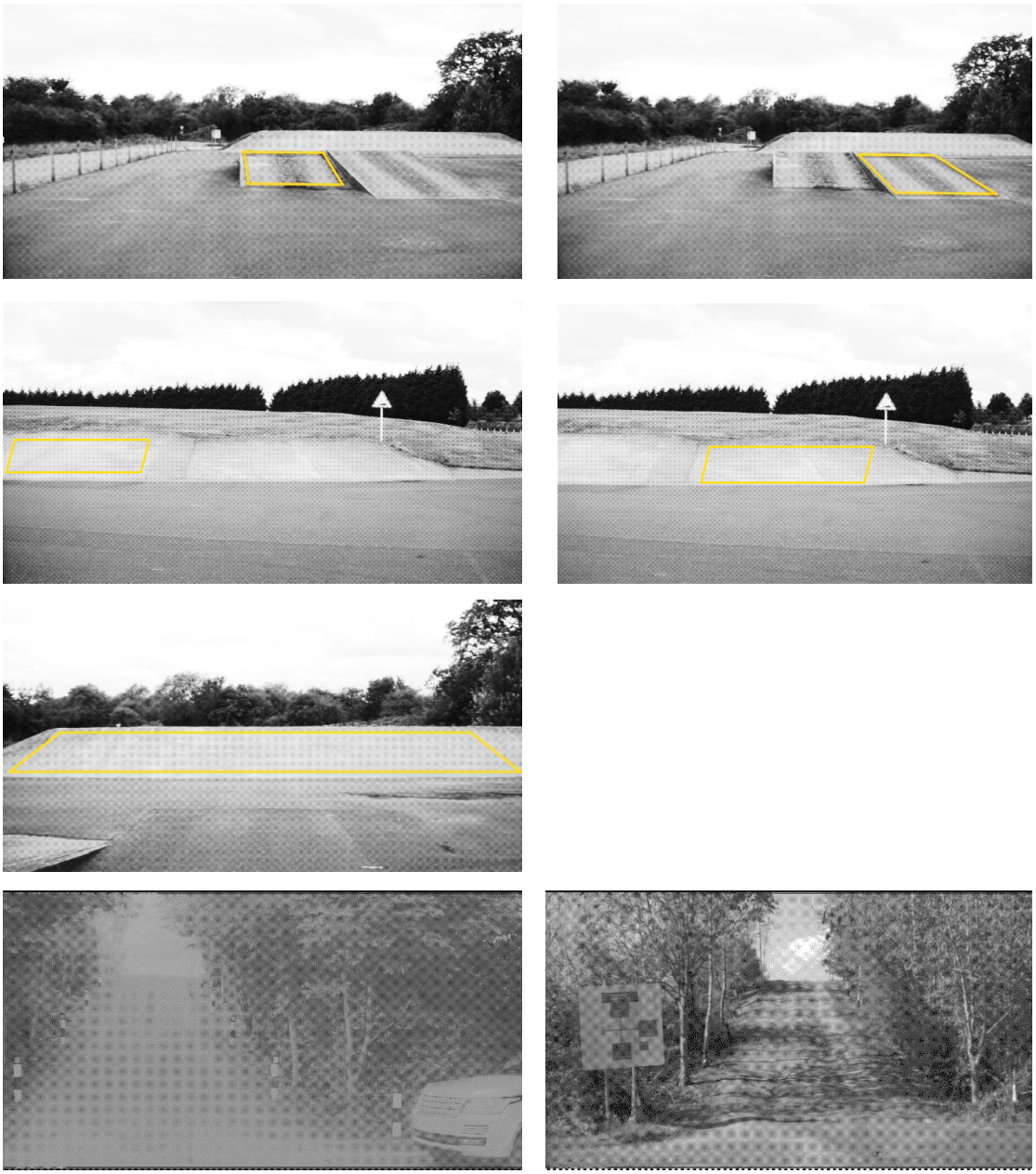

Figure 7.12 Manmade concrete slopes with homogeneous surface and off-road slopes.

Experiments performed on a set of man-made concrete objects presented in Figure 7.12 showed that it is possible to correctly identify slope areas and measure surface slope within +/-2.5° error with standard deviation below 4°. The off-road slopes were excluded from this experiment as they surface is not homogenous hence, it was not possible to establish ground truth for each cell in the MLS *slope map*. These experiments however were performed in a static configuration whereby the vehicle was stationary with respects to the target. The slopes were correctly identified in a range of 20 m. Figure 7.13 shows the plot of the measured slope means, with error bars showing standard deviation. As can be seen from the graph, slope measurements closer to the vehicle are more accurate due to the fact that the uncertainty of the measurements grows with distance. The majority of the available man-made structures have slope

angles between 5° and 8°, with only a single extreme slope with 28° angle. Within this experiment, where surface with homogenous gradient was required, only concrete mane made obstacles were used. Hence, due to the availability of these structures within the test facility, this experiment could not be performed on slopes within the range of 9° to 27°. More detailed results of this experiment are contained within Submission 2 [178].

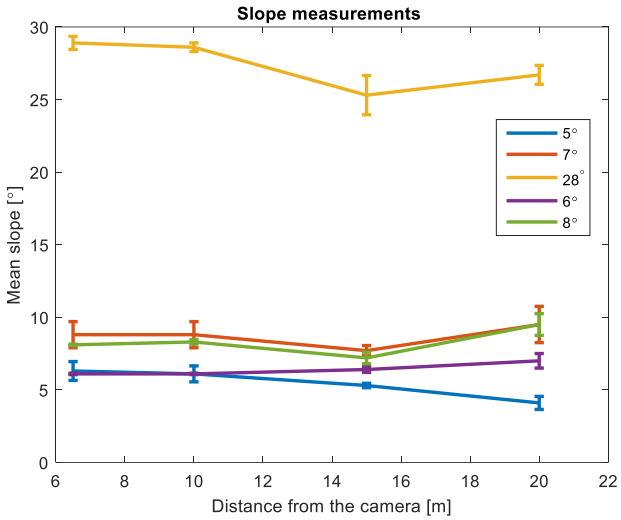

Figure 7.13. Slope measurements at various distances (6.5 m, 10 m, 15 m, 20 m). Each measurement plot shows calculated mean slope values and contains error bar which corresponds to the standard deviation.

In dynamic scenarios when the vehicle is moving, the vehicle pitch angle also affects the measurements obtained from the camera. Additionally only slope corresponding to predicted vehicle path is passed to the control system, hence only subset of measurements of the whole slope is used. In a set of dynamic experiments, it has been established that the slope measurement is still acceptable, and provides measurements within +/-2.5° error. It has also been observed that the standard deviation of measurements on man-made concrete objects was lower than in off-road scenarios (detailed results in Submission 2). In off-road scenarios, first the vehicle pitch movement is much higher and the surface is less homogenous, leading to higher deviation in the measured output as can be seen in Figure 7.14.

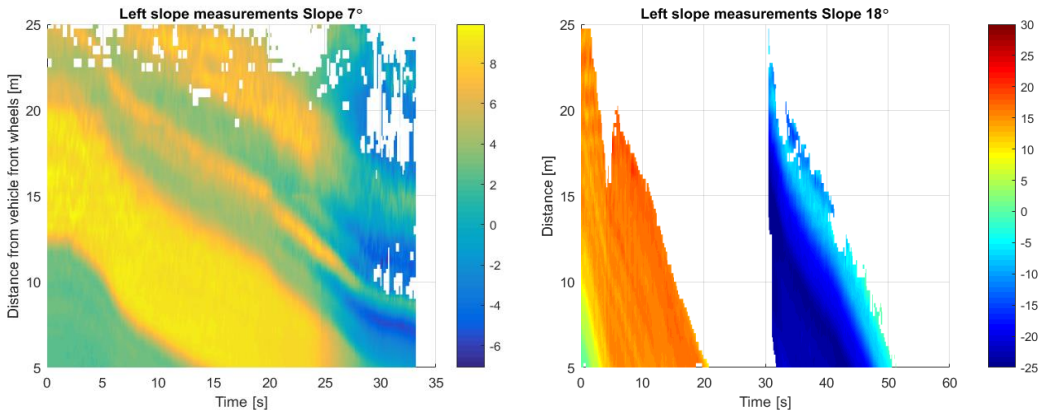

Figure 7.14. Slope profile over time for 7° slope and 18° slope

Figure 7.14 shows the output of slope profile for the predicted left wheel vehicle path over time. This signal for left and right wheel predicted vehicle path is send to the control algorithm. Based on the performed experiments, it can be established that this signal reflects the measured slope within +/-2.5° with a measurement range of 20 m, which is sufficient for controlling the vehicle speed. In addition, as the surface gets closer to the vehicle the measurements become more accurate, as noted in previous experiment, hence the crude speed adjustment can be done in advance and the speed control can be further refined as the object becomes closer to the vehicle.

7.6.2 Ditch and crest detection

Ditches and crests are reported as discrete objects hence the interface to the control system is distance to ditch and crest. The system reports the distance to the closest object in the predicted vehicle path.

The experiments performed on concrete structures with a clearly delimited crest (top two slopes in Figure 7.12) showed that the crest position can be established even for low surface gradient (slope 5°) up to 18 m. The accuracy of distance measurement for the last reported position is within 0.5 m. From the perspective of the vehicle control, if the distance to feature is misreported by 0.5 m the change of the vehicle speed with maximum deceleration rate of $2\,\frac{m}{s^2}$ from worst case scenario of initial speed of 30 kph the speed difference achieved at this distance would be 0.5 kph, at lower speeds this difference is much lower. What is worth noting is that the distance to the object is consistently reported as shown in Figure 7.15.

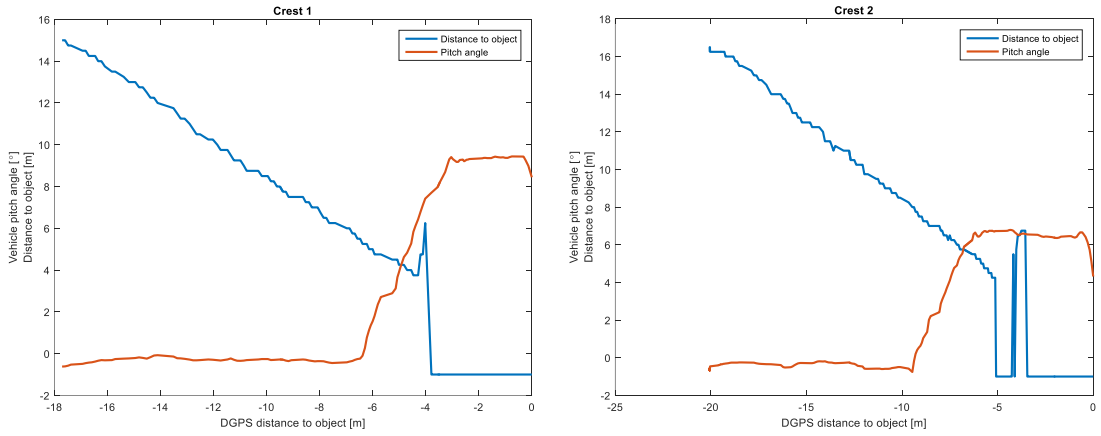

Figure 7.15. Off-road crest detecion results

In off-road scenarios the issue of validating the distance to crest is more complex. As the vehicle approaches the crest, since the crest feature is not a clearly defined edge, with the change of vehicle position and viewpoint the crest rolls forward (see Figure 7.17). This is reflected in the measurements as shown in Figure 7.17, the crest distance is reported consistently up to 5 m, then for next meter fluctuates.

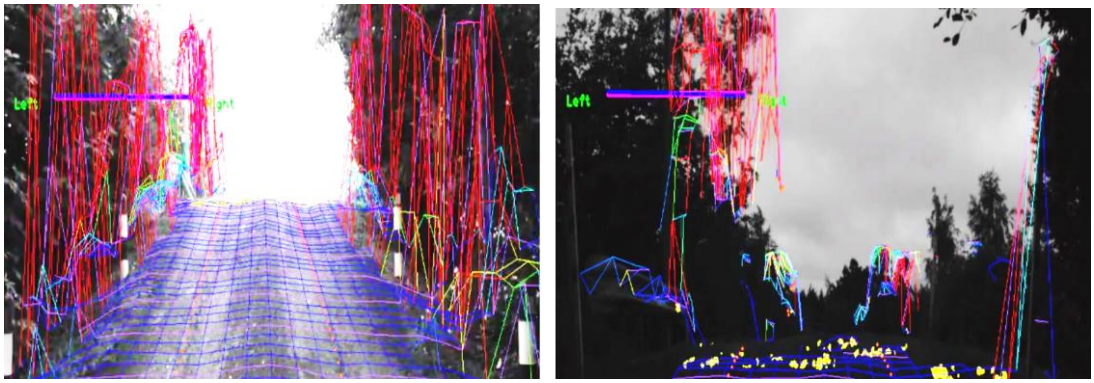

Figure 7.16 Rolling crest. When approaching crest the same object is tracked (left) up until the viewpoint changes resulting in rolling crest.

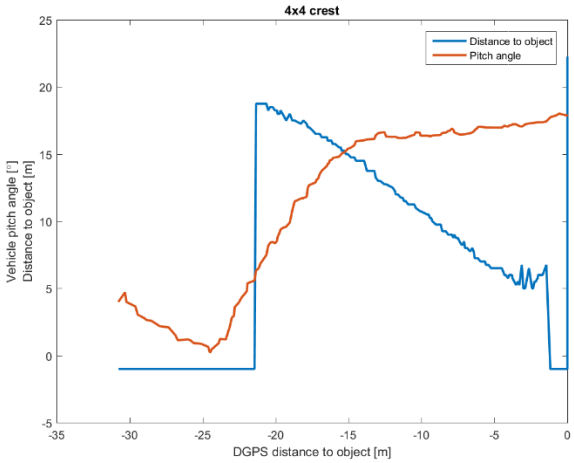

Figure 7.17. Off-road crest detection results.

Ditch detection validation was more difficult from methodological point of view. Only one concrete ditch with clearly delimitated edges were available for testing as shown in Figure 7.18. The larger 1 m wide and 40 cm deep ditch was detected at 12 m and the accuracy of last reported distance was within 0.5 m margin as in case of crests. The distance was also consistently reported as shown in Figure 7.19.

Figure 7.18. Concrete ditch used in experrments

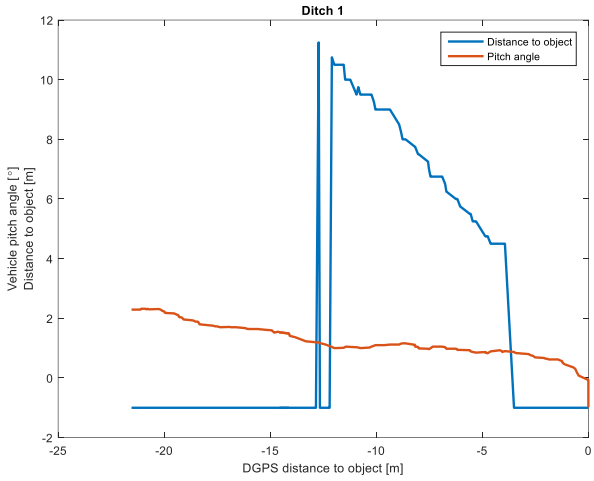

Figure 7.19. Reported distance to ditch.

7.6.3 Off-road performance

Off-road performance of the system was validated on an off-road route with variety of slopes and ditches and different surfaces. The route was 2 km long and consisted of 3 distinctive parts: smooth gravel surface which will be referred to as *Developing World* followed by a rougher section with small rocks and ruts referred to as *Cross Country* and last section of concrete surface high undulation of amplitude more than 30 cm called *Contructors Road*. This route has been chosen as it features 2 fords followed by slopes in the *Developing World* section, slope in the *Cross Country* section and the *Contructors Road* large undulations which are consider ditches. Since the perception system is used as an information source for the speed control this experiment also qualitatively validated the performance of the pre-emptive speed control method based on the terrain geometry identification complimenting reactive system.

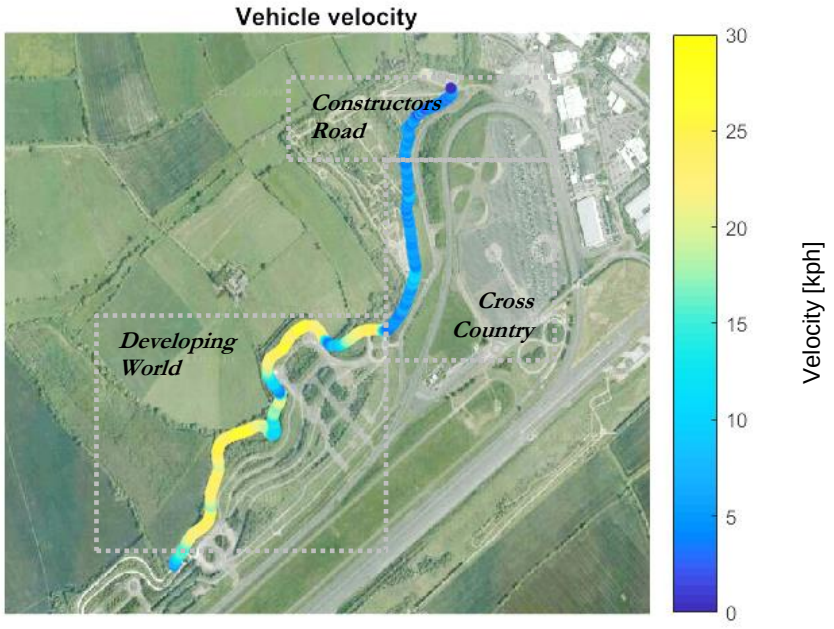

Figure 7.20. Off-road test route illustrating the performance of the pre-emptive and reactive system.

The perception system correctly identified slopes and ditches allowing TBSA system to slow down pre-emptively. The vehicle velocity is significantly affected by the detected ditches and crest (see Figure 7.21). The vehicle slows down before reaching the fords (location 1 and 2). The impact of the features detected later is not significant as the vehicle is already travelling at a lower speed due to rougher surface detected by the reactive system.

The benefit of the pre-emptive system is especially visible when the vehicle travels at higher velocities on a smooth surface hence the macro terrain features become the main driver behind speed adaptation (location 1 and 2). Vehicle speed is adapted before the vehicle follows a downhill slope to the ford as shown in Figure 7.22. In addition, in case of second ford (location 2), when exiting the ford, a crest is detected allowing the vehicle to slow down and the driver to assess the situation. The slope is steeper (see pitch angle) and the transition after the slope is more abrupt, hence the crest is detected.

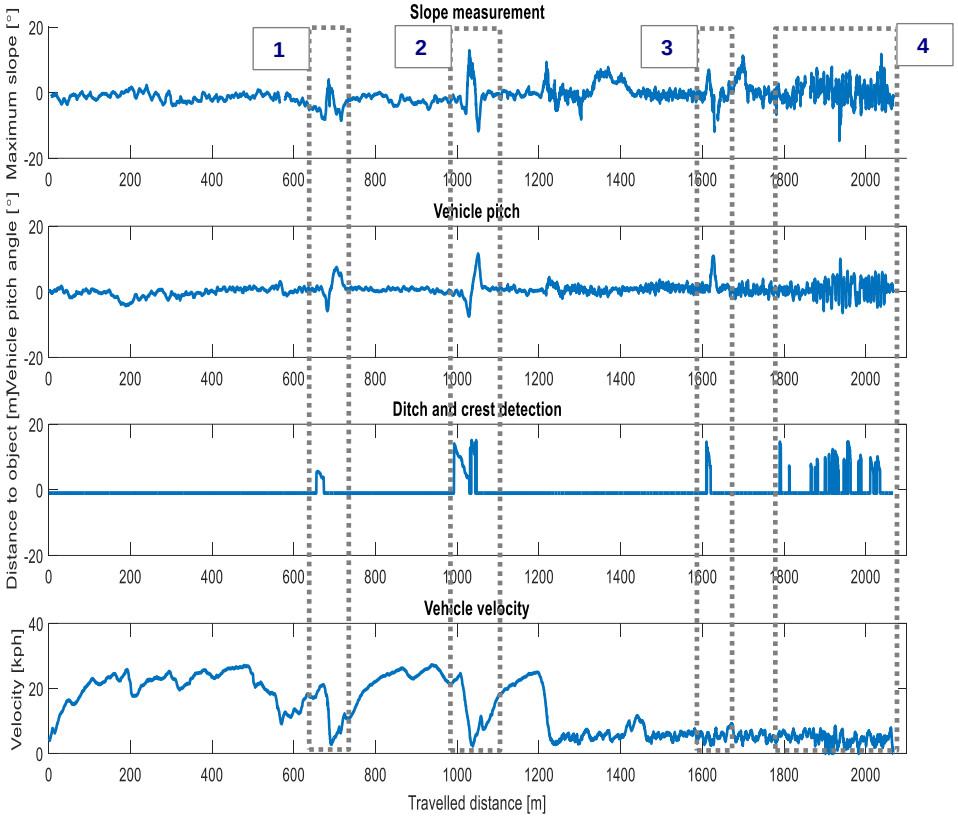

Figure 7.21. Slope measurements, ditch/crest detection results with vehicle velocity and vehicle pitch over the route.

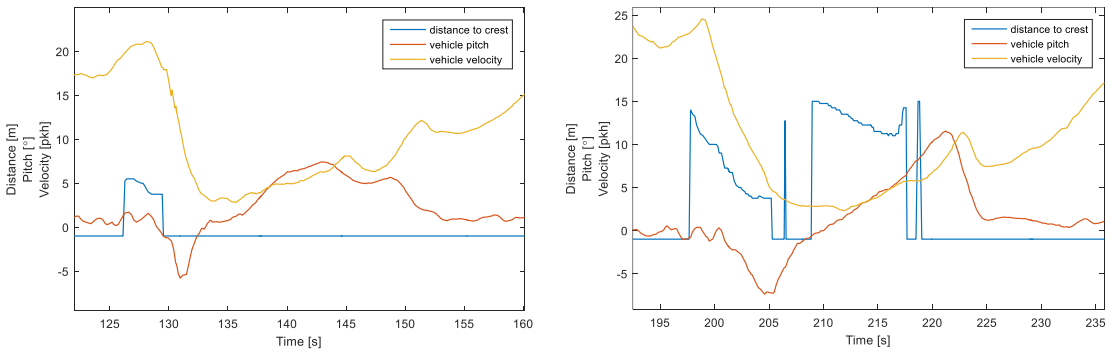

Figure 7.22. Vehicle slowing down before fords: left – location 1, right – location 2.

The perception system identified all the present crests and ditches on the route. The locations of these objects as detected by the system are indicated in Figure 7.23. Location 1 marked on the map is a ford, detected as shown in Figure 7.24. Location 2 marked on the map is a second ford followed by a slope where the crest was detected as shown in Figure 7.25 (a) and (b). The top down view maps in Figure 7.25 show the missing measurements which allows identification of ditches and crest in green, with khaki colour marking obstacles and their shadows. The correctly detected crest in location 3 is shown in Figure

7.26 (a). The examples of detected ditches on *Constructors Road* section (location 4) are shown in Figure 7.26 (b)(c). In this area multiple ditches were correctly identified and for brevity only exemplars are shown. It is important to emphasise that no false positive detections were made.

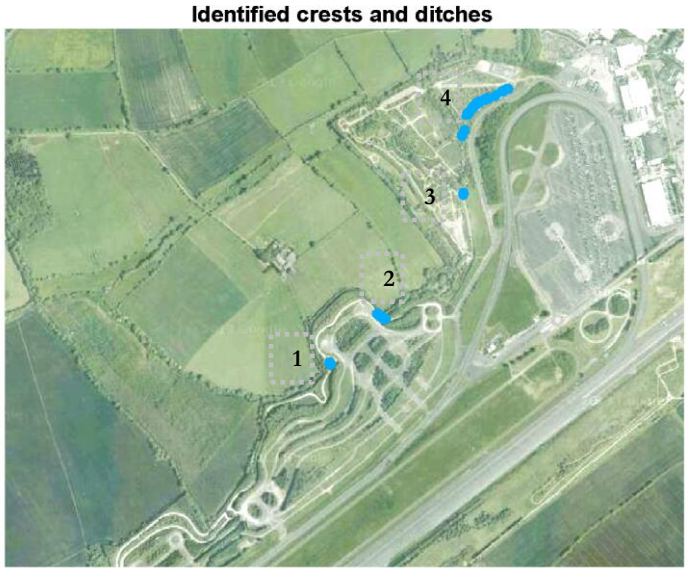

Figure 7.23. Detected crests and ditches.

Figure 7.24. Detected ford corresponding to location 1. On the right – crest/ditch map where green colour corresponds to identified objects

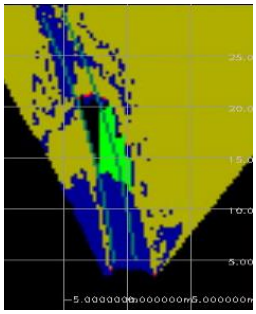

(a)

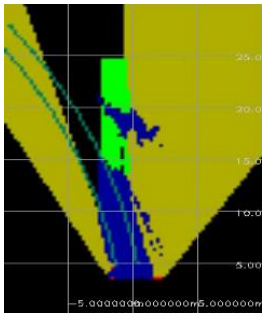

(b)

Figure 7.25. Detected ditches and slopes: (a) ford corresponding to location 2, (b) crest corresponding to location 2. On the right – crest/ditch map where green colour corresponds to identified objects.

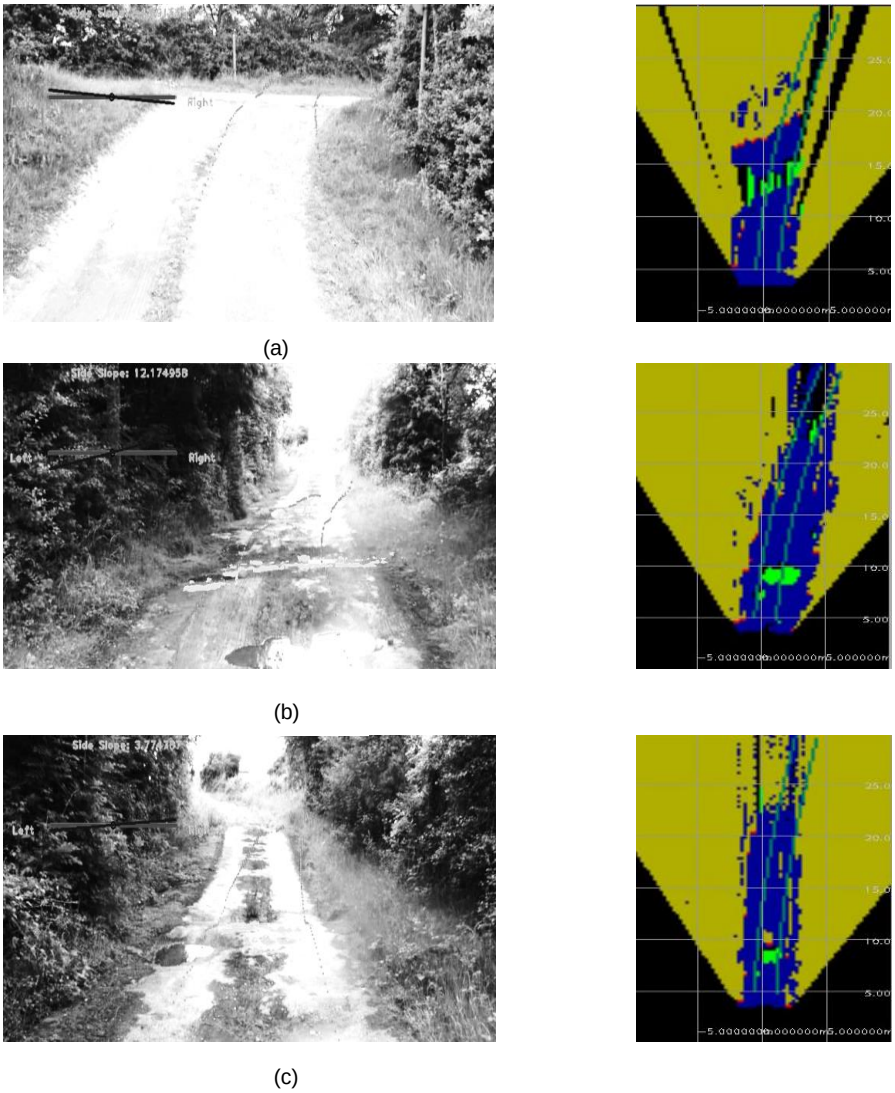

Figure 7.26. Detected ditches and slopes: (a) crest corresponding to location 3, (b) (c) example ditches detected in location 4. On the right – crest/ditch map where green colour corresponds to identified objects.

Another important factor to consider is the detection range. Figure 7.21 shows the distance to the object detected (crest/ditch). The first ford is detected only at a short distance of 8 m whereas the second ford and the crest are detected at 17 m. The difference stems from the fact that the approach towards the first ford is at the bend and the ford becomes visible in the camera field of view only at this distance. Smaller ditch features in the *Constructors road* are detected at a shorter range (10-12 m) due to their smaller size as visible in Figure 7.26 (b)(c). The green areas corresponding to the missing measurements are much smaller and become visible only at a shorter distance.

The performance of the slope measurement also correctly identify the negative slopes preceding the ford and positive slopes following the fords as seen in Figure 7.21. The locations of the slopes correspond to the pitch angle measurements obtained from the IMU unit on the vehicle. There are several spikes in the slope measurements which are incorrect, as the vehicle pitch angle does not show significant changes (between locations 2 and 3; between locations 3 and 4). This is caused by the imprecision of the path

prediction mechanism. As the vehicle approaches bends, incorrect area of the surface is measured where the vehicle is not going to travel. As the steering wheel angle changes this measurements are disregarded by the vehicle speed controller hence it does not affect the vehicle velocity as the vehicle is slowing down due to the steering angle applied.

Only terrain geometry is used as a speed predictor input hence the terrain is assumed to be non-deformable meaning that the measured terrain geometry corresponds to a solid surface. Deformable terrains such as sand and mud exert less force on the vehicle than, for example, concrete surface due to the fact that deformable surfaces will change their geometry once the vehicle traverses them. Although rippled sand surface geometry measurements can be extremely rough the vehicle will not experience excessive acceleration levels since the surface will deform under the vehicle mass. The pre-emptive system takes a conservative, worst case scenario approach and calculates the recommended vehicle speed based on the assumption that the traversed surface is solid. The terrain composition will affect deformability of the surface, however assessment of terrain composition has been shown to be a challenging problem [83]. As discussed in Submission 1 [184], this issue could be alleviated via the augmentation with the terrain recognition system which infers terrain class from visual properties. Further, sensor fusion with other sensing modalities such as radars or ultrasonics could also provide terrain recognition capability [195], [196].

7.7 Conclusions

The research presented in this chapter focused on identification of macro-terrain features for the purpose of vehicle speed adaptation. The aim was to develop a robust, real-time method that can perform in real-world conditions. This work has developed an image processing framework for terrain geometry identification with particular focus on detection of crest and ditches and slope measurement. It has been shown that the proposed method is effective in identifying ditches and crest with accuracy of distance estimation of 0.5 m. Crests were detected up to 18 m, whereas ditch detection range highly depends on the ditch geometry, depending on the ditch size. The slopes were shown to be measured with accuracy of +/- 2.5° in controlled environment on concrete objects.

The proposed system was also validated in conjunction with TBSA in off-road environments showing that the production representative sensors and the proposed method can robustly identify terrain geometry in real-time at 10 fps. In conclusion, the proposed solution addresses a known deficiency of the reactive TBSA system by pre-emptively identifying macro terrain features allowing the vehicle to adjust the speed before reaching the terrain.

8 Pre-emptive speed recommendation using surface roughness

This chapter addresses the question of how to identify surface roughness, which have been identified in Section 5.2 as a crucial element for the pre-emptive perception system for TBSA. As discussed in Section 5.2 the surface roughness measurement should allow the system to identify transitions between surfaces of different roughness and discrete micro terrain features such as kerbs, rocks and logs which will not be identified as macro terrain features. The purpose of identifying surface roughness is to recommend the vehicle speed to achieve a target level of passenger comfort based on the vibration levels experienced by the vehicle as discussed in Section 5.2. Since the relationship between the pre-emptively measured surface roughness and target vehicle speed was unknown, this work also addresses the problem of mapping the proposed roughness metric to target vehicle speed.

Literature in the domain of off-road perception and controls focuses on custom build vehicles and robots with extensive suite of sensors such as lidars and cameras. These systems are designed to operate autonomously hence the focus of perception is to create the world model, describing hazards so the vehicle can avoid them. Adjusting the vehicle speed based on pre-emptive information is either simplified to choosing the speed level based on the pre-defined terrain class [149], using a previously acquired map of the environment with speed limit levels or mapping terrain traversability into vehicle speed. The proposed approaches do not consider the levels of vehicle vibration that will be excerpt on the vehicle but rather try to minimise the risk of severe damage to the vehicle by planning conservative routes. To the author's knowledge adjusting the vehicle speed pre-emptively to maintain passenger comfort has not yet been achieved, both within the realms of automotive industry or the autonomous vehicle research community.

The study presented in this chapter analyses the performance of the method for assessing surface roughness from the remote sensed data on the vehicle and the ability of surface roughness descriptors to distinguish between different rough surfaces. Many different methods are proposed in the literature to assess road surface roughness, but most of them were used to assess the condition of the roads for maintenance or to produce simulation data for vehicle durability testing, and only a small number of methods were used for the purpose of speed adaptation. The roughness descriptors proposed for the purpose of speed adaptation however do not take into account passenger comfort but focus on limiting excessive shock experienced by the vehicle [170]. This work presents a method that enables the vehicle to acquire a roughness measurement for vehicle speed selection taking into account the passenger comfort.

The core contribution of this study is the design and implementation of a novel pre-emptive speed recommendation system that allows the vehicle to adapt the speed dynamically based on the roughness

of the surface ahead. The proposed surface roughness descriptor was used for characterisation of road networks roughness and simulations of the vehicle reliability, but was not used for characterisation of the short surface intervals especially for the purpose of speed adaptation. This work shows novel use of this roughness descriptor and both experimentally and analytically validates its use for the purpose of speed adaptation.

The proposed solution has been implemented on a production ready sensors, showing that the system is feasible to be introduced in the next generation of Land Rover vehicles. Extensive experimental validation quantifies the benefits of employing the pre-emptive system to reduce the number of events causing extreme passenger excitation to compliment the performance of the purely reactive system. In contrast to previous research, the system was designed with limited capability commercially available automotive sensor and the performance of the system was extensively assessed on long stretches of various surfaces showing that the system is capable of adapting the vehicle speed within range of +/- 5 kph.

Section 8.1 introduces the proposed processing pipeline. Section 8.2 describes method for acquiring surface profile. Section 8.3 introduces the training data set used to derive the roughness descriptors and velocity mapping.

Sections 8.4 and 8.6 present the proposed surface roughness descriptor and the speed recommendation methods including a machine learning and a direct functional mapping approach. The roughness descriptors are evaluated qualitatively on a range of different surfaces showing the correlation of the roughness measurement from the stereo camera and the acceleration levels linked to passenger comfort. The speed recommendation performance is analysed on these surfaces with respect to an expert chosen target vehicle velocity (Section 8.7).

Section 8.8 presents an extensive evaluation of the pre-emptive speed recommendation system in contrast with a purely reactive system. The performance is analysed in terms of the potential improvements of speed selection while approaching terrain events that cause discomfort when approached too rapidly by the reactive system while still maintaining speeds similar to the reactive system when the comfort metric is within the acceptable limits to ensure that the overall progress of the vehicle is not hindered.

8.1 Method

In this chapter the method which enables the vehicle to robustly estimate roughness to adjust the vehicle speed is presented. The diagram of the processing pipeline is presented in Figure 8.1. From the Multi Level Surface (MLS) height map and the predicted vehicle path as introduced in section 7.1, the Power Spectral Density (PSD) of the surface height profile is calculated. PSD is then processed by a mapping

function which assigns a recommended vehicle velocity based on the surface roughness described by the PSD.

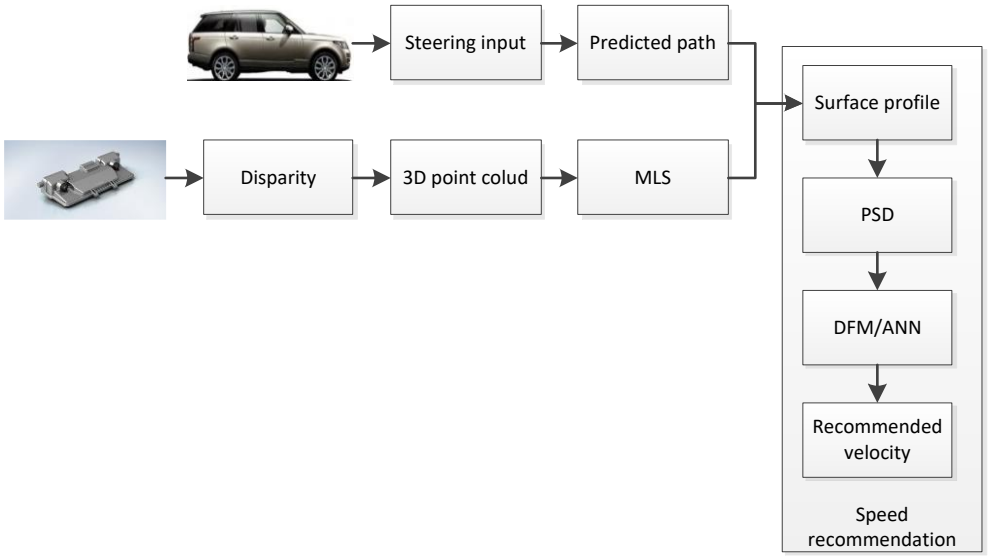

Figure 8.1. Pre-emptive speed recommendation processing pipeline.

The presented method is based on PSD of the surface profile frequency spectrum as discussed in Section 3.7.2. This approach incorporates instantaneous surface profile measurements ahead of the vehicle with the predicted vehicle path to relate the future state of the vehicle with the scene ahead. The key of this approach is that PSD can be directly mapped onto recommended vehicle speeds as PSD represents energy content of the surface profile. The roughness estimator is then used to establish the recommended vehicle speed. This is achieved through two distinct approaches, one using machine learning with Artificial Neural Networks (ANN) [197] and another using a regression model which in this work will be referred to as Direct Functional Mapping (DFM). Training data is obtained by driving through a representative set of surfaces with the target speed assigned by an expert. This acts as a control signal that is used for training as a reference. This data is then used both to train a supervised classifier which is able to predict the vehicle speed and to create a direct mapping function between roughness descriptor and the target vehicle speed. These two approaches were developed in parallel in order to understand which of these would be a more suitable approach. The learning approach should be able to transfer the capability of sensing the surface roughness from the profile ahead to the appropriate vehicle speed.

The method is evaluated on the data sets consisting of different surface samples with varying roughness levels. The experiments measure the ability of the surface roughness descriptor to distinguish between different surfaces and also the ability to recommend the vehicle speeds on homogenous surface types.

The method is derived in three stages. First the surface roughness measurement is derived showing the capability of distinguishing different surfaces based on PSD roughness metric (Section 8.5.1). Secondly,

this relationship is used to build a mapping function for establishing appropriate vehicle speed purely based on the pre-emptive measurements taken with a stereo camera (Section 8.6.3). The relationship between the target speed and surface roughness is then derived.

8.2 Dataset

The set consists of 50 m straight segments of homogeneous surfaces to decouple the effect of varying conditions of the surface as well as the sampling of the surface profile on non-straight paths. It is crucial that the dataset consists of homogenous surfaces in order to establish the correct mapping between the surface roughness descriptor and the chosen target vehicle speed.

The selection of surfaces chosen covers a range of surfaces with varying roughness types requiring different vehicle speeds. The target vehicle velocities for each of the terrain samples were chosen by the off-road experts as safe and comfortable velocities that the vehicle should achieve on these surfaces[1]. The overview of selected surfaces constituting the dataset is summarised in Table 8.1 with example images presented in Figure 8.2. The selection in this section is also limited to exemplars which are used for creating the speed mapping, whereas a more extensive data set is used for the pre-emptive speed recommendation system validation against the reactive speed recommendation system in Section 8.8.

Set	Target speed [kph]	Example image	Description
riverbed	3	a	Extremely rough, rocky surface, any velocity above 5kph will cause vehicle damage
tarmac	30[2]	b	Smooth tarmac surface
dirt 1	30	c	Smooth dirt track with potholes
dirt 2	30	d	Smooth dirt track
perimeter 1	20	e	Relatively smooth surface with small rocks
cross country 1	15	f	Track consisting of dirt and small rocks with undulations and large potholes
cross country 2	10	g	Track consisting of dirt and small rocks with undulations and large potholes

Table 8.1. Surface roughness dataset

Riverbed data set is the most challenging terrain consisting of large rocks and demanding very low vehicle speed of 3kph. *Tarmac*, *dirt 1*, *dirt 2* are the smoothest surfaces allowing maximum vehicle speed of 30 kph. *Perimeter 1* is a relatively smooth surface with potholes and small rocks requesting slower speeds of

[1] Personal communication with JLR Peerless Effortless All Terrain team, June 2015

[2] Maximum system allowable speed due to system limits. Higher vehicle speed can also be recommended for tarmac, however the overall system speed limitation of 30 kph dictates this recommendation.

20 kph. *Cross country* are slightly rutted tracks with undulation and potholes hence the requested vehicle speed is between 10 and 15 kph.

Figure 8.2. Example images representing data set summarised in Table 8.1.

8.3 Acquiring the surface profile

The surface height profile is acquired from the MLS map for the predicted vehicle path of left and right wheel as discussed in Section 7.1.4. The road profile is measured in the range between 5-15 m from the front wheels and can be defined as a vector of elevation measurements with the corresponding vector of distances from the vehicle:

$$\begin{cases} \mathrm{z} = \{z_0, \dots z_i \dots, z_n\} \\ \mathrm{d} = \{d_0, \dots d_i \dots, d_n\} \end{cases} \quad (8.1)$$

where z_i is elevation measurement along the vehicle path and d_i corresponding distance from the vehicle front wheels (x_i = 5 m, x_n = 15 m). Locations of the points on ground plane are derived from the predicted vehicle path as discussed in section 7.1.4.

The surface profile is measured up to 15 m due to the fact that as the uncertainty of measurements grows with distance, it has been observed that the profile height measurements above 15 m were noisy. Although, it has been shown that it is possible to identify macro terrain features up to 20 m, micro terrain features are not accurately represented above 15 m.

8.4 Surface roughness

This section introduces Power Spectral Density as a surface roughness descriptor and analyses the data set showing that PSD can provide discrimination between surfaces of different roughness. Further, the vehicle response in terms of vertical acceleration on different surfaces is compared with PSD based surface roughness descriptor.

8.4.1 Power Spectral Density

Power Spectral Density (PSD) have been chosen as a representation of surface roughness due to the fact that it has been shown to correlate with the weighted mean-square acceleration amplitude representing passenger comfort [159]. As PSD takes into the impact of consecutive height changes, which will affect the vehicle response, it is much more powerful descriptor than local MLS patch roughness descriptors as discussed in section 3.4.

PSD of a discrete signal x_L(n) containing L samples can be calculated from the N-point periodogram estimate of the PSD using fast Fourier Transform:

$$\mathrm{G}(n_k) = \frac{|X_L(n_k)|^2}{n_s L} \qquad n_k = \frac{k n_s}{N}, \quad k = 0,1, \dots., N-1 \quad (8.2)$$

Where the N-point Fast Fourier Transform is defined as follows:

$$X_L(n_k) = \sum_{m=0}^{N-1} x_L(m) e^{-2\pi jkm/N}, \quad (8.3)$$

where $G(n_k)$ is Power Spectral Density as a function of discrete spatial frequency points n_k, $X_L(n_k)$ is the N-point Fast Fourier transform, n_s is the spatial sampling frequency, L is the length of the profile signal.

ISO standard "SO 8608:1995, Mechanical vibration - Road surface profiles - Reporting of measured data" [162] provides recommendation on calculation of PSD from surface profiles, however the data obtained from profilometers or laser meters provide accurate measurements of road profiles over long distances (typically kilometres), where body motion of the measurement device has been compensated for. Therefore the effects of a discontinued signal is only visible for spatial frequencies that are well below 10^{-3} cycles/m and no effects of the measurement device motion are present. Due to the fact that the profile measurement window in our system spans over 10 m the effect of signal discontinuity at the end of measurement will be visible in the PSD. In addition the vehicle motion (pitch) introduces gradient in the profile measurement which affects the PSD. Figure 8.3 illustrates the measured elevation profile with visible gradient introduced by the pitching vehicle. The same elevation profile has been levelled by fitting the line through and offsetting the gradient bias. As seen in the plot of Power Spectral Density, this has two effects: firstly the low spatial frequency component representing the gradient has been removed, secondly the high spatial frequency component has lower amplitude due to limiting the spectrum leakage. In order to limit further the effects of spectral leakage introducing side lobes as spurious frequencies due to the abrupt signal truncation in the spatial domain, a spatial profile signal is windowed with Hamming window filter (as recommended in the ISO standard [162]).

Power Spectral Density is represented in dB/(cycle/m):

$$G_{dB}(n_k) = 20\log(G(n_k)). \quad (8.4)$$

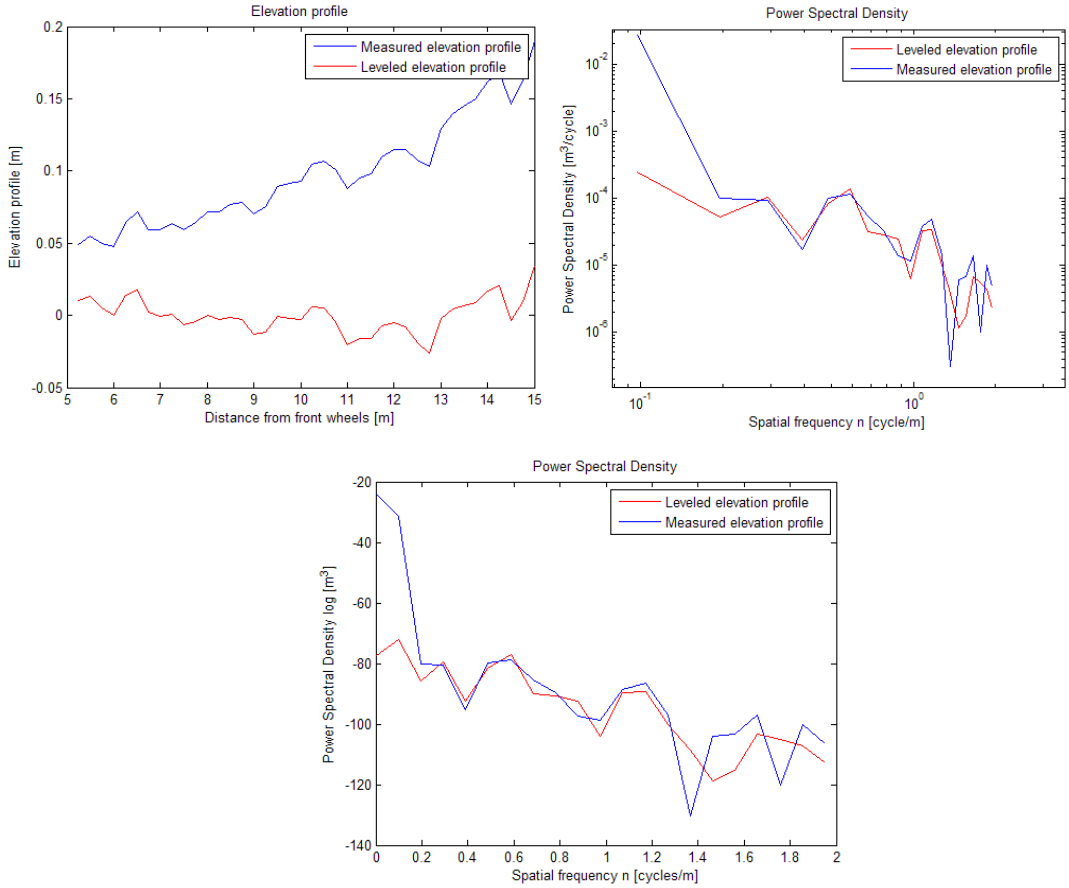

Figure 8.3. Surface profiles (top left) and associated Power Spectral Densities (top right) and Power Spectral Densities in dB (bottom).

8.5 PSD evaluation

In order to evaluate the usefulness of PSD as a roughness descriptor, the average PSD was calculated over a data set presented in Section 8.2. The average PSDs for different surfaces are plotted in Figure 8.4. The magnitude of the PSD diminishes with increased frequency in accordance with the prior research on the use of PSD in paved roads surface measurements [152]. The angle of the line fitted in Figure 8.4 represents the parameter called *weaviness* of the road and is usually similar for all type of roads. The differentiating factor describing the roughness of the surface is the magnitude of PSD. The scaling factor applied corresponds to the line fitted in Figure 8.4, to offset the effect of diminishing magnitudes of higher frequency signals and has been experimentally derived from the presented dataset. A dataset representing a medium roughness surface has been chosen which demands vehicle speed of 15 kph; it is in the middle of operating velocities.

In order to illustrate the correlation of the obtained values with the perceived surface roughness in the vehicle, vehicle vertical acceleration and the speeds for the same data sets are plotted in Figure 8.5. It can be seen that the *riverbed* data set has the highest PSD magnitudes (above -60 dB) and this corresponds to the lowest vehicle speed (below 5 kph) with highest levels of z-acceleration (above 0.5 m/s^2), which can be classified as the roughest surface. In contrast the datasets *tarmac* and *dirt1* have lowest magnitudes

of PSD (below -70 dB) and lowest levels of vertical acceleration (below 0.5 m/s²) even with higher vehicle velocities (above 20 kph).

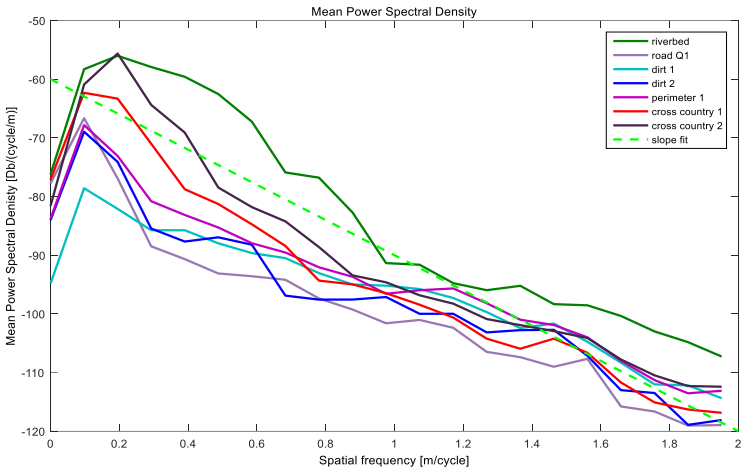

Figure 8.4. Power Spectral Density on different surfaces.

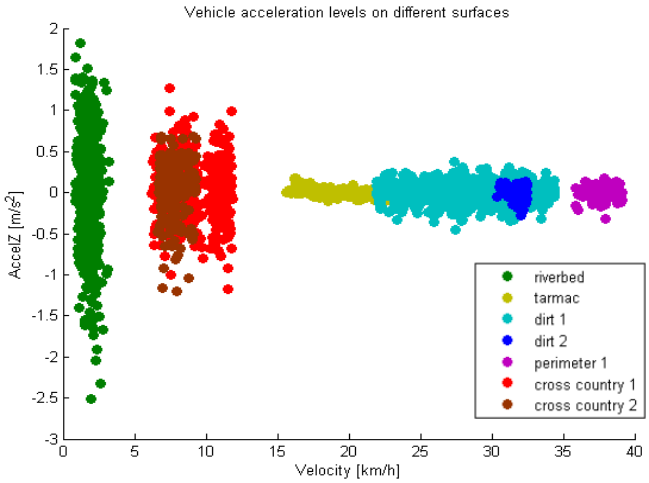

Figure 8.5. Vehicle Z-acceleration and velocities on different surfaces

Rough surfaces such as *riverbed* and *cross country* show high amplitude surface profile changes resulting in high PSD coefficients as shown in Figure 8.6 and Figure 8.7. Surface profiles measured from 5-15 m from the vehicle are composed together over time producing the mosaic showing how terrain features get closer to the vehicle. High amplitude surface profile change as visible in red in Figure 8.6 (*riverbed*) produce high amplitude PSD response also illustrated in red. Smoother surfaces such as *tarmac* and *dirt* have less amplitude variation of the surface profile resulting in PSD coefficients with significantly lower amplitude represented by blue and yellow in Figure 8.6 and Figure 8.7.

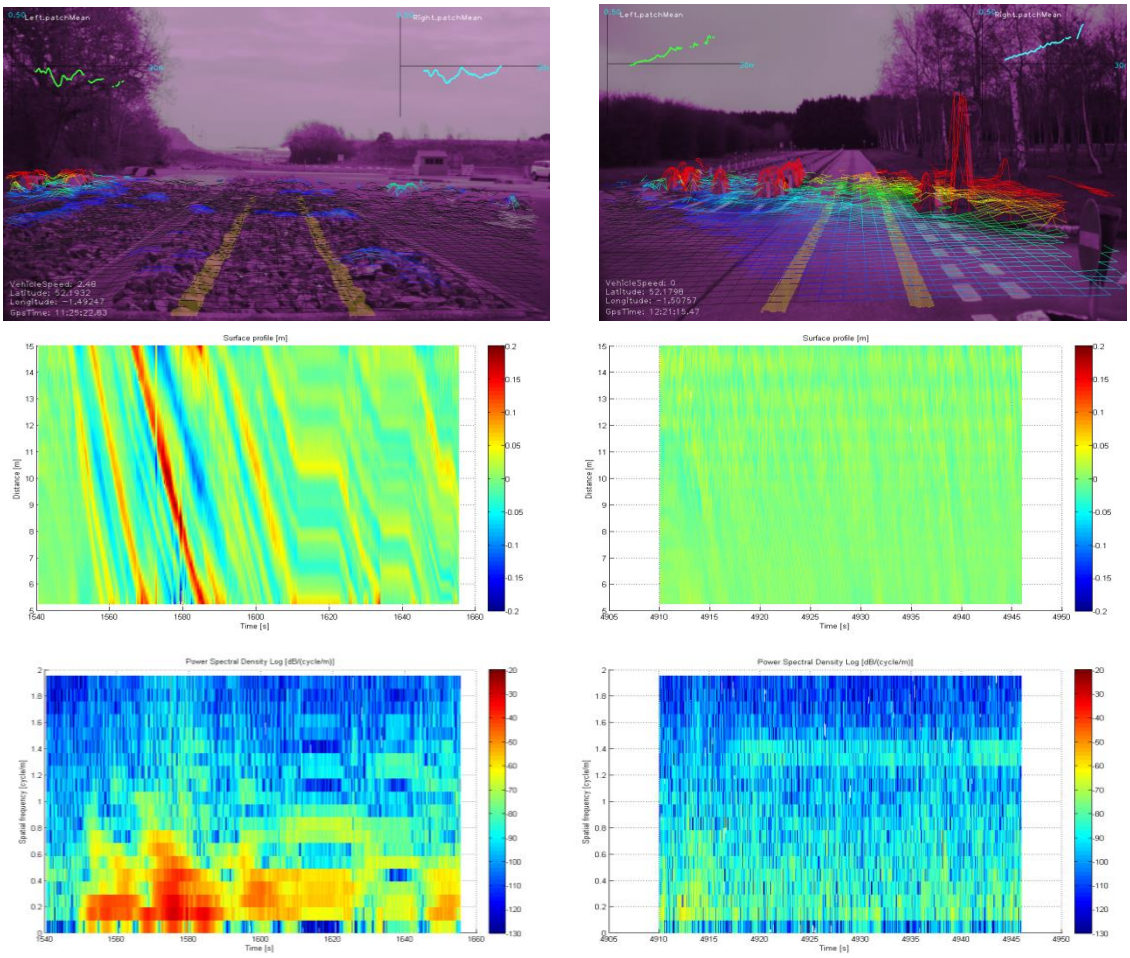

Figure 8.6. Riverbed (left column) and tarmac (right column) datasets: example image (top), surface profile (middle) and Power Spectral Density (bottom) over time.

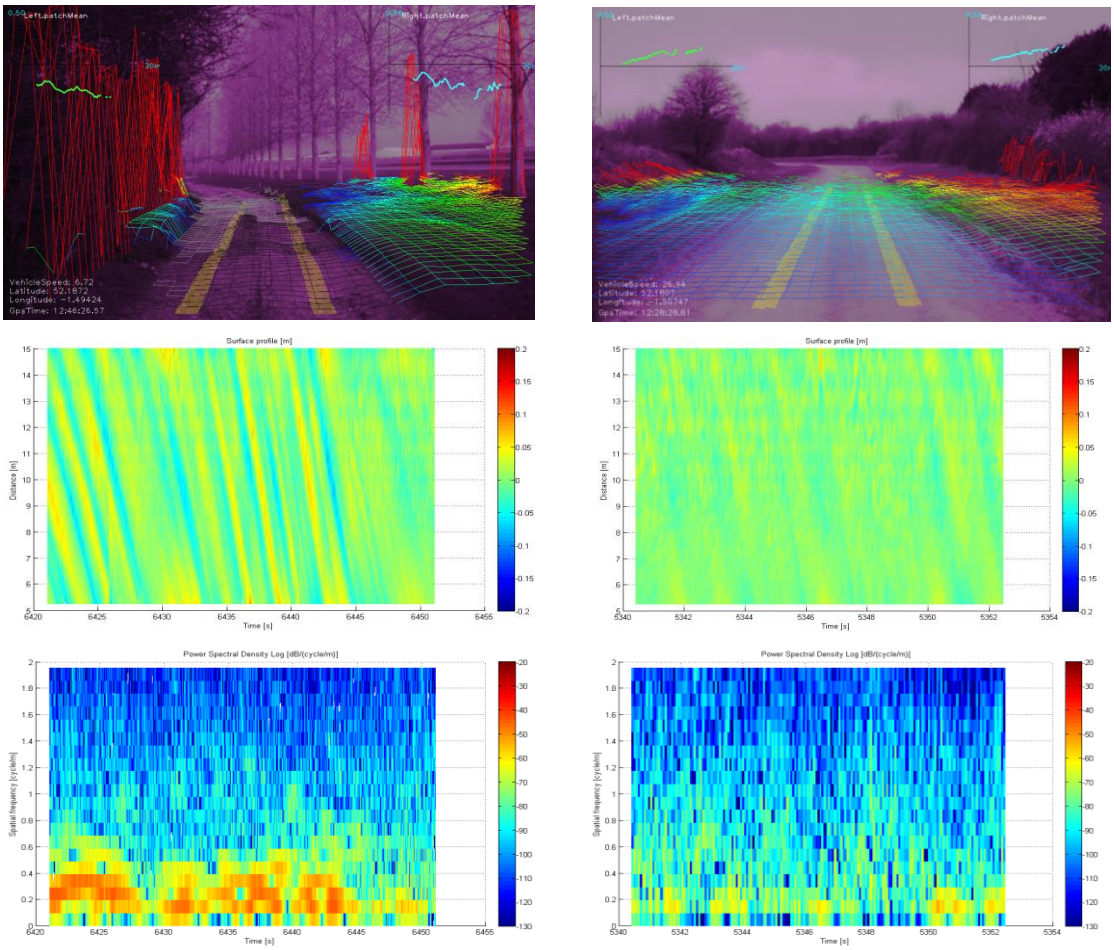

Figure 8.7. CrossCountry1 (left column) and dirt1 (right column) datasets: example image (top), surface profile (middle) and Power Spectral Density (bottom) over time.

8.5.1 Roughness descriptor

In order to simplify PSD to a surface descriptor and offset the effect of diminishing magnitudes of higher frequency signals, the PSD coefficients are scaled and added as follows:

$$r = \sum_{k=0}^{N-1} a_k G_{dB}(n_k)\,, \qquad (8.5)$$

where r is the roughness descriptor, a_k is the scaling factor for each of the spatial frequencies n_k and $G_{dB}(n_k)$ is the PSD in dB. The coefficients have been experimentally derived from the dataset with the detailed description of the experimental results in the following section.

The scaling factor applied corresponds to the line fitted in Figure 8.4, to offset the effect of diminishing magnitudes of higher frequency signals and has been experimentally derived from the presented dataset.

A dataset representing a medium roughness surface has been chosen which demands vehicle speed of 15 kph; it is in the middle of operating velocities.

The computed roughness descriptors correlate to the normalized vertical vehicle acceleration as shown in Figure 8.8. It has been shown that the vertical acceleration is proportional to the vehicle speed [64][170]. Therefore in order to offset the effect of vehicle speed on the perceived acceleration, vertical acceleration is normalised with respect to speed providing indication on how much vertical acceleration was excerpt on a particular surface independent of the velocity.

It can be observed that the sample sets observed of rough surfaces, experiencing higher level of normalised vertical acceleration have much lower roughness descriptor values, whereas sample sets from smoother surfaces generate higher descriptor values. Roughness descriptor values correlate with maximum normalised vertical acceleration which shows that the descriptor can be used for the assignment of target vehicle velocity.

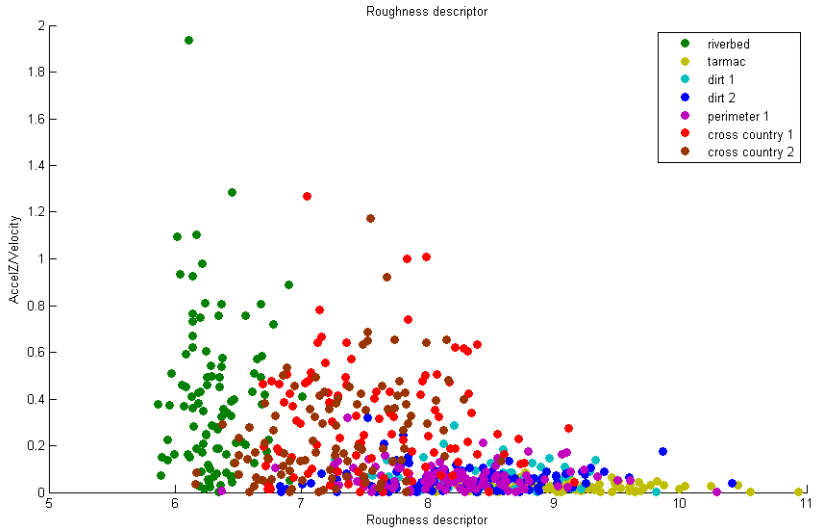

Figure 8.8. Roughness descriptor vs normalised vertical acceleration.

8.6 Velocity mapping

The goal of the speed recommendation system is to recommend vehicle velocity based on the micro terrain features described as surface roughness. As discussed in Section 3.4, some methods proposed in vehicle dynamics literature analyse the vehicle state and specifically vertical acceleration based on the surface roughness input. The predicted vehicle state could be used to define weather the vehicle should slow down or accelerate for the surface ahead. Analytical methods from vehicle dynamic studies use simplified quarter car models which predict vertical acceleration on one wheel and not the whole vehicle. Running a full vehicle dynamic model in real-time on the height profile to predict vehicle vertical acceleration is impractical. Hence, instead of predicting vehicle state from the height profile inputs, this

method rather proposes to find the mapping function between the surface roughness and the target vehicle velocity. This approach follows a *Learning from Demonstration* paradigm as discussed by Silver [104], where complex behaviours are modelled by a mapping function between the available inputs and required output.

The problem of vehicle speed recommendation is hence reformulated as finding a function which maps the surface roughness onto the recommended vehicle velocity. Given a set of roughness descriptors R and a target vehicle velocities V, $D = \{(r_1, v_1), \dots, (r_n, v_n)\}$ the aim is finding a function $g: R \rightarrow V$. Based on the set of homogeneous terrain samples introduces in Section 8.2 and expert assigned target velocities, two methods for mapping vehicle velocity are proposed: an Artificial Neural Network (ANN) and Direct Functional Mapping (DFM). The ANN is a regression based machine learning algorithm whereas DFM is a polynomial regression mapping function. The target vehicle velocities for each of the terrain samples were chosen by the off-road experts as safe and comfortable velocities that the vehicle should achieve on these surfaces.

8.6.1 Data labelling

The data set presented in Section 8.27 was annotated with expert chosen velocities. The sample sets taken on different surfaces in Gaydon varying in roughness from smooth tracks allowing speeds of 30 kph to rough rock surfaces allowing speeds of 3 kph. In total 4900 samples were used split into a training set (70% samples) and a test set (30% samples). The training set is used to derive model parameters whereas the test set is used to establish the model performance.

8.6.2 Artificial Neural Network

The ANN was trained using 5-fold cross validation and the 21 element PSD vector as an input since ANN can derive a mapping function in the multidimensional space. The detail methodology of training ANN is provided in Submission 3 [198]. The resulting ANN has 14 hidden nodes and one output node as illustrated in Figure 8.9.

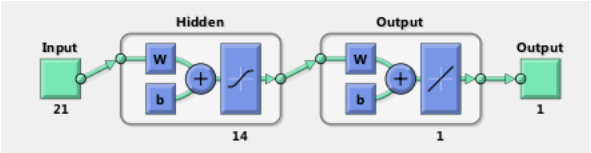

Figure 8.9. Trained ANN structure

8.6.3 Direct Function Mapping

The Direct Function Mapping (DFM) is composed of two stages, firstly a PSD is simplified into a roughness descriptor as described in Section 8.5.1 which then is mapped onto a target vehicle speed. Similarly to a machine learning method the mapping is using target vehicle speeds for each of the sample with associated roughness descriptor.

The DMF was derived from the mean roughness descriptors from each data set to eliminate the influence of the outliers. This initial fit was tested on a test data set to ensure that the data does not overfit the training set. Initially a linear fitting method was used, however second order polynomial provided a better fit function.

The velocity mapping function was derived by fitting a second order polynomial to the mean roughness descriptors from the training set and corresponding target velocities as shown in Figure 8.10, resulting in the following mapping function:

$$V(\mathrm{r}) = p_1 r^2 + p_2 r + p_3 \,, \qquad (8.6)$$

where $V(\mathrm{r})$ is the velocity, r is the roughness descriptor and p_1, p_2, p_3 are polynomial coefficients.

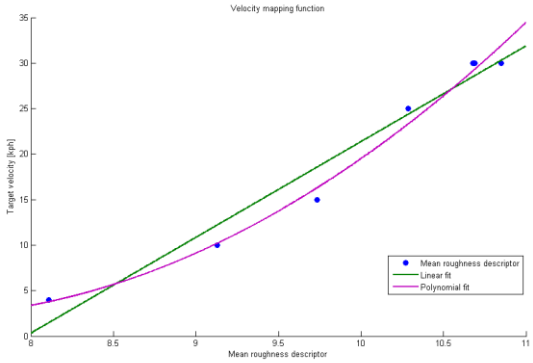

Figure 8.10. Velocity mapping function.

8.7 Speed recommendation performance

The performance of the algorithms is evaluated on the data set presented in Section 8.27. The performance of the two proposed speed recommendation methods is evaluated on raw model outputs and the outputs filtered through the simplified vehicle model which takes into account the maximum acceleration and deceleration rates as discussed in Section 5.2.4. Although raw model output error metric provides indication on the discrepancy between the expert chosen velocity and the recommendation velocity, the unfiltered velocity recommendations do not represent the actual velocity the vehicle is capable of achieving. The velocity recommendations do not take into account any constraints of the vehicle such as limited acceleration and deceleration rate as it is not feasible to accelerate above certain limits within short periods of time between the samples (60 ms). This can be modelled by post processing the recommended velocities and the sampling distances with limitations on acceleration and deceleration rates. In the current implementation the maximum deceleration rate is 2.25 m/s2 due to safety reasons to ensure the vehicle can maintain traction and to limit passenger discomfort associated with rapid decelerations. Similarly a limit of 1.5 m/s2 is applied to the acceleration rate. DFM and ANN speed recommendations results are compared with the expert chosen velocities for each of the samples in the data set. The error is calculated for each of the samples as:

$$e_{rec}(i) = v_{rec}(i) - v_{target}(i), \quad (8.7)$$

where v_{rec} is the recommended velocity and v_{target} is the expert chosen target velocity. Whereas average error is calculated as:

$$e_{rec} = \frac{\sum_{i=1}^{N} e_{rec}(i)}{N}, \quad (8.8)$$

where N is the number of samples.

Figure 8.11 shows the histogram of velocity recommendation error for both unfiltered recommendations and filtered recommendation. Mean errors show that both approaches match the target vehicle velocity reasonably well. However, the standard deviation of the error is higher for unfiltered recommended velocities than the vehicle constraint filtered signal. The normalised histogram of the velocity error shows the spread of error around the mean values for both velocity recommendation methods. Although the results are similar the DFM shows a higher spread of the recommended velocity error. The filtered vehicle velocity error histogram for both DFM and ANN is skewed towards negative error indicating that the velocity recommendation is rather conservative and it is more likely that the system will recommend lower velocity rather than higher velocity in comparison to the target value.

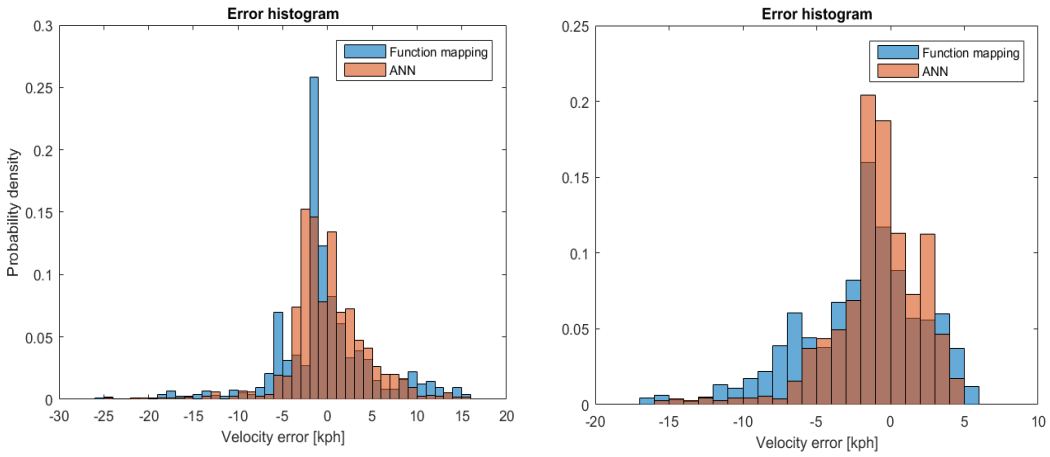

Figure 8.11. Histograms of error: unfiltered recommended velocity (left), recommended velocity with applied vehicle acceleration constraints (right)

Figure 8.12 shows the time history of the recommended vehicle velocities on different surfaces from the dataset. Applying vehicle acceleration constraints significantly reduces the variation and the error of the speed recommendation as can be seen in Figure 8.12. Although the speed recommendation overshoots in the *reverbed* data sat even up to 14 kph, the vehicle velocity is contained within the 8 kph limit. A similar trend is visible in the plots from *cross country* and *perimeter* data sets. The rough surfaces which have high surface undulation, may produce temporary higher speed targets when only a portion of the undulation is visible in the surface profile or a flat plateau is present in a short interval. Significant temporary peaks in the velocity recommendations are filtered by applying vehicle constraints.

Smooth surfaces such as tarmac and dirt show smaller variations of the recommended velocities and actual vehicle velocities, due to no undulation present in the surface. DFM shows more conservative performance in comparison to the ANN which recommends higher vehicle velocities, matching closer the vehicle target speed.

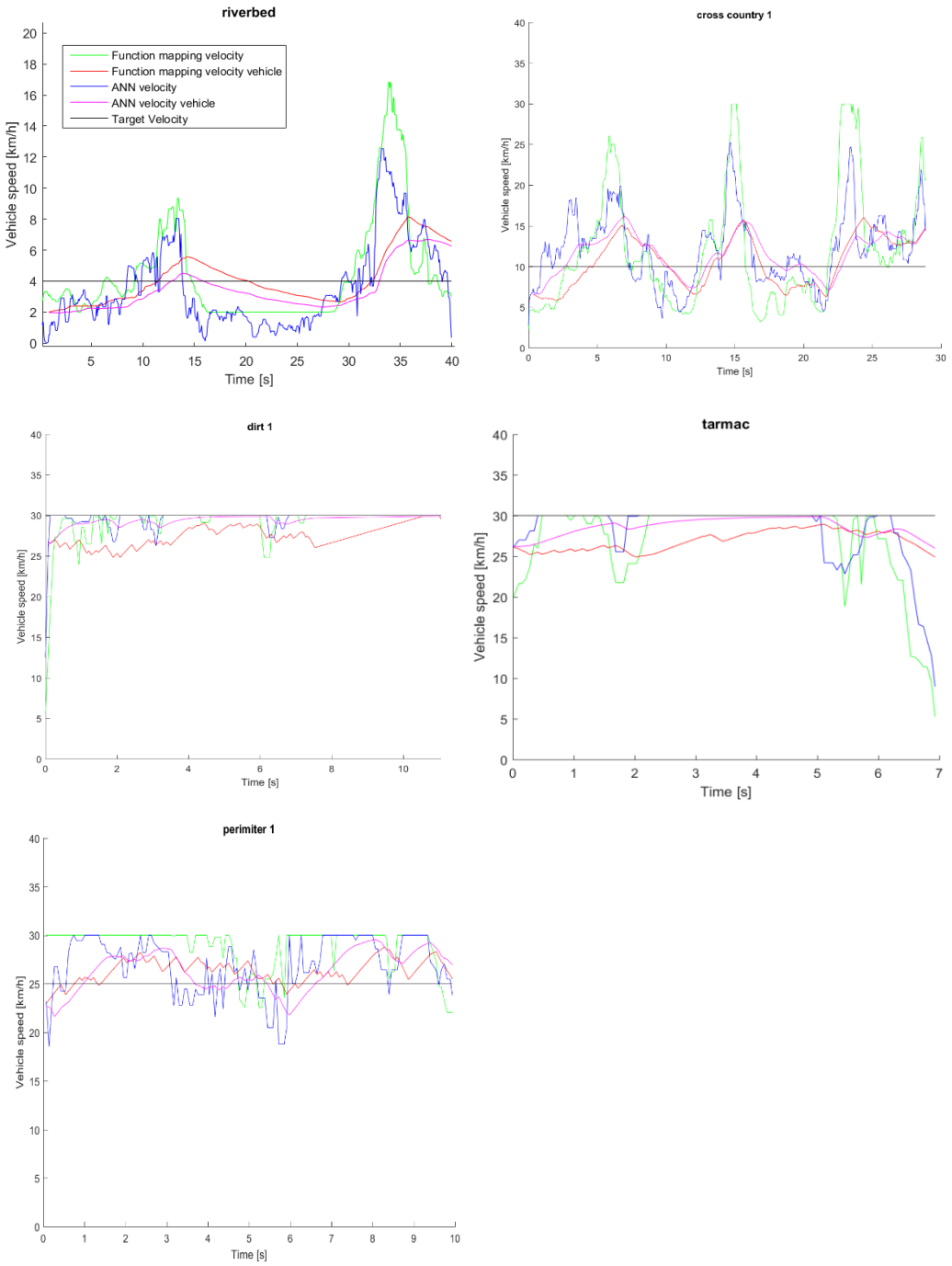

Figure 8.12. Recommended vehicle velocities on selected data sets.

The results show that the speed recommendation system tracks the target vehicle speed value with acceptable accuracy, as the velocity variations of +/- 5 kph can be accepted by the system. For practical reasons due to tractability and ability to tune the mapping function, DFM mapping is the approach chosen for further validation. More detailed discussion on applicability of both methods is contained within Submission 3.

8.8 Experimental evaluation

The experimental evaluation focuses on the comparison of the performance between the reactive and pre-emptive speed recommendation systems in a variety of different environments, showing the benefits and improved performance of the pre-emptive system. For the pre-emptive system it is intractable to compare its performance against a human driver as no driver will drive the same route in exactly the same fashion. On the contrary, the reactive system is deterministic and will maintain the same speed on the same route over multiple runs. In order to compare the performance of the pre-emptive system with the reactive system, several situations need to be considered:

- Change of surface type – the reactive system cannot anticipate the change of the surface roughness hence two situations can occur: the vehicle will hit a rough surface patch too quickly causing shock to the vehicle resulting in passenger discomfort or the vehicle will transition to a smooth surface and only after a delay will the vehicle speed increase. The pre-emptive system should be able to anticipate these changes and reduce passenger discomfort and eliminate the delays.
- Homogeneous surface – the reactive system speed should provide consistent speed and levels of passenger comfort, the pre-emptive system should provide similar target speeds to avoid the vehicle being too slow and limiting the vehicle progress, or too fast potentially inducing passenger discomfort.
- Discrete events – distinct surface features such as rocks, step changes, small obstacles which do not form a continuous rough surface segment hence the reactive system would not be able to adjust the speed accordingly due to the fact that the surface after the event is not as rough. Pre-emptive system should be able to anticipate this event, slow down accordingly and after the obstacle is surpassed speed up.

The effectiveness of the pre-emptive speed recommendation system is therefore assessed based on the following metrics:

- The difference in speed between the pre-emptive and the reactive system for events where the reactive system experiences high level of passenger discomfort. This signifies the situation where the reactive system speed was inappropriate (too fast) causing excessive vehicle excitation. In these scenarios the pre-emptive system should provide an advantage as the recommendation is

provided before the vehicle hits the surface event. The threshold for passenger events signifying discomfort has been chosen experimentally as discussed in Submission 3. This can be defined as follows:

$$\Delta V_{ExctMax}(i) = V_{react}(i) - V_{pre-empt}(i), \quad i \in S \mapsto IsoPsngrExct(i) > PsngrExctMax \tag{8.9}$$

$$\overline{\Delta V}_{ExctMax} = \frac{\sum_{i=0}^{N} \Delta V_{ExctMax}(i)}{N}, \tag{8.10}$$

where $V_{react}(i)$ is a reactive vehicle speed sample at location i, $V_{pre-empt}(i)$ is pre-emptive system speed sample at location i, location i is defined based on the excessive passenger excitation events and S is a set of all sample locations, $IsoPsngrExct$ is a passenger comfort metric as described in Section 5.2 $PsngrExctMax = 10$ is maximum passenger excitation threshold. $\overline{\Delta V}_{ExctMax}$ is the average difference in speed between the pre-emptive and the reactive system for events where the reactive system experiences high level of passenger discomfort.

This metric has been calculated for all the points where the speed recommendation was available, and excluded the instances where no data was available due to the path of the vehicle exceeding camera field of view.

- The difference in speed between pre-emptive and reactive system for events where the passenger comfort values where low signifying relatively smooth surfaces, where vehicle could have travelled faster.

$$\Delta V_{ExctMin}(i) = V_{react}(i) - V_{pre-empt}(i), \quad i \in S \mapsto IsoPsngrExct(i) < PsngrExctMin \tag{8.11}$$

$$\overline{\Delta V}_{ExctMin} = \frac{\sum_{i=0}^{N} \Delta V_{ExctMin}(i)}{N}, \tag{8.12}$$

where $V_{react}(i)$ is a reactive vehicle speed sample at location *i*, $V_{pre-empt}(i)$ is pre-emptive system speed sample at location *i*, location *i* is defined based on the excessive passenger excitation events and *S* is a set of all sample locations, $IsoPsngrExct$ is a passenger comfort metric as described in Section 5.2 $PsngrExctMin = -10$ is minimum passenger excitation threshold. $\overline{\Delta V}_{ExctMin}$ is the average difference in speed between the pre-emptive and the reactive system for events where the passenger comfort values where low signifying relatively smooth surfaces, where vehicle could have travelled faster.

- The average speed difference between the reactive and pre-emptive system. The average speed difference considers the entire route and includes the situations where passenger comfort was

below the target value, where the vehicle could travel faster, as well as situations where the passenger comfort reached excessive values where the vehicle travelled too fast over the terrain. In general, the average speed difference signifies if the vehicle would travel the overall route faster or slower.

$$\Delta V(i) = V_{react}(i) - V_{pre-empt}(i), \qquad i \in S \tag{8.13}$$

$$\overline{\Delta V} = \frac{\sum_{i=0}^{N} \Delta V(i)}{N}, \tag{8.14}$$

where $V_{react}(i)$ is a reactive vehicle speed sample at location *i*, $V_{pre-empt}(i)$ is pre-emptive system speed sample at location *i*, location *i* is a location along the test route, $IsoPsngrExct$ is a passenger comfort metric as described in Section 5.2. $\overline{\Delta V}$ is the average difference in speed between the pre-emptive and the reactive system for all the locations on the route.

The detailed methodology of this experimental evaluation is presented in Submission 3.

8.8.1 Test routes

The particular routes chosen in these experiments comprise a varied selection of routes with varying levels of surface topography and roughness from relatively smooth surfaces of the developing world circuit, the rougher *Cross Country* track, *Quarry Lane* with sections of different surface roughness, hills, dips to *Constructors Road* with highly undulating surface. *Developing World* is a limestone road which becomes rutted and potholed with use providing severe suspension and tyre inputs, designed to simulate roads found in developing world countries. The route contains varying radius curves, short and long straights with two fords. *Cross Country* track consists of hard-core material and large stones with small aggregate filling in certain areas. Part of the cross country track is linked through an island to the *Developing World* circuit. *Quarry Lane* section is similar to the cross country track with large undulating hills and dips, smooth sections in the straights covered with gravel and a ford. *Constructors Road* consists of a smooth concrete mix, shaped to simulate construction roads. The summary of different circuits used in testing is presented in Table 8.2.

These circuits provide a large range of longer stretches of the different surface type which allow testing the transition between the smooth and rough surfaces and validate the behaviour of the system in real-world conditions. The terrain is very challenging including narrow passes between the tree lines with undulating terrain, hills, dips and fords. In particular the routes with bends are challenging for the pre-emptive system as the measurements of the path may not be visible in the camera's field of view due to high path curvature. Transitions between surfaces of different roughness on the other hand are challenging for the reactive system and these are particular points of interested where the pre-emptive system should provide a more suitable speed recommendation.

Table 8.2. Test routes summary

Circuit	Length	Width	Average speed	Description	
Developing World	1000 m	4 m	25 kph	Non metalled limestone road which becomes rutted and potholed with use providing severe suspension and tyre inputs, designed to simulate roads found in developing world countries. 4.8km long x 4m wide consisting of varying radius bends, short and long straights with two fords.	
Cross Country	400 m	3 m	10 kph	Track consists of hard-core material and large stones with small aggregate filling in certain areas. Part of the cross country track is linked through an island to the developing world circuit.	
Quarry Lane	900 m	3 m	10 kph	Track consists of packed soil, in areas soil patches are separated by a band of grass in the centre of the track. Similar to the cross country track with undulating hills and dips.	
Quarry Lane Straights	400 m	3 m	15 kph	Straight areas composed of gravel, with transition between medium roughness undulating surface and smooth gravel.	
Constructors Road	200 m	2.5 m	5 kph	Consists of a smooth concrete mix, shaped to simulate construction roads	

8.8.2 Results

The graphical representation of results is presented in Figure 8.13. Results obtained from the comparison of reactive and pre-emptive system show that the pre-emptive system can significantly reduce the vehicle speed in case of events when the reactive system exceeded maximum passenger excitation limit, with the speed difference ranging between 12% to 68% speed reduction. . In case of events where the passenger excitation is below the target level the pre-emptive system does not slow down the vehicle on average more than 1 kph. More detailed set of results is presented in Submission 3.

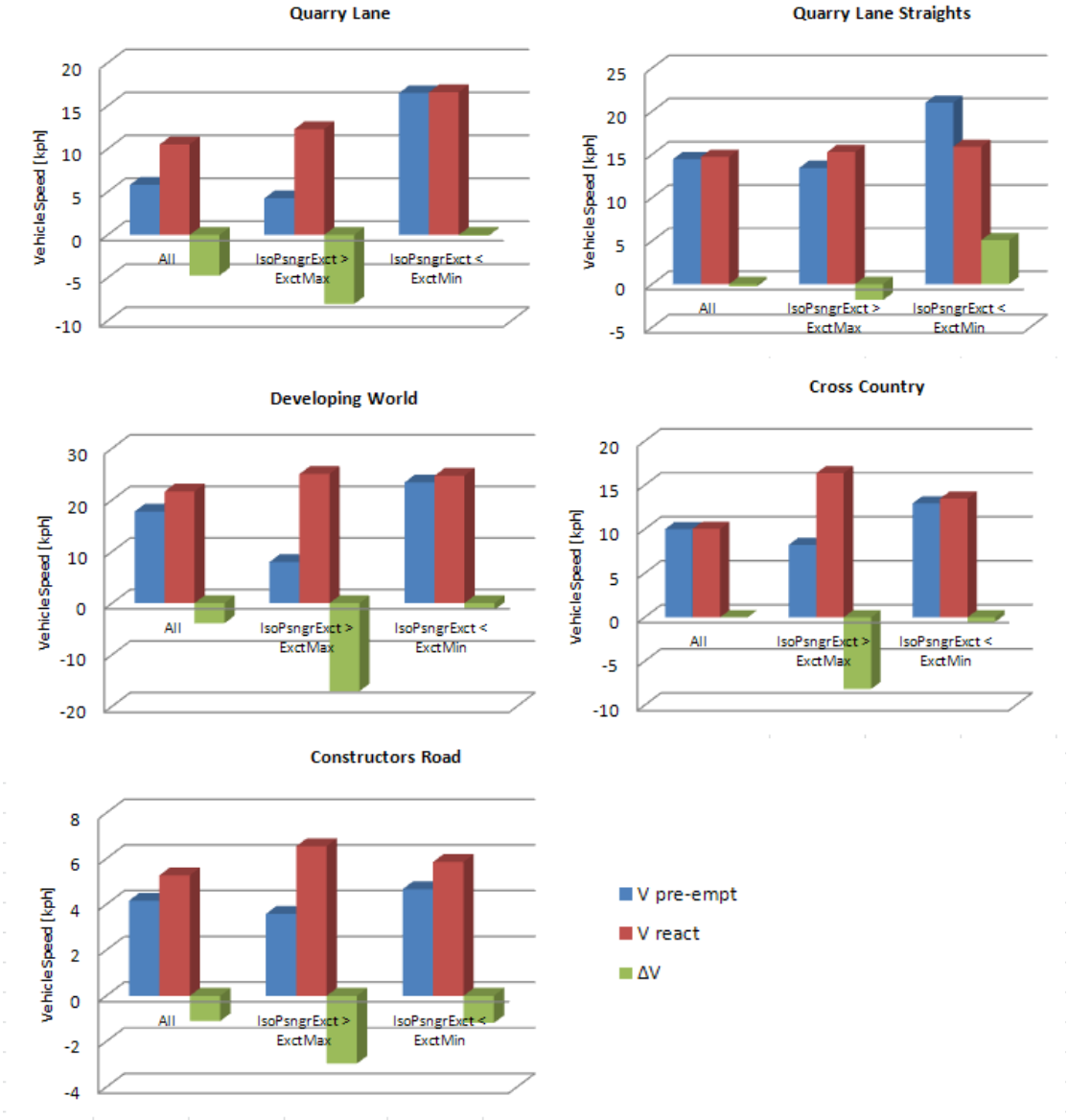

Figure 8.13. Bar charts representing average vehicle speeds for pre-emptive and reactive system split into groups: entire data set (All), classified excessive passenger excitation levels excitation (IsoPsngrExct > ExctMax) and below target passenger excitation (IsoPsngrExct < ExctMin).

The detailed qualitative analysis of all the scenarios presented in Submission 3, shows the benefits of the proposed pre-emptive speed recommendation. In cases of surface roughness change, particular transition between smooth surface and rough surface, these changes were properly identified by the pre-emptive system. Figure 8.14 shows the excessive passenger excitation levels due to surface roughness change, followed by vehicle speed reduction bringing the passenger excitation level down. In contrast, the pre-emptive speed recommendation would reduce the vehicle speed before approaching rough terrain, as shown in Figure 8.14.

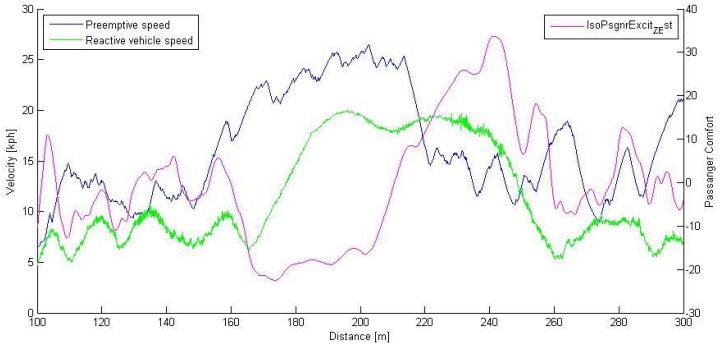

Figure 8.14. Passenger excitation (comfort axis) and associated vehicle speeds over the portion of the course illustrating faster response of the pre-emptive system.

In total reactive system caused excessive levels of passenger excitation in 21 instances. In all these instances, the pre-emptive system recommended lower speeds, which would lead to lower passenger excitation levels. These instances were surface roughness changes as illustrated Figure 8.15, Figure 8.16, Figure 8.17 and discrete macro terrain features such as ditches (see Figure 8.18) and fords (see Figure 8.19). The detailed qualitative evaluation of the performance for each of the routes is presented in Submission 3.

Figure 8.15. Example images from the Quarry Lane dataset. The smooth gravel surface (left) is followed by coarser track with small rocks (right)

Figure 8.16. Example images from Quarry Lane Straights data set – transition between surfaces (left) detected correctly by the pre-emptive system.

Figure 8.17. Smooth section of Cross Country route (left) followed by rougher potholed surface (right)

Figure 8.18. Ford in the developing world track. White points depict the predicted vehicle path.

Figure 8.19. Example image from Constructors Road data set.

Obtained results also highlighted issues with the proposed solution. The predicted vehicle path is known and is calculated based on the steering inputs from the driver. Surface roughness measurements are taken from a longitudinal profile using the steering input provided by the driver as the path traversed by the wheels excites the vehicle. Hence any inaccuracies in the prediction of the vehicle kinematic state in the

future will inherently result in the measurement of the surface that do not correspond to the travelled vehicle path.

The current limitation of the pre-emptive system is its performance on the highly curved roads. This limitation stems from the fact that the measurement area is ahead of the vehicle on it predicted future path. The prediction of the path is based on the driver's steering inputs as the driver is in control of the vehicle and decides on the vehicle trajectory. When the vehicle approaches the bend following a straight the correct road area is measured (Figure 8.20 left). When the vehicle traverses two consecutive bends the measurements are incorrect due to the fact that the vehicle is still in the curve (steering angle applied) causing the measurements to be taken outside of the road area (Figure 8.20 right).

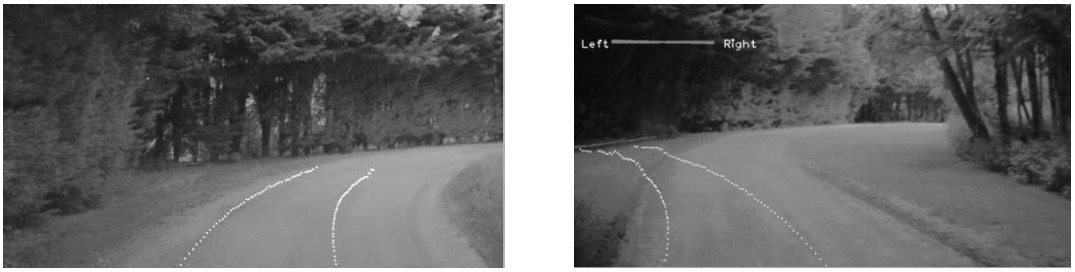

Figure 8.20.Surface profile measurements are based on the predicted vehicle path taking into account the driver steering inputs (measurement points are denoted as white dots).

This causes the lower pre-emptive speed recommendations as the measured profile contains the edge of the path transitioning from smooth gravel to grass. This however can be mitigated by the reactive system measuring the changes in the applied steering wheel angle. When the changes in the steering angle are significant, singling that to the pre-emptive measurements are not valid as the vehicle changes its course, the pre-emptive recommendations can be disregarded.

In addition, when approaching a tight bend the path lies outside of the camera field of view resulting in complete lack of measurements as illustrated in Figure 8.21. In this situation pre-emptive system would not be able to provide any recommendation and the reactive system would need to take over.

Figure 8.21. Sharp curve resulting in lack of measurements as the path is outside of the camera field of view.

8.9 Conclusions

In this chapter a novel pre-emptive speed recommendation system was proposed that allows the vehicle to adapt the speed dynamically based on the roughness of the surface ahead. The proposed method draws from experience in the domain of vehicle dynamics and road surface metrology; the proposed surface roughness descriptor has been used for characterization of road networks roughness and simulations of the vehicle reliability, but has not been used for characterization of the short surface intervals especially for the purpose of speed adaptation. The selected surface roughness descriptor has been shown to correlate with the levels of vertical acceleration, which indicate the shock experienced by the vehicle. This work presents novel use of this roughness descriptor and both experimentally and analytically validates its use for the purpose of speed adaptation.

The proposed solution was implemented on production ready sensors, showing that it is feasible to introduce the system in the next generation of Land Rover vehicles. In contrast to previous research, the system was designed with limited capability automotive sensors to suit particular requirements of Terrain Based Speed Adaptation system

Performance evaluation of the system with data gathered in real-world off-road conditions showed that the system is capable of recommending appropriate vehicle speed based on surface roughness. Performance evaluation on initial set of homogeneous surfaces of different roughness showed that the system can track expert recommended vehicle velocity within +/- 5 kph.

Further performance evaluation quantified the benefits of complimenting the reactive system with the proposed pre-emptive speed recommendation system to provide the vehicle with anticipatory speed facilities. The results show that the pre-emptive system performance offers significant improvement in the situations in which the reactive system cannot cope, such as changes in the terrain roughness, as the reactive system can only adapt once it has reached a particular surface. Such scenarios cause high levels of passenger excitation, hence indicating passenger discomfort and potentially needing the driver to intervene. The pre-emptive system achieves speed reduction ranging from 12% to 68%in comparison to the reactive speed recommendation system, in cases when an excessive passenger excitation event occurred while using the reactive system... Hence the pre-emptive system can improve passenger comfort and eliminate the need for driver intervention. Although, the vehicle speed recommendation is designed with respect to the expert chosen velocity, which may be treated as a baseline, there is also a scope for customisation of vehicle speed dependant on the customer perception of comfort. By adjusting the mapping between the roughness descriptor values or passenger excitation index and the target velocity, the users may decide to choose a trade-off between the progress and comfort.

9 Discussion

This research was undertaken at Jaguar Land Rover, as a part of a new off-road Advance Driver Assistance System (ADAS) feature development. The main objectives of this work were to design and implement a vision-based system that would enable new off-road functionality, hence enabling the company to deliver new customer facing features.

9.1 Commercial impact

The technology and methodology developed during this research have many commercial benefits for Jaguar Land Rover including the development of new ADAS features, Intellectual Property generation and decreased feature development time and cost.

New off-road functionality enabled by the proposed sensing solutions builds allows Land Rover to maintain its off-road leadership position, which is a key company strategy. At the moment it is expected that Land Rover will be the first vehicle manufacturer to introduce speed adaptation for off-road vehicles. New features generate additional revenue streams and provide competitive advantage.

This research focused on employing the existing sensor set and understanding its capability with the proposed new computer vision algorithms. Reusing the existing vehicle sensors means that there is no significant hardware cost required to implement this technology. Moreover, the discussions with suppliers confirmed that the proposed perception solution could be implemented on the target automotive platform in series development.

The research also resulted in generation of new Intellectual Property (IP) for Jaguar Land Rover. Considering only the vision-development, seven patent applications were filed; three of which have already been granted. The patents cover utilisation of surface geometry for speed adaptation, speed adaptation based on surface roughness, adapting vehicle settings depending on terrain geometry, adapting vehicle settings based on surface type and visualisation of terrain geometry to aid the driver. Generated IP provides competitive advantage, limiting the employment of proposed technology by other manufactures. Moreover, licencing IP to suppliers or other manufacturers may also generate revenue.

The proposed perception system was implemented on a recent Terrain Based Speed Adaption prototype vehicle which was demonstrated to the press during the Land Rover Future Technology Showcase [199] as a part of All-Terrain Self-Driving Research portfolio. The event generated publicity for Land Rover, showing its commitment to developing all-terrain automation and strengthening its position as a leader in off-road technology.

9.2 Technology impact

In a wider context the proposed methods are a step towards a full semantic representation of the off-road/unstructured environment. The perception of terrain geometry, surface roughness and terrain type is a building block towards comprehensive perception which will allow further vehicle automation. Allowing the vehicle to control its speed based on the surface and adjust vehicle systems based on the terrain type are the basis for autonomy. In the context of autonomous vehicles, full vehicle autonomy should not only be constrained to on-road scenarios, but rather allow the vehicle to travel to its destination, even if it is along a rough track or gravel road.

The proposed perception methods can potentially be applied in other automated driving applications. Autonomous parking in multi-storey car parks will require more detailed knowledge of the geometry of the environment such as locations of ramps and kerbs. Even in urban environments, micro features of the surface will need to be identified e.g. large potholes and ramps will require vehicle speed adjustment.

With the advancement of automotive hardware, including automotive GPU development by NVIDIA [200], introduction of new sensing functionality will become more affordable as vehicles will have specific processing units designed for computer vision applications. Further developments in the Deep Learning approaches to classification with aforementioned hardware support, may also create new opportunities to provide more complex classification mechanism, which show promise in the area of off-road [201] and on-road perception [202], [203].

9.3 Limitations

The performance of the terrain recognition method is, mostly, limited to daylight conditions and does not perform as well in night time conditions. Due to the nature of the changing colour of light sources and degraded image quality at night, the classifier does not always properly capture the terrain type colour distribution. A generic limitation of visual-based terrain classification, which causes the afore-mentioned night time limitation, is that it identifies terrain class based on the visual appearance hence only indirectly infers terrain properties based on the terrain class. With the increased integration of more sensors on the vehicle, sensor fusion approaches combining multiple sensor modalities (radar returns, ultrasonic returns and infrared signatures) could be used to alleviate this problem [195], [196], [204].

The limitations of the proposed terrain geometry approach include limited accuracy of the world model, camera specification, the mechanism of predicting vehicle path and the assumptions made about the composition of the terrain.

The control system is provided with the information about the terrain features in the predicted vehicle path. The mechanism of predicting vehicle path is based on the steering input provided by the driver. In certain cases, such as exiting a corner, the predicted vehicle path lies outside of the actual path taken by

the driver resulting in reported terrain features that are not on the actual path. This effect is only temporary since the steering angle changes quickly, hence this information is disregarded by the control system. In future, the predicted vehicle path information may be augmented with semantic segmentation identifying a most probable drivable path, which could potentially help identifying relevant terrain features further in advance. When the functionality will be extended with automated steering, this situation will not be problematic as the vehicle will plan its own path.

Terrain geometry and surface roughness are used as a speed predictor input. The limitation of the system stems from the assumption that the terrain is non-deformable meaning that the measured terrain geometry corresponds to a solid surface. Deformable terrains such as sand an mud excerpt less force on the vehicle than for example concrete surface due to the fact that deformable surface will change its geometry once the vehicle traverses it. Although rippled sand surface geometry measurement can be extremely rough the vehicle will not experience excessive acceleration levels since the surface will deform under the vehicle mass. The pre-emptive system takes a conservative, worst case scenario approach and calculates the recommended vehicle speed based on the assumption that the traversed surface is solid.

Another limitation, is the performance of the vision based sensing in low light conditions. It is know that in low light conditions the camera performance is degraded. In the terrain geometry studies it was assumed that the camera provides diagnostic information on the quality of the disparity estimation. In cases when the disparity estimation is not available or low quality, the pre-emptive system will not be operational. In future, this limitation might be overcome by the introduction of more sensitive cameras or non-visible light sources and sensors, which will provide depth information even in low light conditions.

A general limitation of all the studies is the variability of the environments, which can affect the system performance. The limited access to off-road facilities and the cost of testing meant that the system was evaluated in the available off-road facility in Gaydon. Usually the more extensive testing in more challenging environments and conditions is performed once the algorithms are implemented by a supplier on a target hardware platform, at a later stage of development. The initial testing provides indication on the applicability of the proposed concept, and further robustness testing is performed in series development. In future the system should be tested especially on snow and sand surfaces, as less prominent visual texture of such surfaces may potentially affect the capability of the system to reconstruct 3D world model using stereo camera.

10 Conclusions and Future Work

This Innovation Report described the development of a novel perception system for off-road driver assistance. The focus of the work was on feasible engineering solutions within a constrained sensor set to provide the semantic representation of terrain composition and terrain topography. As discussed in Chapter 1, the barrier that previously hindered the development of off-road ADAS features included a lack of off-road perception capability from available automotive sensing solutions. The research presented in this report has demonstrated that the vision-based perception system *can* provide an understanding of the off-road environment to enable next generation of off-road ADAS features within the constraints of automotive systems. The next generation off-road ADAS features were the two systems that Jaguar Land Rover was interested in developing: Terrain Response 3 and Terrain Based Speed Adaptation. Within the context of development of these features the research question was answered through meeting the following objectives:

Objective 1 Develop and validate a terrain classification system capable of detecting grass surfaces

Based on the requirement posed by the Terrain Response 2 system, an image processing framework for grass detection was developed, including the choice of discriminative image features, classifier choice and the performance evaluation method. The developed terrain recognition system robustly and accurately classified grass and non-grass terrain surfaces with 98% accuracy in daytime conditions. In the night time conditions the performance of the system was unsatisfactory with accuracy of 65% due to varying colour of light sources such as street lamps hence not conforming to the employed colour models. The proposed novel terrain classification method was shown to be applicable for deployment on an in-vehicle system providing a new source of information for the next generation of Terrain Response system. The proposed validation methodology focused on the evaluation of computational constraints and robustness against various environmental conditions.

Objective 2 Develop and validate a terrain geometry identification system.

A terrain identification system utilising production representative stereo-camera sensors was proposed. The novelty of this work in automotive context included identification of the relevant macro terrain features including slopes, ditches and crests which affect the vehicle progress capability. The capability of the proposed system was validated to understand the operational envelope. Identification of ditches and crest was achieved with accuracy of distance estimation of 0.5 m. Crests were detected up to 18 m, whereas ditches were detected at ranges varying from 6-15 m depending on size of a ditch. The slopes were measured with accuracy of +/- 2.5°. The proposed terrain geometry identification system was also validated in conjunction with its intended application TBSA. The perception system was shown to be effective in identifying the terrain features hence allowing the vehicle to slow down pre-emptively, improving the system performance. In contrast to reactive TBSA the vehicle was able to anticipate terrain ahead eliminating the need of driver to intervene.

Objective 3 Develop and validate a pre-emptive speed recommendation system based on surface roughness

A novel surface roughness measurement and speed recommendation method was also proposed, utilising a production representative stereo camera sensor. Performance evaluation of the system with data gathered in real-world off-road conditions showed that the system is capable of recommending appropriate vehicle speed based on surface roughness. Performance evaluation on initial set of homogeneous surfaces of different roughness showed that the system can track expert recommended vehicle velocity within +/- 5 kph. Further performance evaluation on more than 2 km of off-road routes quantified the benefits of complimenting the reactive system with the proposed pre-emptive speed recommendation system to provide the vehicle with anticipatory speed facilities. The results show that the pre-emptive system performance offers significant improvement in the situations in which the reactive system cannot cope, such as changes in the terrain roughness, as the reactive system can only adapt once it has reached a particular surface. Such scenarios cause excessive levels of passenger excitation, hence indicating passenger discomfort and potentially needing the driver to intervene. The pre-emptive system achieves speed reduction ranging from 12% to 68% for the events with excessive passenger excitation in comparison to the reactive system baseline. Therefore, the pre-emptive system can improve passenger comfort and eliminate the need for driver intervention.

Existing unmanned off-road vehicles are designed to operate autonomously and the sensor set and the data processing methods are designed to suit that particular task. This promotes a top-down approach where little consideration is given the limitations of the sensor set. In contrast, this work promotes a bottom-up approach where the perception solution is designed around the constraints of a single perception modality – vision based system. Within the automotive industry, the cost of a sensor, packaging and styling constraints are of paramount importance; it is not only the functionality and performance that is taken into account. Furthermore, the perception solution must fulfil the requirements of a specific ADAS application. This research showed that off-road perception can be achieved within the automotive constraints and fulfils the requirements of certain ADAS applications.

The aforementioned systems could be brought together in future off-road control systems to facilitate further development of fully autonomous off-road vehicle. Considering that the perceptions system was shown to support longitudinal motion controller, the next step would require perception system to support lateral motion controller to steer the vehicle. Although, the research has shown the particular application of the technology which was constrained by the use of single colour camera for grass identification and non-colour stereo camera for terrain geometry measurement, the proposed solutions can be readily implemented on a next generation of colour camera system.

10.1 Future work

Future work in the area of perception should address the deficiencies of the sensors performance in low light conditions. Use of structured light approaches or use of infrared sensors could provide the necessary performance in all light conditions. Further, sensor fusion with other sensors such as radar and ultrasonic could provide more information on terrain composition.

Another interesting area of extending this work would be to extend the perception capability to identify a trajectory of an off-road track. This could facilitate automated path following as a next step towards higher levels of automation. Although individual lateral and longitudinal motion control is a level 2 automated system (as discussed in Section 2.2), the combination of both track following and TBSA could potentially facilitate level 3 automation. The difficulty of track detection is that the appearance of the off-road tracks may vary drastically and the track may not have a defined structure as road in urban environment. An on-line learning approach could allow the perception system to learn the appearance of the track and combine it with geometry and traversability information. This would allow the vehicle to detect a path without the need to gather large amounts of data and a priori learning samples.

As an ultimate goal a perception system would facilitate full off-road autonomy. An interesting aspect of the autonomy is considered when travelling repeatedly on the same routes e.g. driving to a country house every weekend. This could be facilitated by learning from examples or Simultaneous Localisation and Mapping (SLAM) based approaches. The vehicle traversing the route in the manual mode, could build an environment map to later follow the known route in autonomous mode. The challenging aspect of SLAM in this context is how to ensure that the build map is actually correct, if system operates without human supervision, and how to diagnose when the system fails. The environment also changes with seasons and weather conditions, hence another challenge would be to create a map that describes the environment in a way that these changes do not impact localisation performance.

Full autonomy will require information on the destination and available routes. This is an open question as unpaved, off-road areas may not be mapped. The increased connectivity of the vehicles may allow gathering the information from fleets of vehicles. This could enable creating topographic or geometric maps of the areas not served by the suppliers of navigation solutions.

References

[1] E. D. Dickmanns, *Dynamic vision for perception and control of motion*. Springer, 2007.

[2] R. Behringer, "Results on visual road recognition for road vehicle guidance," in *Intelligent Vehicles Symposium*, 1996, pp. 415–420.

[3] D. Braid, a. Broggi, and G. Schmiedel, "The TerraMax Autonomous Vehicle concludes the 2005 DARPA Grand Challenge," *2006 IEEE Intell. Veh. Symp.*, pp. 534–539, 2006.

[4] S. Thrun, M. Montemerlo, H. Dahlkamp, D. Stavens, A. Aron, J. Diebel, P. Fong, J. Gale, M. Halpenny, G. Hoffmann, K. Lau, C. Oakley, M. Palatucci, V. Pratt, P. Stang, S. Strohband, C. Dupont, L. E. Jendrossek, C. Koelen, C. Markey, C. Rummel, J. van Niekerk, E. Jensen, P. Alessandrini, G. Bradski, B. Davies, S. Ettinger, A. Kaehler, A. Nefian, and P. Mahoney, "Stanley: The robot that won the DARPA Grand Challenge," *Springer Tracts Adv. Robot.*, vol. 36, pp. 1–43, 2007.

[5] M. Montemerlo, S. Thrun, H. Dahlkamp, D. Stavens, and S. Strohband, "Winning the DARPA Grand Challenge with an AI Robot," *Artif. Intell.*, vol. 21, no. Gat 1998, pp. 982–987, 2006.

[6] M. Buehler, K. Iagnemma, and S. Singh, "The DARPA Urban Challenge," in *The DARPA Urban Challenge*, vol. 49, no. 0, M. Buehler, K. Iagnemma, and S. Singh, Eds. Springer, 2010, p. 626.

[7] S. Kammel, J. Ziegler, B. Pitzer, M. Werling, T. Gindele, D. Jagzent, J. Schöder, M. Thuy, M. Goebl, F. Von Hundelshausen, O. Pink, C. Frese, and C. Stiller, "Team AnnieWAY's autonomous system for the DARPA Urban Challenge 2007," in *Springer Tracts in Advanced Robotics*, 2009, vol. 56, pp. 359–391.

[8] M. Montemerlo, J. Becker, S. Bhat, H. Dahlkamp, D. Dolgov, S. Ettinger, D. Haehnel, T. Hilden, G. Hoffmann, B. Huhnke, D. Johnston, S. Klumpp, D. Langer, A. Levandowski, J. Levinson, J. Marcil, D. Orenstein, J. Paefgen, I. Penny, A. Petrovskaya, M. Pflueger, G. Stanek, D. Stavens, A. Vogt, and S. Thrun, "Junior: The stanford entry in the urban challenge," in *Springer Tracts in Advanced Robotics*, 2009, vol. 56, pp. 91–123.

[9] C. Urmson, J. Anhalt, D. Bagnell, C. Baker, R. Bittner, M. N. Clark, J. Dolan, D. Duggins, T. Galatali, C. Geyer, M. Gittleman, S. Harbaugh, M. Hebert, T. M. Howard, S. Kolski, A. Kelly, M. Likhachev, M. McNaughton, N. Miller, K. Peterson, B. Pilnick, R. Rajkumar, P. Rybski, B. Salesky, Y. W. Seo, S. Singh, J. Snider, A. Stentz, W. Whittaker, Z. Wolkowicki, J. Ziglar, H. Bae, T. Brown, D. Demitrish, B. Litkouhi, J. Nickolaou, V. Sadekar, W. Zhang, J. Struble, M. Taylor, M. Darms, and D. Ferguson, "Autonomous driving in Urban environments: Boss and the Urban Challenge," in *Springer Tracts in Advanced Robotics*, 2009, vol. 56, pp. 1–59.

[10] Google, "Google Self-Driving Car Testing Report on Disengagements of Autonomous Mode," *Technical Report*, 2015. [Online]. Available: https://www.google.com/selfdrivingcar/files/reports/report-annual-15.pdf.

[11] A. Broggi, M. Buzzoni, S. Debattisti, P. Grisleri, M. C. Laghi, P. Medici, and P. Versari, "Extensive tests of autonomous driving technologies," *IEEE Trans. Intell. Transp. Syst.*, vol. 14, no. 3, pp. 1403–1415, 2013.

[12] J. Ziegler, T. Dang, U. Franke, H. Lategahn, P. Bender, M. Schreiber, T. Strauss, N. Appenrodt, C. G. Keller, E. Kaus, C. Stiller, and R. G. Herrtwich, "Making Bertha Drive — An Autonomous Journey on a Historic Route," *Intell. Transp. Syst. Mag. IEEE*, vol. 11, no. 2, pp. 1–10, 2013.

[13] Tesla Energy, "Press Kit | Tesla Motors UK," 2015. [Online]. Available: http://www.teslamotors.com/en_GB/presskit. [Accessed: 26-Apr-2015].

[14] Volkswagen, "Traffic Jam Assist from Volkswagen | Think New." [Online]. Available: http://thinknew.volkswagen.com/int/en/innovations/driver-assistance/traffic-jam-assist.html. [Accessed: 03-Aug-2016].

[15] Mercedes-Benz, "Mercedes-Benz Intelligent Drive." [Online]. Available:

https://www.mercedes-benz.com/en/mercedes-benz/innovation/mercedes-benz-intelligent-drive/. [Accessed: 10-Jun-2016].

[16] A. Hillel, R. Lerner, D. Levi, and G. Raz, "Recent progress in road and lane detection a survey.pdf," *Mach. Vis. Appl.*, 2014.

[17] Euro NCAP, "Euro NCAP | Ratings Review Report 2015," 2015. [Online]. Available: https://cdn.euroncap.com/media/16470/ratings-group-report-2015-version-10-with-appendix.pdf. [Accessed: 02-Apr-2016].

[18] F. Stein, "The challenge of putting vision algorithms into a car," *IEEE Comput. Soc. Conf. Comput. Vis. Pattern Recognit. Work.*, pp. 89–94, 2012.

[19] S. Committee, "Towards Europe-wide Safer , Cleaner and Efficient Mobility : The First Intelligent Car Report," 2009.

[20] I. Wilmink, W. Janssen, E. Jonkers, M. K, M. Noort, G. Klunder, P. Rämä, N. Sihvola, R. Kulmala, A. Schirokoff, and G. Lind, "Impact assesment of intelligent vehicle safety systems," 2008.

[21] Y. Takada and O. Shimoyama, "Evaluation of driving-assistance systems based on drivers' workload," *Proc. First Int. Driv. Symp. Hum. Factors Driv. Assessment, Train. Veh. Des.*, pp. 208–213, 2001.

[22] R. Ma and D. B. Kaber, "Situation awareness and workload in driving while using adaptive cruise control and a cell phone," *Int. J. Ind. Ergon.*, vol. 35, no. 10, pp. 939–953, 2005.

[23] J. C. F. De Winter, R. Happee, M. H. Martens, and N. A. Stanton, "Effects of adaptive cruise control and highly automated driving on workload and situation awareness: A review of the empirical evidence," *Transportation Research Part F: Traffic Psychology and Behaviour*, vol. 27, no. PB. pp. 196–217, 2014.

[24] C. Grover, I. Knight, and F. Okoro, "Automated emergency brake systems: Technical requirements, costs and benefits," … *Brake Syst. Tech.* …, 2008.

[25] T. Hummel, M. Kühn, J. Bende, and A. Lang, "Advanced Driver Assistance Systems - An investigation of their potential safety benefi ts based on an analysis of insurance claims in Germany," *Ger. Insur. Assoc.*, 2011.

[26] ABI Research, "ABI Research Values Global ADAS Market at $132 Billion in 2026 with Vulnerable User Detection Systems Showing Strongest Growth," 2016. [Online]. Available: https://www.abiresearch.com/press/abi-research-values-global-adas-market-132-billion/. [Accessed: 20-May-2016].

[27] A. Dunoyer and D. Rangarajan, "A Camera for every occasion : Technical & Market trends for camera-based ADAS in EU," 2013.

[28] "Regulation (EC) No 661/2009 of the European Parliament and of the Council concerning typeapproval requirements for the general safety of motor vehicles, their trailers and systems, components and separate technical units intended therefor."

[29] A. Knapp, M. Neumann, M. Brockmann, R. Walz, and T. Winkle, "Code of Practice for the Design and Evaluation of ADAS," 2009.

[30] C. W. Elverum and T. Welo, "On the use of directional and incremental prototyping in the development of high novelty products: Two case studies in the automotive industry," *J. Eng. Technol. Manag. - JET-M*, vol. 38, pp. 71–88, 2015.

[31] M. Broy, I. H. Kruger, A. Pretschner, and C. Salzmann, "Engineering automotive software," *Proc. IEEE*, vol. 95, no. 2, pp. 356–373, 2007.

[32] T. M. Gasser and D. Westhoff, "BASt-study: Definitions of automation and legal issues in Germany," in *Proceedings of the 2012 Road Vehicle Automation Workshop*, 2012.

[33] Sociatey of Automotive Engineers, "Taxonomy and Definitions for Terms Related to On-Road Motor Vehicle Automated Driving Systems," *SAE J3016*, 2014.

[34] World Bank, "The World Bank DataBank," *Data Bank*, 2016. [Online]. Available: http://databank.worldbank.org/data/home.aspx.

[35] M. I. Skolnik, *Introduction to Radar Systems*, vol. 1081. 2009.

[36] J. Hasch, E. Topak, R. Schnabel, T. Zwick, R. Weigel, and C. Waldschmidt, "Millimeter-wave technology for automotive radar sensors in the 77 GHz frequency band," *IEEE Trans. Microw. Theory Tech.*, vol. 60, no. 3 PART 2, pp. 845–860, 2012.

[37] D. Rangarajan, A. Dunoyer, and SBD, "Safe Car An Overview of Next Generation Tier-1 ADAS Solutions," 2014.

[38] A. Dickmann, J., Klappstein, J., Hahn, M., Muntzinger, M., Appenrodt, N., Brenk, C., & Sailer, "Present research activities and future requirements on automotive radar from a car manufacturer's point of view," in *2015 IEEE MTT-S International Conference on Microwaves for Intelligent Mobility (ICMIM)*, 2015, pp. 1–4.

[39] K. Werber, M. Barjenbruch, J. Klappstein, and C. Dickmann, Jurgen Waldschmidt, "How do traffic signs look like in radar?," in *2014 44th European Microwave Conference*, 2014.

[40] C. Fischer and F. Ruf, "Evaluation of different super-resolution techniques for automotive applications," … *(Radar 2012), IET* …, 2012.

[41] D. Kellner, M. Barjenbruch, J. Klappstein, J. Dickmann, and K. Dietmayer, "Instantaneous full-motion estimation of arbitrary objects using dual Doppler radar," in *IEEE Intelligent Vehicles Symposium, Proceedings*, 2014, pp. 324–329.

[42] M. Rapp, M. Hahn, M. Thom, J. Dickmann, and K. Dietmayer, "Semi-markov process based localization using radar in dynamic environments," in *2015 IEEE 18th International Conference on Intelligent Transportation Systems*, 2015, pp. 423–429.

[43] M. Heuer, A. Al-Hamadi, A. Rain, and M. M. Meinecke, "Detection and tracking approach using an automotive radar to increase active pedestrian safety," in *IEEE Intelligent Vehicles Symposium, Proceedings*, 2014, pp. 890–893.

[44] D. Z. Wang, In. Posner, and P. Newman, "Model-free detection and tracking of dynamic objects with 2D lidar," *Int. J. Rob. Res.*, vol. 34, no. 7, pp. 1039–1063, 2015.

[45] M. Himmelsbach, "LIDAR-based 3D Object Perception," *Proc. 1st Int. Work. Cogn. Tech. Syst.*, 2008.

[46] Continental, "Continental Industrial Sensors -SRL 1 Short Range Lidar (Infrared sensor)." [Online]. Available: http://www.conti-online.com/www/industrial_sensors_de_en/themes/srl_1_en.html. [Accessed: 16-Nov-2014].

[47] P. Radecki, M. Campbell, and K. Matzen, "All Weather Perception: Joint Data Association, Tracking, and Classification for Autonomous Ground Vehicle," *arXiv Prepr. arXiv1605.02196*, 2016.

[48] J. Levinson, J. Askeland, J. Becker, J. Dolson, D. Held, S. Kammel, J. Z. Kolter, D. Langer, O. Pink, V. Pratt, M. Sokolsky, G. Stanek, D. Stavens, A. Teichman, M. Werling, and S. Thrun, "Towards fully autonomous driving: Systems and algorithms," in *IEEE Intelligent Vehicles Symposium, Proceedings*, 2011, pp. 163–168.

[49] R. Benenson, M. Omran, J. Hosang, and B. Schiele, "Ten years of pedestrian detection, what have we learned?," in *Lecture Notes in Computer Science (including subseries Lecture Notes in Artificial Intelligence and Lecture Notes in Bioinformatics)*, 2015, vol. 8926, pp. 613–627.

[50] P. Dollar, C. Wojek, B. Schiele, P. Perona, and P. Dollár, "Pedestrian detection: An evaluation of the state of the art," *Pattern Anal. Mach. Intell. IEEE Trans.*, vol. 34, no. 4, pp. 743–761, 2012.

[51] Z. Sun, G. Bebis, and R. Miller, "Monocular precrash vehicle detection: Features and classifiers," *IEEE Trans. Image Process.*, vol. 15, no. 7, pp. 2019–2034, 2006.

[52] S. Sivaraman and M. M. Trivedi, "Looking at vehicles on the road: A survey of vision-based vehicle detection, tracking, and behavior analysis," *IEEE Trans. Intell. Transp. Syst.*, vol. 14, no. 4, pp. 1773–1795, 2013.

[53] Z. Sun, G. Bebis, and R. Miller, "On-road vehicle detection: A review," *IEEE Transactions on Pattern Analysis and Machine Intelligence*, vol. 28, no. 5. pp. 694–711, 2006.

[54] A. Møgelmose, M. M. Trivedi, and T. B. Moeslund, "Vision-based traffic sign detection and analysis for intelligent driver assistance systems: Perspectives and survey," *IEEE Trans. Intell. Transp. Syst.*, vol. 13, no. 4, pp. 1484–1497, 2012.

[55] J. C. McCall and M. M. Trivedi, "Video-based lane estimation and tracking for driver assistance: Survey, system, and evaluation," *IEEE Transactions on Intelligent Transportation Systems*, vol. 7, no. 1. pp. 20–37, 2006.

[56] R. Benenson, "Perception for urban driverless vehicles: design and implementation," Ecole des Mines de Paris, 2008.

[57] Z. Papp, "Situational awareness in intelligent vehicles," in *Handbook of Intelligent Vehicles*, 2012, pp. 61–80.

[58] C. a. Brooks, K. Iagnemma, and S. Dubowsky, "Vibration-based Terrain Analysis for Mobile Robots," *IEEE Int. Conf. Robot. Autom.*, no. April, pp. 3415–3420, 2005.

[59] S. Chhaniyara, C. Brunskill, B. Yeomans, M. C. Matthews, C. Saaj, S. Ransom, and L. Richter, "Terrain trafficability analysis and soil mechanical property identification for planetary rovers: A survey," *J. Terramechanics*, vol. 49, no. 2, pp. 115–128, 2012.

[60] D. Helmick, A. Angelova, and L. Matthies, "Terrain adaptive navigation for planetary rovers," *J. F. Robot.*, vol. 26, pp. 391–410, 2009.

[61] T. Gator, B. Nation, D. Armstrong, A. Baker, C. Crane, D. Dankel, G. Garcia, N. Johnson, J. Lee, S. Ridgeway, E. Thorn, S. Velat, J. H. Yoon, and J. Washburn, "Autonomous Navigation Technologies Developed to Support the 2007 DARPA Urban Challenge," pp. 1–25, 2007.

[62] U. Ozguner, K. a. Redmill, and a. Broggi, "Team TerraMax and the DARPA grand challenge: a general overview," *IEEE Intell. Veh. Symp. 2004*, pp. 232–237, 2004.

[63] M. M. Ben Upcroft Alexei Makarenko,David Johnson, "DARPA Urban Challenge Technical Paper:Sydney-Berkeley Driving Team," 2007.

[64] D. Stavens and S. Thrun, "A Self-Supervised Terrain Roughness Estimator for Off-Road Autonomous Driving," *Proc. Twenty-Second Conf. Annu. Conf. Uncertain. Artif. Intell.*, pp. 469–476, 2006.

[65] A. Broggi, C. Caraffi, R. I. Fedriga, and P. Grisleri, "Obstacle detection with stereo vision for off-road vehicle navigation," *IEEE Comput. Soc. Conf. Comput. Vis. Pattern Recognit.*, 2005.

[66] S. Buehler, Martin; Iagnemma, Karl; Singh, *Springer Tracts in Advanced Robotics; The 2005 DARPA Grand Challenge; The Great Robot Race*. Springer Tracts In Advanced Robotics, 2007.

[67] H. Dahlkamp, A. Kaehler, D. Stavens, S. Thrun, and G. Bradski, "Self-supervised Monocular Road Detection in Desert Terrain," *Proc Robot. Sci. Syst. RSS*, 2006.

[68] D. Lieb, A. Lookingbill, and S. Thrun, "Adaptive Road Following using Self-Supervised Learning and Reverse Optical Flow," *Methods*, 2005.

[69] A. Broggi and S. Cattani, "An agent based evolutionary approach to path detection for off-road vehicle guidance," *Pattern Recognit. Lett.*, vol. 27, no. 11, pp. 1164–1173, 2006.

[70] KPMG, "Self-driving cars : The next revolution," 2013.

[71] E. Ackerman, "UK Unveils 'Affordable' Self-Driving RobotCar," *IEEE Spectrum*, 2013. [Online]. Available: http://spectrum.ieee.org/automaton/robotics/artificial-intelligence/uk-affordable-self-driving-robotcar/. [Accessed: 26-Apr-2015].

[72] M. Bajracharya and A. Howard, "Autonomous off-road navigation with end-to-end learning for the LAGR program," *J. F.* …, 2009.

[73] T. K. Marks, A. Howard, M. Bajracharya, G. W. Cottrell, and L. H. Matthies, "Gamma-SLAM: Visual SLAM in unstructured environments using variance grid maps," *J. F. Robot.*, vol. 26, no. 1, pp. 26–51, Jan. 2009.

[74] K. Konolige, M. Agrawal, M. R. Blas, R. C. Bolles, B. Gerkey, J. Solà, and A. Sundaresan, "Mapping, navigation, and learning for off-road traversal," *J. F. Robot.*, vol. 26, no. 1, pp. 88–113, Jan. 2009.

[75] L. Jackel, E. Krotkov, M. Perschbacher, J. Pippine, and C. Sullivan, "Path-following algorithms and experiments for an autonomous surface vehicle," *J. F. Robot.*, vol. 23, pp. 945–973, 2006.

[76] R. Hadsell, A. Erkan, P. Sermanet, M. Scoffier, U. Muller, and Y. LeCun, "Deep belief net learning in a long-range vision system for autonomous off-road driving," *2008 IEEE/RSJ Int. Conf. Intell. Robot. Syst. IROS*, vol. 1, no. 1, pp. 628–633, 2008.

[77] P. Moghadam and W. S. Wijesoma, "Online, self-supervised vision-based terrain classification in unstructured environments," in *Conference Proceedings - IEEE International Conference on Systems, Man and Cybernetics*, 2009, no. October, pp. 3100–3105.

[78] A. Howard, M. Turmon, L. Matthies, B. Tang, A. Angelova, and E. Mjolsness, "Towards learned traversability for robot navigation: From underfoot to the far field," *J. F. Robot.*, vol. 23, no. 2006, pp. 1005–1017, 2006.

[79] M. J. Procopio, J. Mulligan, and G. Grudic, "Learning terrain segmentation with classifier ensembles for autonomous robot navigation in unstructured environments," *J. F. Robot.*, vol. 26, no. 2, pp. 145–175, Feb. 2009.

[80] W. H. Huang, M. Ollis, M. Happold, and B. A. Stancil, "Image-based path planning for outdoor mobile robots," *J. F. Robot.*, vol. 26, no. 2, pp. 196–211, Feb. 2009.

[81] J. M. Alvarez and A. M. Lopez, "Road Detection based on Illumination Invariance," *IEEE Trans. Intell. Transp. Syst.*, vol. 12, p. 184, 2010.

[82] J. M. Álvarez, a. López, and R. Baldrich, "Illuminant-invariant model-based road segmentation," *IEEE Intell. Veh. Symp. Proc.*, pp. 1175–1180, 2008.

[83] S. Shoop, "Terrain Characterization for Trafficability," in *Cold Regions Research and Engineering Lab. Tech Report*, 1993.

[84] K. Cibulova and S. Sobotkova, "Different Ways of Judging Trafficability," *Adv. Mil. Technol.*, vol. 1, no. 2, pp. 77–88, 2006.

[85] C. A. Brooks and K. Iagnemma, "Vibration-based terrain classification for planetary exploration rovers," *IEEE Trans. Robot.*, vol. 21, no. 6, pp. 1185–1190, Dec. 2005.

[86] C. Weiss, N. Fechner, M. Stark, and A. Zell, "Comparison of different approaches to vibration-based terrain classification," … *3Rd* …, pp. 1–6, 2007.

[87] C. Weiss, H. Tamimi, and A. Zell, "A combination of vision- and vibration-based terrain classification," in *2008 IEEE/RSJ International Conference on Intelligent Robots and Systems, IROS*, 2008, pp. 2204–2209.

[88] E. M. DuPont, C. A. Moore, and R. G. Roberts, "Terrain classification for mobile robots traveling at various speeds: An eigenspace manifold approach," *Proc. - IEEE Int. Conf. Robot. Autom.*, pp. 3284–3289, 2008.

[89] K. Iagnemma, S. Kang, H. Shibly, and S. Dubowsky, "Online terrain parameter estimation for

wheeled mobile robots with application to planetary rovers," *IEEE Trans. Robot.*, vol. 20, pp. 921–927, 2004.

[90] K. Iagnemma, C. Brooks, and S. Dubowsky, "Visual, tactile, and vibration-based terrain analysis for planetary rovers," in *IEEE Aerospace Conference Proceedings*, 2004, vol. 2, pp. 841–848.

[91] I. Halatci, C. a. Brooks, and K. Iagnemma, "A study of visual and tactile terrain classification and classifier fusion for planetary exploration rovers," *Robotica*, vol. 26, p. 767, 2008.

[92] A. Kelly and A. Stentz, "Rough Terrain Autonomous Mobility Part 2 : An Active Vision , Predictive Control Approach," *Auton. Robots*, vol. 5, pp. 163–198, 1998.

[93] A. Howard and H. Seraji, "Vision-based terrain characterization and traversability assessment," *J. Robot. Syst.*, vol. 18, pp. 577–587, 2001.

[94] J. Larson, M. Trivedi, and M. Bruch, "Off-Road Terrain Traversability Analysis and Hazard Avoidance for UGVs," *Calif. Univ. San Diego Dept Electr. Eng.*, pp. 1–7, 2011.

[95] I. Bogoslavskyi, O. Vysotska, J. Serafin, G. Grisetti, and C. Stachniss, "Efficient traversability analysis for mobile robots using the Kinect sensor," *2013 Eur. Conf. Mob. Robot.*, pp. 158–163, 2013.

[96] A. Rankin and L. Matthies, "Daytime water detection based on color variation," *IEEE/RSJ Int. Conf. Intell. Robot. Syst.*, pp. 215–221, 2010.

[97] M. Bibuli, M. Caccia, and L. Lapierre, "Path-following algorithms and experiments for an autonomous surface vehicle," *IFAC Proc. Vol.*, vol. 7, no. 2, pp. 81–86, 2007.

[98] A. L. Rankin, A. Huertas, and L. H. Matthies, "Stereo-vision-based terrain mapping for off-road autonomous navigation," *Proc. SPIE*, vol. 7332, pp. 210–217, 2009.

[99] A. Howard, H. Seraji, and E. Tunstel, "A rule-based Fuzzy Traversability Index for mobile robot navigation," in *Proceedings - IEEE International Conference on Robotics and Automation*, 2001, vol. 3, pp. 3067–3071.

[100] K. Ho, T. Peynot, and S. Sukkarieh, "Traversability estimation for a planetary rover via experimental kernel learning in a Gaussian process framework," *Proc. - IEEE Int. Conf. Robot. Autom.*, pp. 3475–3482, 2013.

[101] J. Gu, Q. Cao, and Y. Huang, "Rapid traversability assesment in 2.5 d grid based map on rough terrain," *Int. J. Adv. Robot.*, vol. 5, no. 4, pp. 389–394, 2008.

[102] H. Seraji, "New Traversability Indices and Traversability Grid for Integrated Sensor/Map-Based Navigation," *J. Robot. Syst.*, vol. 20, no. 3, pp. 121–134, Mar. 2003.

[103] A. Dargazany and K. Berns, "Terrain Traversability Analysis using Organized Point Cloud , Superpixel Surface Normals-based segmentation and PCA-based Classification," 2014.

[104] D. Silver, J. a. Bagnell, and a. Stentz, "Learning from Demonstration for Autonomous Navigation in Complex Unstructured Terrain," *Int. J. Rob. Res.*, vol. 29, pp. 1565–1592, 2010.

[105] J. Larson, "Off-road obstacle classification and traversability analysis in the presence of negative obstacles," University of California, 2011.

[106] C. Caraffi, S. Cattani, and P. Grisleri, "Off-road path and obstacle detection using decision networks and stereo vision," *IEEE Trans. Intell. Transp. Syst.*, vol. 8, no. 4, pp. 607–618, 2007.

[107] À. Navarro, "Terrain Classification in Complex Three dimensional Outdoor Environments," *J. F.* …, 2015.

[108] F. V. Hundelshausen, M. Himmelsbach, F. Hecker, A. Mueller, and H. J. Wuensche, "Driving with tentacles - Integral structures for sensing and motion," *Springer Tracts Adv. Robot.*, vol. 56, pp. 393–440, 2009.

[109] J. F. Lalonde, N. Vandapel, D. F. Huber, and M. Hebert, "Natural terrain classification using

three-dimensional ladar data for ground robot mobility," *J. F. Robot.*, vol. 23, no. 10, pp. 839–861, Oct. 2006.

[110] J. Larson and M. Trivedi, "Lidar based off-road negative obstacle detection and analysis," in *IEEE Conference on Intelligent Transportation Systems, Proceedings, ITSC*, 2011, pp. 192–197.

[111] M. Bellone, G. Reina, N. I. Giannoccaro, and L. Spedicato, "Unevenness point descriptor for terrain analysis in mobile robot applications," *Int. J. Adv. Robot. Syst.*, vol. 10, pp. 1–10, 2013.

[112] J. Loh, G. Elkaim, and R. Curry, "Roughness map for autonomous rovers," *Proc. 2013 Am. Control Conf.*, 2013.

[113] A. Elfes, "Using occupancy grids for mobile robot perception and navigation," *Computer (Long. Beach. Calif).*, vol. 22, pp. 46–57, 1989.

[114] S. Thrun, "Learning occupancy grid maps with forward sensor models," *Auton. Robots*, vol. 15, pp. 111–127, 2003.

[115] M. Perrollaz, A. Spalanzani, and D. Aubert, "Probabilistic representation of the uncertainty of stereo-vision and application to obstacle detection," *IEEE Intell. Veh. Symp. Proc.*, pp. 313–318, 2010.

[116] F. Oniga and S. Nedevschi, "Processing dense stereo data using elevation maps: Road surface, traffic isle, and obstacle detection," *IEEE Trans. Veh. Technol.*, vol. 59, pp. 1172–1182, 2010.

[117] F. Malartre, T. Feraud, C. Debain, and R. Chapuis, "Digital elevation map estimation by vision-lidar fusion," in *2009 IEEE International Conference on Robotics and Biomimetics, ROBIO 2009*, 2009, pp. 523–528.

[118] S. Lacroix, I. K. Jung, and a. Mallet, "Digital elevation map building from low altitude stereo imagery," *Rob. Auton. Syst.*, vol. 41, pp. 119–127, 2002.

[119] S. Pascal, S. Weiss, and T. Rudolph, "Multi Level Surface Mapping using Sparse Point Clouds," 2010.

[120] R. Triebel, P. Pfaff, and W. Burgard, "Multi-level surface maps for outdoor terrain mapping and loop closing," *IEEE Int. Conf. Intell. Robot. Syst.*, pp. 2276–2282, 2006.

[121] A. Persson, "3 D Scan-based Navigation using Multi-Level Surface Maps A ndreas P ersson," Örebro University, 2009.

[122] A. Hornung, K. M. Wurm, M. Bennewitz, C. Stachniss, and W. Burgard, "OctoMap: An efficient probabilistic 3D mapping framework based on octrees," *Auton. Robots*, vol. 34, pp. 189–206, 2013.

[123] R. Zou, "Free Space Detection Based On Occupancy Gridmaps," no. April, 2012.

[124] A. Huertas, L. Matthies, and A. Rankin, "Stereo-based tree traversability analysis for autonomous off-road navigation," *Proc. - Seventh IEEE Work. Appl. Comput. Vision, WACV 2005*, pp. 210–217, 2007.

[125] C. Ye, "Polar traversability index: A measure of terrain traversal property for mobile robot navigation in urban environments," in *Conference Proceedings - IEEE International Conference on Systems, Man and Cybernetics*, 2007.

[126] J. Collier, G. Broten, and J. Giesbrecht, "Traversability analysis for unmanned ground vehicles," *Def. Res. Dev. Canada*, no. DRDC Suffield TM 2006-175, 2006.

[127] A. Chilian and H. Hirschmuller, "Stereo camera based navigation of mobile robots on rough terrain," *2009 IEEE/RSJ Int. Conf. Intell. Robot. Syst.*, pp. 4571–4576, 2009.

[128] S. B. Goldberg, M. W. Maimone, and L. Matthies, "Stereo vision and rover navigation software for planetary exploration," *IEEE Aerosp. Conf. Proc.*, vol. 5, pp. 2025–2036, 2002.

[129] A. El-Kabbany, "Terrain Assessment for High Speed Navigation of Unmanned Ground

Vehicles," University of Calgary, 2014.

[130] A. el-Kabbany and A. Ramirez-Serrano, "Terrain Roughness Assessment for High Speed Ugv Navigation in Unknown Heterogeneous Terrains," *Int. J.* …, 2010.

[131] A. Hornung, "3D Mapping with OctoMap."

[132] G. Vallicrosa, A. Palome, D. Ribas, and P. Ridao, "Realtime AUV terrain based navigation with octomap in a natural environment," in *Advances in Intelligent Systems and Computing*, 2014, vol. 252, pp. 41–53.

[133] A. Rankin, A. Huertas, and L. Matthies, "Evaluation of stereo vision obstacle detection algorithms for off-road autonomous navigation," *Jet Propuls. Lab. Natl. Aeronaut. Sp. Adm.*, 2005.

[134] R. Manduchi, A. Castano, A. Talukder, and L. Matthies, "Obstacle detection and terrain classification for autonomous off-road navigation," *Auton. Robots*, vol. 18, no. 1, pp. 81–102, Jan. 2005.

[135] G. Dubbelman, W. Van Der Mark, J. C. Van Den Heuvel, and F. C. a. Groen, "Obstacle detection during day and night conditions using stereo vision," *2007 IEEE/RSJ Int. Conf. Intell. Robot. Syst.*, pp. 109–116, 2007.

[136] A. Rankin, T. Ivanov, and S. Brennan, "Evaluating the performance of unmanned ground vehicle water detection," *Proc. 10th Perform. Metrics Intell. Syst. Work. - Permis '10*, vol. 16, p. 305, 2010.

[137] R. Labayrade, D. Aubert, and J.-P. Tarel, "Real time obstacle detection in stereovision on non flat road geometry through 'v-disparity' representation," in *Intelligent Vehicle Symposium, 2002. IEEE*, 2002.

[138] A. Howard and H. Seraji, "Vision-based terrain characterization and traversability assessment," *J. Robot. Syst.*, vol. 18, no. 10, pp. 577–587, 2001.

[139] I. Katramados, S. Crumpler, and T. P. Breckon, "Real-time traversable surface detection by colour space fusion and temporal analysis," in *Lecture Notes in Computer Science (including subseries Lecture Notes in Artificial Intelligence and Lecture Notes in Bioinformatics)*, 2009, vol. 5815 LNCS, pp. 265–274.

[140] A. Angelova, L. Matthies, D. Helmick, and P. Perona, "Fast terrain classification using variable-length representation for autonomous navigation," *Proc. IEEE Comput. Soc. Conf. Comput. Vis. Pattern Recognit.*, pp. 1–8, Jun. 2007.

[141] S. D. Buluswar and B. a. Draper, "Color machine vision for autonomous vehicles," *Eng. Appl. Artif. Intell.*, vol. 11, no. 2, pp. 245–256, Apr. 1998.

[142] S. D. Buluswar and B. a. Draper, "Color Models for Outdoor Machine Vision," *Comput. Vis. Image Underst.*, vol. 85, no. 2, pp. 71–99, Feb. 2002.

[143] J. Batlle, A. Casals, J. Freixenet, and J. Martí, "Review on strategies for recognizing natural objects in colour images of outdoor scenes," *Image Vis. Comput.*, vol. 18, no. 6, pp. 515–530, 2000.

[144] P. Jansen, W. Van Der Mark, J. C. Van Den Heuvel, and F. C. A. Groen, "Colour based off-road environment and terrain type classification," in *IEEE Conference on Intelligent Transportation Systems, Proceedings, ITSC*, 2005, vol. 2005, pp. 61–66.

[145] C. S. Dima, N. Vandapel, and M. Hebert, "Classifier fusion for outdoor obstacle detection," *IEEE Int. Conf. Robot. Autom. 2004. Proceedings. ICRA '04. 2004*, vol. 1, pp. 665–671, 2004.

[146] R. Castano and R. Manduchi, "Classification experiments on real-world texture," in *Third Workshop on Empirical Evaluation Methods in Computer Vision*, 2001, pp. 3–20.

[147] G. Amayeh, A. Tavakkoli, and G. Bebis, "Accurate and efficient computation of Gabor features in real-time applications," in *Lecture Notes in Computer Science (including subseries Lecture Notes in Artificial Intelligence and Lecture Notes in Bioinformatics)*, vol. 5875 LNCS, no. PART 1, Springer, 2009, pp. 243–252.

[148] L. Mioulet, T. P. Breckon, A. Mouton, H. Liang, and T. Morie, "Gabor features for real-time road environment classification," in *Proceedings of the IEEE International Conference on Industrial Technology*, 2013, pp. 1117–1121.

[149] H. Seraji and A. Howard, "Behavior-based robot navigation on challenging terrain: A fuzzy logic approach," *IEEE Trans. Robot. Autom.*, vol. 18, no. 3, pp. 308–321, Jun. 2002.

[150] A. Dargazany and K. Berns, "Stereo-based Terrain Traversability Estimation using Surface Normals," *41st Int. Symp. Robot. Robot. 2014*, 2014.

[151] T. D. Gillespie, *Fundamentals of Vehicle Dynamics*. Society of Automotive Engineers, 1992.

[152] M. W. Sayers and S. M. Karamihas, "The little book of profiling," *Basic Inf. about Meas. Interpret. Road Profiles*, no. September, p. 100, 1998.

[153] B. Smoothness and T. Workshop, "Introduction to the International Roughness Index," *Training*, 2007.

[154] M. W. Sayers and S. M. Karamihas, "Interpretation of road roughness profile data," no. June, p. 178, 1996.

[155] L. Xiandong, W. Haixia, S. Yingchun, and H. Tian, "Construction of road roughness in left and right wheel paths based on PSD and coherence function," vol. 61, pp. 668–677, 2015.

[156] F. Tyan, Y. Hong, S. Tu, and W. Jent, "Generation of random road profiles," *J. Adv.* …, pp. 1373–1378, 2009.

[157] P. Johannesson and I. Rychlik, "Modelling of road profiles using roughness indicators," *Int. J. Veh. Des.*, vol. 66, no. 4, p. 317, 2014.

[158] M. W. Sayers, T. D. Gillespie, and W. D. . Paterson, *Guidelines for conducting and calibrating road roughness measurements*, no. 46. 1986.

[159] X. Hou, L. Shan, and S. Ma, "Influence of Pavement Roughness on Riding Comfort Based on Whole Vehicle Model," in *International Conference on Transportation Engineering*, 2007, pp. 655–662.

[160] G. Fichera and M. Scionti, "Experimental Correlation between the Road Roughness and the Comfort Perceived In Bus Cabins," no. 724, 2007.

[161] G. Cantisani and G. Loprencipe, "Road Roughness and Whole Body Vibration: Evaluation Tools and Comfort Limits," *J. Transp. Eng.*, vol. 136, no. 9, pp. 818–826, Sep. 2010.

[162] I. T. 108/Sc 2, "ISO 8608:1995, Mechanical vibration - Road surface profiles - Reporting of measured data," p. 34, 1996.

[163] ISO, "ISO 2631-1:1997 Mechanical vibration and shock - Evaluation of human exposure to whole-body vibration," 1997.

[164] K. Shafizadeh and F. Mannering, "A statistical analysis of factors associated with driver-perceived poad roughness on urban highways," 2002.

[165] S. Tehrani, S. Lynne, C. Falls, and D. Mesher, "Road users' perception of roughness and the corresponding IRI threshold values," *Can. J. Civ. Eng.*, vol. 42.4, pp. 233–240, 2015.

[166] P. Bellutta, R. Manduchi, L. Matthies, K. Owens, and A. Rankin, "Terrain perception for DEMO III," *Proc. IEEE Intell. Veh. Symp. 2000*, pp. 326–331, 2000.

[167] A. S. El-Kabbany and A. Ramirez-Serrano, "Terrain roughness assessment for human assisted UGV navigation within heterogeneous terrains," in *2009 IEEE International Conference on Robotics and Biomimetics, ROBIO 2009*, 2009, pp. 1501–1506.

[168] M. Castelnovi, R. Arkin, and T. R. Collins, "Reactive speed control system based on terrain roughness detection," *Proc. - IEEE Int. Conf. Robot. Autom.*, vol. 2005, pp. 891–896, 2005.

[169] F. Neuhaus, D. Dillenberger, J. Pellenz, and D. Paulus, "Terrain drivability analysis in 3D laser range data for autonomous robot navigation in unstructured environments," *2009 IEEE Conf.*

Emerg. Technol. Fact. Autom., pp. 3–6, 2009.

[170] D. Stavens, G. Hoffmann, and S. Thrun, "Online speed adaptation using supervised learning for high-speed, off-road autonomous driving," in *IJCAI International Joint Conference on Artificial Intelligence*, 2007, pp. 2218–2224.

[171] K. Iagnemma and S. Dubowsky, "Terrain estimation for high-speed rough-terrain autonomous vehicle navigation," *Proc. SPIE*, vol. 4715, no. 617, pp. 256–266, 2002.

[172] G. N. Wilson, A. Ramirez-Serrano, and Q. Sun, "Vehicle state prediction for outdoor autonomous high-speed off-road UGVs," in *2015 IEEE International Conference on Robotics and Automation (ICRA)*, 2015, pp. 467–472.

[173] J. Kelly, S. Zuberi, and A. Fairgrieve, "VEHICLE SPEED CONTROL," *US Pat. 20 150 217 771*, 2015.

[174] V. Sezer, Z. Ercan, H. Heceoglu, S. Bogosyan, and M. Gokasan, "A new fuzzy speed planning method for safe navigation," in *2012 IEEE International Conference on Vehicular Electronics and Safety (ICVES 2012)*, 2012, pp. 381–386.

[175] D. Stavens, "Learning To Drive : Perception for Autonomous Cars a Dissertation Submitted To the Department of Computer Science and the Committee on Graduate Studies of Stanford University in Partial Fulfillment of the Requirements for the Degree of," no. May, 2011.

[176] G. N. Wilson, "High Speed Navigation of UGVs in Rough Unknown Terrains," University of Calgary, 2013.

[177] G. Dubey and P. Korupolu, "Shock Reduction for Autonomous Navigation on Rough Terrain: A Difference of Normals Approach," in *Proceedings of Conference on Advances In Robotics*, 2013.

[178] A. Gaszczak, "Off-road Terrain Geometry Identification - Submission 2," Univerity of Warwick, 2016.

[179] A. Gaszczak, "M8 report|Terrain type recognition," Jaguar Land Rover, 2011.

[180] British Standards, "Intelligent transport systems — Adaptive Cruise Control systems — Performance requirements and test procedures," *BS ISO 156222010*.

[181] Z. Wu, Y. Liu, and G. Pan, "A Smart Car Control Model for Brake Comfort Based on Car Following," *IEEE Trans. Intell. Transp. Syst.*, vol. 10, no. 1, pp. 42–46, Mar. 2009.

[182] R. O. Duda, P. E. Hart, and D. Stork, *Pattern Classification and Scene Analysis*, 2nd ed. John Wiley & Sons, 2012.

[183] D. A. Forsyth and J. Ponce, *Computer Vision: A Modern Approach*, vol. 25, no. 3. Prentice-Hall, 2002.

[184] A. Gaszczak, "Terrain Type Recognition Camera-based grass detection feasibility study - Submission 1," University of Warwick, 2012.

[185] R. Szeliski, "Computer Vision : Algorithms and Applications," *Computer (Long. Beach. Calif).*, vol. 5, pp. 183–195, 2010.

[186] H. Bay, A. Ess, T. Tuytelaars, and L. Van Gool, "Speeded-Up Robust Features (SURF)," *Comput. Vis. Image Underst.*, vol. 110, no. 3, pp. 346–359, 2008.

[187] D. G. Lowe, "Distinctive image features from scale-invariant keypoints," *Int. J. Comput. Vis.*, vol. 60, no. 2, pp. 91–110, 2004.

[188] S. Battiato, G. M. Farinella, E. Messina, G. Puglisi, D. Ravì, A. Capra, and V. Tomaselli, "On the Performances of Computer Vision Algorithms on Mobile Platforms," vol. 8299, p. 82990L–82990L–6, 2012.

[189] K. Van De Sande, T. Gevers, and C. Snoek, "Evaluating color descriptors for object and scene recognition," *IEEE Trans. Pattern Anal. Mach. Intell.*, vol. 32, no. 9, pp. 1582–1596, 2010.

[190] J. C. B. Christopher, "A tutorial on support vector machines for pattern recognition," *Data Min. Knowl. Discov.*, vol. 2, no. 2, pp. 121–167, 1998.

[191] P. Jansen, W. Van Der Mark, J. C. Van Den Heuvel, and F. C. a Groen, "Colour based off-road environment and terrain type classification," in *IEEE Conference on Intelligent Transportation Systems, Proceedings, ITSC*, 2005, vol. 2005, pp. 61–66.

[192] R. Manduchi, "Learning outdoor color classification," *IEEE Trans. Pattern Anal. Mach. Intell.*, vol. 28, no. 11, pp. 1713–1723, 2006.

[193] J. C. Platt, "Probabilistic Outputs for Support Vector Machines and Comparison to Regularized Likelihood Methods," *B Schölkopf C J C Burges A J Smola Ed. Adv. Kernel Methods Support Vector Learn.*, pp. 61–74, 2000.

[194] P. Pfaff, R. Triebel, and W. Burgard, "An Efficient Extension to Elevation Maps for Outdoor Terrain Mapping and Loop Closing," *Int. J. Rob. Res.*, vol. 26, pp. 217–230, 2007.

[195] A. Bystrov, M. Abbas, E. Hoare, T.-Y. Tran, N. Clarke, M. Gashinova, and M. Cherniakov, "Remote Road Surface Identification Using Radar and Ultrasonic Sensors," in *11th European Radar Conference 2014*, 2014, pp. 185–188.

[196] A. Bystrov, M. Abbas, E. Hoare, T. Tran, N. Clarke, M. Gashinova, and M. Cherniakov, "Analysis of Classification Algorithms Applied to Road Surface Recognition," *Radar Conf. (RadarCon), 2015 IEEE*, pp. 0907–0911, 2015.

[197] T. M. Mitchell, *Machine Learning*. 1997.

[198] A. Gaszczak, "Vehicle speed recommendation by pre-emptive surface roughness measurements - Submission 3," University of Warwick, 2016.

[199] Land Rover, "All-Terrain Self-Driving Research Demonstrated at Land Rover Future Tech Showcase." [Online]. Available: http://www.landrover.com/experiences/news/all-terrain-self-driving-research.html. [Accessed: 25-Aug-2016].

[200] NVIDIA, "Automotive Technology Solutions Overview | NVIDIA." [Online]. Available: http://www.nvidia.com/object/drive-automotive-technology.html. [Accessed: 10-Jul-2016].

[201] C. Holder, T. Breckon, and X. Wei, "From on-road to off: transfer learning within a deep convolutional neural network for segmentation and classification of off-road scenes," *Eur. Conf. Comput.*, 2016.

[202] C. Chen, A. Seff, and A. Kornhauser, "Deepdriving: Learning affordance for direct perception in autonomous driving," *Proc. IEEE*, 2015.

[203] B. Huval, T. Wang, S. Tandon, J. Kiske, and W. Song, "An empirical evaluation of deep learning on highway driving," *arXiv Prepr. arXiv*, 2015.

[204] G. Reina, A. Milella, and J. Underwood, "Self-learning classification of radar features for scene understanding," *Rob. Auton. Syst.*, vol. 60, no. 11, pp. 1377–1388, 2012.